

FILMUNIVERSITÄT
BABELSBERG
KONRAD WOLF

Filmuniversity Babelsberg *KONRAD WOLF*

degree program Sound (B.FA.)

Design and implementation of the 2-microphone wave
separation method for impedance measurement using
commercially available components, with special regard to
differences in phase alignment of different measurement
microphones

- Bachelor's thesis -

Submitted by: Ingolf-Christopher Facius
Matriculation number: 10385
1st assessor: Prof. Dr.-Ing. Klaus Hobohm
2nd assessor: Prof. Ingo Kock
Date of submission: September 15, 2020

Contents

Contents	i
List of Figures	vi
Nomenclature	vii
1 Introduction	1
2 Theoretical foundation	6
2.1 Sound propagation in a tube	6
2.1.1 Types of sound waves	6
2.1.2 Plane-wave sound field	7
2.2 Influence of obstacles in the sound field on sound propagation	8
2.2.1 Reflection	9
2.2.2 Absorption	9
2.2.3 Acoustic impedance	10
2.2.4 Loss Factor	11
2.3 Standing waves	13
2.4 The Kundt impedance tube	14
2.5 EN ISO 10534-2	15
2.5.1 Structural parameters of the impedance tube	17
2.5.2 Operating frequency range	17
2.5.3 Microphones	18
2.5.4 Sample Holder	18
2.5.5 Signal generation and processing	19
2.5.6 Loudspeaker	20
2.5.7 Temperature and air pressure	20
2.5.8 Before the measurement	20
2.5.9 Performing Measurements in compliance with <i>EN ISO 10534-2</i>	22
3 Application of the theory	24
3.1 The Measurement System	24
3.1.1 Design drawing	24

3.1.2	The impedance tube	25
3.1.3	Electroacoustic transducers	27
3.1.4	Processing Hardware	30
3.1.5	Software	33
3.1.6	Subsumption of the individual setup used in this thesis	33
3.2	Determination of the transfer function	34
3.3	Calibrating the system	35
3.3.1	Calibration of speaker and microphone levels	35
3.3.2	Tube component calibration	36
3.3.3	System calibration using the sensor-switching-method	36
3.4	Determination of acoustic parameters	38
3.5	Retrieval of important data for evaluation	40
3.6	Error analysis for measurements in the impedance tube	41
3.6.1	Systematic errors	41
3.6.2	Random errors	42
3.6.3	Gross errors	43
3.6.4	Preparatory and preconception errors	44
4	Examination of the phase response of different measurement microphone pairs	45
4.1	Importance of phase information for the 2-microphone method	45
4.2	Taking differences in phase alignment out of the equation	47
4.3	Testing the theory	48
4.3.1	Experimental setup	49
4.3.2	Measuring phase frequency response of different microphones at the same position	51
4.3.3	Measurements with different microphone pairs	53
4.4	Evaluation of results	62
4.5	Error analysis	64
5	Conclusion and prospects	66
	References	69

Appendix	75
A Measuring the filter responses of the Brüel & Kjær Type 4206	75
A.1 Measurement Setup	75
A.2 Graphical comparison of all filters	76
A.3 Middle poti position: Linear	77
A.4 Left poti position: Low-Pass	78
A.5 Right poti position: High-Pass	80
B Software Overview and Module Description	82
B.1 Call Graph	83
B.2 Directory Tree - Overview of all required files	84
B.3 Operational and computational modules	87
B.4 Graphical User Interfaces (GUI-Modules)	100
B.5 Visualization modules	112
B.6 Auxiliary modules	114
B.7 Protocol module	117
C Measurement data for phase comparison of different microphone pairs . .	123
C.1 Product and measurement data of Microtech Gefell MK301E	123
C.1.1 Product Data (Microtech Gefell n.d.)	123
C.1.2 Measurement Data	125
C.2 Product data of Superlux ECM888B (Superlux 2018: 1-5)	127
C.3 Measuring the microphones' phase frequency responses	132
C.3.1 Microtech Gefell MK301 with serial number 0556	132
C.3.2 Microtech Gefell MK301 with serial number 0557	132
C.3.3 Superlux ECM888B with serial number E888B5A0528	133
C.3.4 Superlux ECM888B with serial number E888B5A0530	133
C.4 Comparing the microphones' phase frequency responses	134
C.4.1 Complete comparison of all four microphones	134
C.4.2 Comparison of both Microtech Gefell MK301E	134
C.4.3 Comparison of both Superlux ECM888B	135

C.4.4	Comparison of Microtech Gefell MK301E with serial number 0556 and Superlux ECM888B with serial number E888B5A0528	135
C.4.5	Comparison of Microtech Gefell MK301E with serial number 0556 and Superlux ECM888B with serial number E888B5A0530	136
C.4.6	Comparison of Microtech Gefell MK301E with serial number 0557 and Superlux ECM888B with serial number E888B5A0528	136
C.4.7	Comparison of Microtech Gefell MK301E with serial number 0557 and Superlux ECM888B with serial number E888B5A0530	137
D	Measurement data for the observation of the influences of different phase responses	138
D.1	Specimen	138
D.1.1	Calibration specimen	139
D.1.2	Specimen under investigation (measurement specimen)	140
D.2	Individual measurements	141
D.2.1	Impedance measurement using 2 Microtech Gefell MK301E with Calibration	141
D.2.2	Impedance measurement using 2 Microtech Gefell MK301E without Calibration	142
D.2.3	Impedance measurement using 2 Superlux ECM 888B with Calibration	143
D.2.4	Impedance measurement using 2 Superlux ECM 888B without Calibration	144
D.2.5	Impedance measurement using Microtech Gefell MK301E (ser. 0557) and Superlux ECM 888B (ser. E888B5A0530) with Calibration	145
D.2.6	Impedance measurement using Microtech Gefell MK301E (ser. 0557) and Superlux ECM 888B (ser. E888B5A0530) without Calibration	146
D.3	Comparison of measurements	147
D.3.1	Impedance measurements using 2 Microtech Gefell MK301E	147
D.3.2	Impedance measurements using 2 Superlux ECM 888B	148
D.3.3	Impedance measurements using Microtech Gefell MK301E (ser. 0557) and Superlux ECM 888B (ser. E888B5A0530)	149

D.3.4	All impedance measurements with Calibration	150
D.3.5	All impedance measurements without Calibration	151
D.4	Comparison of calibration data	152
D.4.1	Calibration data of measurement using 2 Microtech Gefell MK301E	152
D.4.2	Calibration data of measurement using 2 Superlux ECM 888B . .	153
D.4.3	Calibration data of measurement using Microtech Gefell MK301E (ser. 0557) and Superlux ECM 888B (ser. E888B5A0530)	154
D.4.4	Calibration data of all microphone combinations	155
	Declaration/Selbstständigkeitserklärung	D

List of Figures

2.1	Different types of sound waves (Hobohm 2018-2019)	6
2.2	Propagation of a) plane waves and b) spherical waves.	7
2.3	Influence of obstacles in the sound field on sound propagation	8
2.4	Locational progressions of a standing waves' pressure and velocity with sinusoid signal pattern (Moeser 2015: 41)	14
2.5	Kundt's impedance tube (Macho-Stadler; Elejalde-Garcia 2019: 1)	15
2.6	Drawing of the impedance tube (ISO 10534-2:2001: 7)	19
3.1	Design drawing of the impedance measurement system (ISO 10534-2:2001: 9)	25
3.2	The Brüel & Kjær Type 4206 Impedance Tube (Bruel Kjaer 2019: 1) . . .	26
3.3	Information on the dimensions of the B&K 4206 (Bruel Kjaer 2019: 6) . .	26
3.4	Individual setup for measuring acoustical impedance	34
4.1	Dispersion in transmission systems (Lerch et al. 2009: 186)	46
4.2	Comparison of phase frequency responses of both Microtech Gefell MK301E	51
4.3	Comparison of phase frequency responses of both Superlux ECM888B . .	52
4.4	Comparison of phase frequency responses of Microtech Gefell MK301E ser. 0557 and Superlux ECM888B ser. E888B5A0530	53
4.5	Comparison of the microphone combinations' measurement results with- out and with calibration	55
4.6	Calibration data from measurement with Microtech Gefell MK301E . . .	56
4.7	Comparison of measured absorption data using Microtech Gefell MK301E	57
4.8	Calibration data from measurement with Superlux ECM 888B	58
4.9	Comparison of measured absorption data using Superlux ECM 888B . . .	59
4.10	Calibration data from measurement with Microtech Gefell MK301E + Superlux ECM 888B	60
4.11	Comparison of measured absorption data using Microtech Gefell MK301E + Superlux ECM 888B	61
4.12	Comparison of measured absorption data from the three microphone com- binations	62

Nomenclature

α	Absorption coefficient
β	Loss factor of a material
bufferSize	Buffer size of a digital audio processing system (in samples)
c	Velocity of sound in a medium (in m/s)
c_g	Group velocity (in m/s)
c_p	Phase velocity (in m/s)
d	Diameter of a round impedance tube (in m) Maximum side length of a rectangular tube (in m)
D	Density of a medium (in kg/m ³)
δ	Dissipation coefficient
Δt	Delay time of a signal passing through a system dependent on the frequency (in s)
f	Frequency (in Hz)
f_l	Lower cut-off frequency (in Hz)
$f_{\text{operation}}$	Operating frequency range (in Hz)
f_s	Sampling rate of a digital audio signal (in Hz)
f_u	Upper cut-off frequency (in Hz)
G	Normal surface admittance
H_{12}	Transfer function from microphone positions one to two
H_c	Calibration factor data, specified as vector of calibration factors H_c at any given frequency f
k	Wave count
κ	Adiabatic exponent
λ	Wavelength (in m)
n	Number of averaged independent (non-overlapping) spectra

ω	Angular frequency (in rad)
\underline{P}_+	Impacting power (in W)
p_0	Pressure amplitude of the incident sound wave (in Pa)
p_a	Measured air pressure (in kPa)
\underline{P}_β	Power loss component (in W)
\underline{P}_δ	The actual power loss part resulting from the conversion of sound energy into other forms of energy (in W)
φ	Phase shift (in $^\circ$)
P	Power (in W)
p	Sound pressure (in Pa)
\underline{P}_ρ	Power component caused by reflection (in W)
\underline{P}_τ	Power component, describing the transport of sound energy behind a material after transmission (in W)
R	Modulus of reflection coefficient ρ
ρ	Reflection coefficient
S_{11}	Auto spectrum (in Pa)
S_{12}	Cross spectrum (in Pa)
σ	Standard error
s	Distance between the two measurement microphones (measured at center of the capsule) (in m)
τ	Transmission coefficient
T	Temperature (in K)
u_n	Normal component of particle velocity (in m/s^2)
v	Particle velocity (in m/s^2)
x_1	Distance of the microphones to the probe (in m)
x	Position at which the reference plane is set (in m)

Z_a Acoustic impedance

Z_c Characteristic impedance

1 Introduction

For acousticians, planners, architects, sound engineers, and many more alike, it is imperative to know the acoustic properties of materials they work with in architectural acoustics. While most materials are both well documented and provide stable characteristics, more often than not, it is important to measure or re-measure the properties before being able to use them or to find out their in-situ characteristics and efficiency. While many practices to measure these acoustical properties exist, most are set up for complex and sophisticated laboratory environments and only a few are available as mobile units. Consequently, ease of use is rarely guaranteed.

The objective of this thesis is therefore to extract a widespread procedure to determine acoustic impedance values of a material from the laboratory. In combining it with easy to acquire commercial components, in order to create an easy to use experimental setup that can be used on the go without much technical knowledge, it is the intention to be able to quickly disclose the looked-for results.

The practice used in this paper is the measurement with the Kundt impedance tube. A relatively straight forward concept to verify the efficaciousness of a material's acoustical impedance properties. It is based upon the theory of standing waves and transfer functions. Whilst this test setup has been used by many over a long period of time and standardized at the turn of the century, most components used have become outdated and need revision. Subsequently a modernized and optimized setup for the 2-microphone wave separation method will be proposed and its efficiency tested and evaluated.

This thesis will begin by covering the underlying theoretical basis. The measurement technique will be described and other options to measure the same parameters addressed. This development of theoretical fundamentals will include a more in-depth treatment of the *EN ISO 10534-2* standard as it is imperative to implement the guidelines described within the standard to prevent systematic errors. Conformity with *EN ISO 10534-2* will result in more trustworthy and conclusive measurement results.

The paper will focus on the 2-microphone wave separation method and the underlying principle of the transfer function method. Furthermore, it will critically examine its benefits and disadvantages. The components used in commercially available setups, like the Brüel & Kjær Type 4206, shall be evaluated and potentially replaced. The observations shall motivate the derivation of a new, modernized setup, again taking into account the features of the components to be swapped in. These modern components will be commercially available products, like ASIO Audio Interfaces, 1/4" measurement microphones with XLR connectors and a computer running a current operating system, as well as modern software. This should make it a lot easier for anyone to be able to measure

acoustic impedance parameters with the impedance tube itself being the hardest component to acquire.

The phase alignment between different pairs of 1/4" measurement microphones will be taken into special consideration. In order to optimize the setup to be able to use it with any two 1/4" measurement microphones, different microphones from both high-end and affordable categories will be tested and evaluated. To date, while many researchers have written papers about the impedance tube and its many forms of operation, the importance of the phase information and differences in the phase frequency response of different microphone pairs have not gotten as much attention. For this reason, the phase will be treated in a more detailed manner.

The software section of the bachelor thesis will be implemented using Matlab R2018b. It is the objective to create a platform-independent program that can easily be run, understood, and can run on any computer that runs Matlab.

Possibilities to measure acoustic impedance

As mentioned above, it is imperative for people working with acoustics regularly to acquire knowledge about the acoustical parameters of the used materials. The acoustic impedance, therefore, is an important parameter, especially when working with the propagation of sound and the hindering thereof, i.e. when trying to minimize or equalize sound absorption and transmission in a room. For that purpose, many methods have been created to measure the acoustic impedance of materials. Some of the more well-known methods will be described in the following.

Reverberant room¹

One of the most commonly used and well-known measurement techniques is the impedance measurement in the reverberant room. This method has been standardized in the International Organization for Standardization's [ISO] standard no. 354: 2003. The sound field of a well-built reverberant room is nearly identical to the diffuse sound field. If a material is introduced to the room its frequency response may change. Through comparison of the room's original impulse response and the impulse response with the specimen in the room, considering important values like the sound absorption area and area of the test object, the absorption coefficient can be determined. However, while widespread, this method is neither a well accessible option, nor does it work for in-situ measurements. The specimen needs to be of a certain minimal size to deliver any conclusive results but at

¹ cf. ISO 354:2003

the same time needs to be small enough to fit into the room (and through the door). A big disadvantage of this method is presented by it only returning the information about the absorption coefficient. It is, unfortunately, not possible to find information on transmission or dissipation. Yet, for certain probes, this may be the best option to measure their absorption coefficient, like i.e. wall coverings as they can basically be put into an in-situ position.

Window test bench²

The window test bench is another example of a not easily-accessible measuring method. For this method, two conjoining rooms connected by the “window” are needed. Both rooms need to be reverberant, nearly diffuse, and need to share the same properties. When a specimen is placed in the window a loudspeaker and a microphone are placed in room A and another microphone in room B. In room A a test signal, usually a random noise signal, is played back. The responses from the microphones can be compared and information about diffusion and transmission derived. While this test setup is highly efficient in being able to return all interesting values for the acoustic impedance, including reflection, absorption, dissipation, and transmission it is not easily accessible, takes a lot of time to set up, as the probe needs to be fit for the window and built in flush and sealed. It is also not viable if the specimen has a small size.

“The standard two-room method for assessing sound insulation (sound transmission loss) of a constructive element requires complex and big facilities such as test chambers, and a tough procedure where many variables must be controlled” (Rodriguez-Fernandez; Fernandez-Comesana 2017: 1).

Options using the Kundt impedance tube³

The Kundt impedance tube is probably the most well-known experimental setup to measure acoustic impedance. The most used techniques have been standardized under *EN ISO 10534* and its two sub-standards *EN ISO 10534-1*, the standing wave method, and *EN ISO 10534-2*, the transfer function method.

The impedance tube is a small specimen experiment. Probes of materials are created and observed in the impedance tube. The techniques themselves will be described in chapters 2.4 and 2.5.

Further modifications of the impedance tube are common. These use 3, 4 or more microphones. In those cases, the impedance tube is extended behind the specimen. This

² cf. Meier 2000: 42 ff.

³ cf. ISO 10534-1:2001 & ISO 10534-2:2001

makes it possible to measure the transmission and to be incident-determined about the dissipation.

The impedance tube poses a suitable and easily-accessible option for most situations to acquire information about the acoustic impedance of material probes. Through its extensions, all parameters that might be of interest can be determined. The biggest issue poses the need to cut perfect specimens, so the measurements are not negatively influenced by systematic errors. Also, not many possibilities to measure in-situ with the impedance tube exist with the extended tube measurements excluding in-situ possibilities altogether.

As mentioned before, this thesis will provide a way to make this experimental setup even more accessible and easy to use, while also trying to get the experiment out of laboratory environments. The following options using Microflown have been included to show different and new approaches to impedance measurement, especially for in-situ measuring. Some of which have only been created in recent years and are therefore new modern-day approaches.

Options using Microflown technology

With the invention of the Microflown at the University of Twente in 1994, a couple of possibilities of measuring acoustical impedance have been enabled.

“The Microflown is an acoustic sensor measuring particle velocity instead of sound pressure, which is usually measured by conventional microphones. Since its recent invention it is mostly used for measurement purposes (1D and 3D-sound intensity measurement and acoustic impedance)” (Bree 2003: 1).

The impedance measurement using the Kundt’s tube, both following *EN ISO 10534-1* and *EN ISO 10534-2* guidelines are possible (cf. Bree 2003: 8). Yet, many more possibilities have been made viable and even been created using Microflown technology. For example, it enables PU (pressure-velocity) probes. An application of which is piston-on-a-sphere measurement using the so-called impedance gun. It enables in-situ measurement of acoustic impedance in any space the impedance gun fits in. With it, most surfaces can be measured quickly and within minutes using a small spherical loudspeaker and a Microflown on-axis, recording the test signal and the material’s reflection (cf. Tijss 2013).

Another method uses the PU-probe for sound intensity measurements combined with the Scan & Paint method. “The acoustic signals of the sound field are acquired by manually moving a single transducer across a measurement plane whilst filming the event with a camera. In the post-processing stage, the sensor position is extracted by applying automatic color detection to each frame of the video. It is then possible to split the long recording into multiple segments by applying a spatial grid algorithm. Each fragment of

the signal will be linked to a grid cell, depending upon the position of the probe during the measurement. Spectral variations across the space are computed by analyzing the signal segments of each grid section” (Rodriguez-Fernandez; Fernandez-Comesana 2017: 1). This method also makes in-situ measurements relatively easy. Whilst not as handy as the impedance gun it returns very easy to interpret visualized results over a greater area of a material and is therefore ideal to find i.e. acoustical leakage in a material. Yet, its main objective is to provide information about sound transmission loss and may not be as effective in providing information about reflective properties.

2 Theoretical foundation

Subsequently, the fundamentals will be described to create a basis for a better understanding of the applied principles. This will, first of all, include a description of the propagation of sound within a tube, the influence obstacles in the sound field have, and then move on to the Kundt impedance tube and the *EN ISO 10534-2* standard.

2.1 Sound propagation in a tube

2.1.1 Types of sound waves

When the particles of a medium are excited, i.e. when air molecules are being animated by a speaker's membrane, the particles are transmitting the energy through wavelike propagation. In order to understand and evaluate the physical processes of sound propagation it is important to reflect upon the different types of sound waves.

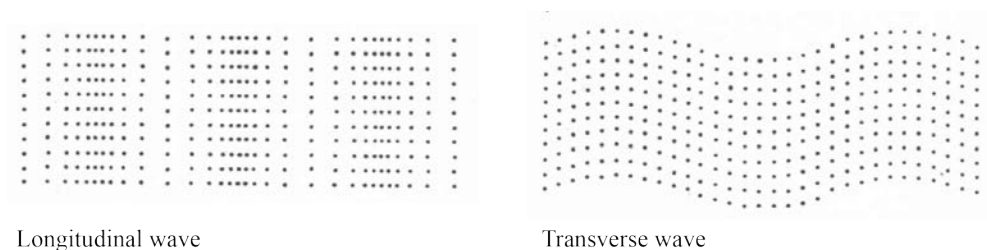


Fig. 2.1: Different types of sound waves (Hobohm 2018-2019)

As shown in Figure 2.1 wave propagation is generally subcategorized into two categories: longitudinal and transverse waves. In a real environment, a single type of wave is rarely encountered. Even though only longitudinal waves can propagate in gases and liquids, the excitation of adjacent solids must always be expected in a real environment. Therefore there are overlaps of both types.

“In a longitudinal wave the particle displacement is parallel to the direction of wave propagation. [...] The particles do not move down the tube with the wave; they simply oscillate back and forth about their individual equilibrium positions. [...] The wave is seen as the motion of the compressed region (i.e., it is a pressure wave). [...]

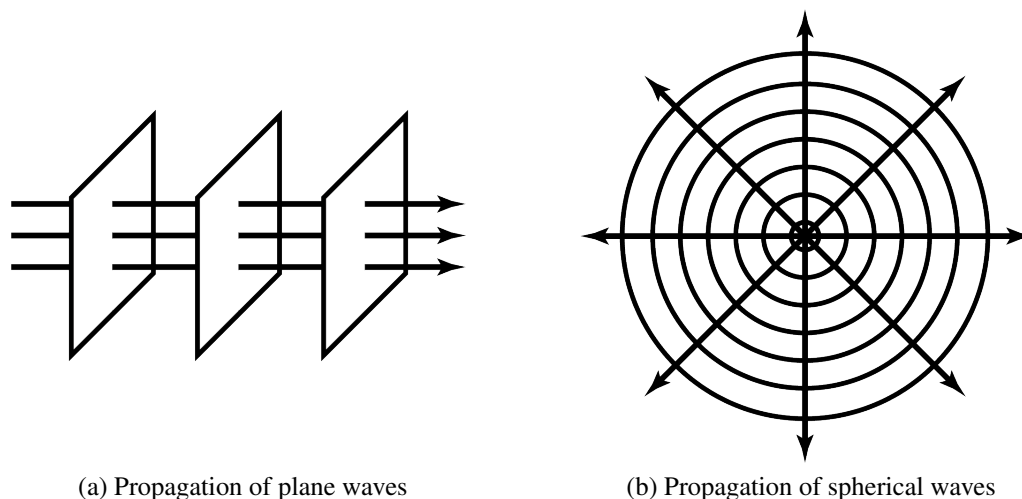
In a transverse wave the particle displacement is perpendicular to the direction of wave propagation. [...] The particles do not move along with the wave; they simply oscillate

up and down about their individual equilibrium positions as the wave passes by.” (Russell 1998)

For the measurement within the impedance tube, longitudinal waves within a plane sound field will be produced by the speaker. Only if the direction of oscillation is parallel to the propagation direction the time and phase information of the signal can be measured correctly.

2.1.2 Plane-wave sound field

To describe sound propagation, a distinction is made between two elementary types of sound fields: the spherical sound field and the plane-wave sound field.



(a) Propagation of plane waves

(b) Propagation of spherical waves

Fig. 2.2: Propagation of a) plane waves and b) spherical waves.

The spherical sound field is prototypical with its main characteristic of propagating sound omnidirectional with equal energy.

The plane-wave sound field, on the other hand, is characterized by every wavelet in its wavefront “moving to the same direction perpendicular to the crest of the wave”, as shown in Figure 2.2 (Tikander 2002: 9). It is difficult to realize a plane-wave sound field, especially for low-frequency signal components. The farther away from the center of the acoustic source you examine the plane-wave sound field in the free field, the more it turns into a spherical sound field. This is due to particles in a free field freely exciting other particles around them, thus not moving on a single straight axis but rather in all directions of the three-dimensional space.

This is caused, just as the propagation of both sound fields is, by Huygens’ principle. This states that “all points of a wavefront [...] may be regarded as new sources of wavelets

that expand in every direction at a rate depending on their velocities” (Encyclopaedia Britannica; Huygens 2016).

In a controlled environment, such as a tube, it is much easier to create a plane-wave sound field. In the case of the impedance tube, the tube has non-absorbent, hard-to-excite, and very smooth boundary surfaces. Consequently, a plane-wave sound field remains plane and a perpendicular sound incidence can be achieved, as is required.

2.2 Influence of obstacles in the sound field on sound propagation

If a sound wave is incident on an obstacle or boundary surface, its further propagation is altered depending on the properties of the obstacle’s material properties. The material will most likely reflect a part of the incident sound and absorb the rest, as visualized in Figure 2.3. If the incident sound’s energy is assumed as the value ‘ I ’ the following rela-

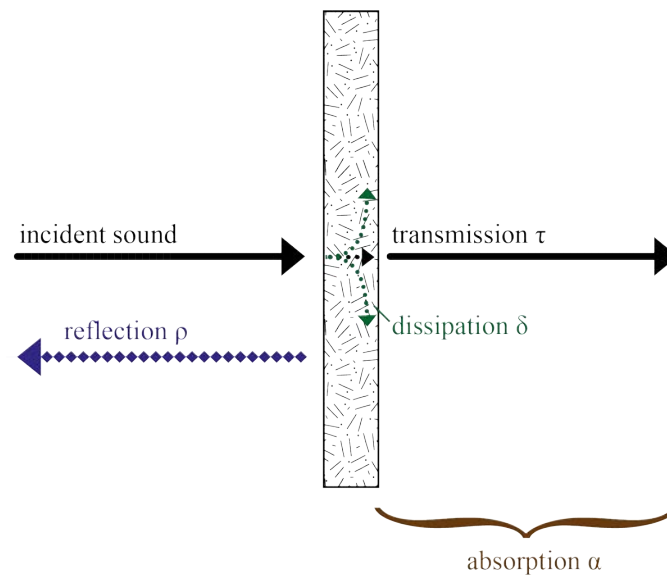


Fig. 2.3: Influence of obstacles in the sound field on sound propagation

tional equation can be applied, where ρ is the reflection coefficient and α the absorption coefficient:

$$1 = \rho + \alpha. \quad (2.1)$$

Both reflection, as well as absorption, are frequency-dependent.

2.2.1 Reflection

The reflection is the part of the signal that is recoiled on impact with the obstacle. The more rigid and harder to excite the material the higher the reflection. The reflection coefficient ρ can contain values between '0' and '1'. The direction of the reflection is determined by the surface texture of the obstacle's material. If the material has a plane surface and the sound hits it perpendicularly then the returning sound wave of the reflection assumes the same path as the incident wave. If the material has a complex texture the reflection is composed of more than one returning wavefront and through angled parts of the texture, the reflected parts will assume different paths. Thus causing running time and phase differences. This effect is called diffusion.

As Prof. Möser evaluates in his book "Technische Akustik" it is important for the examination using the impedance tube to be aware that the reflection coefficient ρ is a complex number (cf. Moeser 2015: 191 f.):

$$\rho = R \cdot e^{j\varphi}. \quad (2.2)$$

With R being the modulus of ρ and φ being the phase shift he continues: "For example, the sound field penetrating the sound absorber layer with fully reflecting backside must pass the layer's thickness twice until it leaves the surface as a reflected wave. The associated running time must inevitably be expressed as a complex-valued reflection factor"⁴ (Moeser 2015: 191). This change in running time causes a shift in phase, considered with φ .

2.2.2 Absorption

The second, absorbed part of the signal is in itself split into two parts again, as shown in Figure 2.3. The transmission τ and dissipation δ shares can easily be related to the absorption:

$$\alpha = \tau + \delta. \quad (2.3)$$

As a result, formula 2.4 can be derived from formulas 2.1 and 2.3:

$$\tau + \delta = 1 - \rho. \quad (2.4)$$

⁴ "Zum Beispiel muss das in eine rückseitig schallhart begrenzte Absorberschicht eindringende Schallfeld zweimal die Schichtdicke passieren, bis es als reflektierte Welle die Schichtoberfläche wieder verlässt. Die damit verbundene Laufzeit muss notwendigerweise durch einen komplexwertigen Reflexionsfaktor erfasst werden." [Original text]

The absorption coefficient α , and as conclusions from the equation 2.3 transmission τ and dissipation δ coefficients as well, can contain values between '0' and '1'.

The dissipating shares of the absorption are converted into other forms of energy, i.e. thermal energy. The transmission allows the energy, in case of acoustic examination sound, to pass through the material and continue its propagation behind the material.

Both dissipation and transmission can be defined by relating the impacting power \underline{P}_+ and the fraction of the power which describes the corresponding transport of energy \underline{P}_τ and \underline{P}_δ respectively. This is expressed for the transmission coefficient as $\tau = \frac{\underline{P}_\tau}{\underline{P}_+}$ and for the dissipation coefficient as $\delta = \frac{\underline{P}_\delta}{\underline{P}_+}$ (cf. Moeser 2015: 194).

2.2.3 Acoustic impedance

The acoustic impedance of a material is closely dependent on its reflective properties. The resistance towards incident sound propagation a material possesses is declared as this complex factor. It is defined as the ratio between pressure and speed (cf. Deter 2013: 4):

$$Z_a = \frac{p}{v}. \quad (2.5)$$

The acoustic impedance Z_a is therefore dependent on the sound pressure p and the volume's particle velocity v indicating the speed at which the air particles oscillate around their idle position.

Additionally, the characteristic impedance Z_c of a material can be calculated by using the pressure p and the normal component of the particle velocity u_n (cf. Tikander 2002: 14):

$$Z_c = \frac{p}{u_n}. \quad (2.6)$$

Mr. Tikander continues to specify the characteristic impedance for lossless materials as $Z_c = Dc$, D being the medium's density and c the velocity of sound in that medium. It has been observed that air can be approximated to be lossless over short distances.

The subsequent observations to illustrate the dependence of the impedance on the reflection factor were adopted from the investigations of Mr. Deter's bachelor thesis (cf. Deter 2013: 4f.).

If pressure and velocity curves are observed in front of a material in the impedance tube, taking into account the law of acoustic inertia, the impedance can be ascertained as:

$$\frac{Z_a}{Dc} = \frac{1 + \rho}{1 - \rho}. \quad (2.7)$$

This formula can be converted to better illustrate the dependency of Z_a and ρ

$$\rho = \frac{Z_a - Dc}{Z_a + Dc} = \frac{\frac{Z_a}{Dc} - 1}{\frac{Z_a}{Dc} + 1}. \quad (2.8)$$

2.2.4 Loss Factor

Often instead of a material's reflection factor R one can find values for the loss factor β .

The loss factor can be defined by relating the impacting power \underline{P}_+ and the power loss \underline{P}_β (cf. Moeser 2015: 194):

$$\beta = \frac{\underline{P}_\beta}{\underline{P}_+}. \quad (2.9)$$

However, it is now important to look back upon equation 2.3, as the loss factor can also be defined as:

$$\beta = \tau + \delta. \quad (2.10)$$

Therefore, the loss factor and the absorption coefficient may be equated:

$$\beta = \alpha. \quad (2.11)$$

This can be traced back to the definition of the term absorption. Some definitions that can be found in literature, as i.e. in Prof. Möser's book "Technische Akustik", define the term absorption differently. Often, for simplification purposes, the term absorption is defined as the shares of energy that are converted into different forms of energy, like thermal energy or light energy. The correct term for this is dissipation as defined in chapter 2.2.2. Yet, Mr. Möser never uses the term dissipation when writing about sound propagation and the impedance tube. Therefore, a substantial conundrum is presented. As the usage of the absorption term varies, so does the definition of the loss factor. Subsequently, it is considerably more difficult to correctly interpret the term absorption, for example when used on specification sheets for a material. It is then when it becomes crucial for the specification sheet to also provide information about how the values behind the term absorption have been measured. Often it is then necessary to look up the technique or standard by which the values were measured to be able to correctly interpret the given information, as only then it is possible to find the information of whether $\alpha = \tau + \delta$ or $\alpha = \delta$. If not considered, significant errors may be introduced to one's observations.

Especially, when using the 2-microphone wave-separation method with the impedance tube it is very difficult to find out the exact values for δ and τ . The returned information only provides values for the overall losses. The analysis is often simplified, with the interpretation usually being simple, as Prof. Möser summarizes (Moeser 2015 194):

- “For absorbent samples with a sound-proof seal on their backside, one concludes $\beta = \delta$, it is almost always such samples that are under observation in the impedance tube.
- For thin, light finishes without an absorbent layer, $\beta = \tau$. Such very light probes are practically not found very often; they are more importantly named here for purposes of full disclosure. An example would be a small mass per unit area (i.e. a curtain of non-porous material) to separate a part of the room.”⁵

The following derivation was adopted from Moeser 2015: 195. If we now observe the power based on the law of conservation of energy, where \underline{P}_ρ is the reflected power:

$$\underline{P}_+ = \underline{P}_\beta + \underline{P}_\rho \quad (2.12)$$

and consider the circumstance of plane waves with:

$$\underline{P}_\rho = R^2 \underline{P}_+ \quad (2.13)$$

The loss factor β can be defined as:

$$\beta = 1 - R^2 \quad (2.14)$$

The relation to the impedance can also be established, as in Deter 2013: 6-7 using the law of adaptation:

$$\beta = \frac{4 \operatorname{Re} \left\{ \frac{Z_a}{D_c} \right\}}{\left(\operatorname{Re} \left\{ \frac{Z_a}{D_c} \right\} + 1 \right)^2 + \left(\operatorname{Im} \left\{ \frac{Z_a}{D_c} \right\} \right)^2} \quad (2.15)$$

5

- “Bei absorbierenden Proben mit rückseitigem schallhartem Abschluss ist immer $\beta = \delta$; es sind fast immer solche Proben, die praktisch interessieren.
- Bei dünnen, leichten Abschlüssen ohne absorbierende Schicht ist $\beta = \tau$. Solche sehr leichten Abschlüsse kommen praktisch nicht sehr oft vor; sie werden hier mehr der vollständigen Beschreibung wegen aufgeführt. Ein Beispiel bestünde in einer kleinen Flächenmasse (einem Vorhang aus nicht-porösem Material) zur Abtrennung eines Raumteiles.”

”It can be understood that for the adaptation case $Z_a = Dc$ the loss factor becomes maximum, $\beta = 1$. Furthermore, it can be concluded that the imaginary part of the impedance reduces the loss factor and therefore the absorption is worsened”⁶ (Deter 2013: 7).

2.3 Standing waves

In a space with parallel boundary surfaces, standing waves can develop. A cylindrical, sealed tube, like the impedance tube, must therefore also be regarded for standing waves. It is sufficient to make an one-dimensional observation, as in a cylindrical tube, standing waves can only emerge on the axis of sound propagation. In a sinusoidal observation, the incident wave is superimposed on the rebounding wave reflected by the sound-reflective tube end. Wave crests and wave valleys overlap each other and form the characteristic image of standing waves.

The following derivation was adopted from Moeser 2015: 39-40. The complex sound pressure magnitude composed of the two parts of the incident and returning waves can be expressed as:

$$p(x) = p_0 \cdot (e^{-jkx} + \rho e^{jkx}) \quad (2.16)$$

where p_0 represents the amplitude of the incident sound wave, the first summand the incident wave, and the second summand the returning wave. Should complete reflection not have taken place the returning wave may be attenuated. This attenuation is expressed via a reflection factor ρ . The variable k considers the wave number. The particle velocity then can be contextualized as:

$$v(x) = \frac{p_0}{D_0c} \cdot (e^{-jkx} + \rho e^{jkx}). \quad (2.17)$$

For simplification, the location of the reflector is assumed with $x = 0$ and the reflector itself is presumed to be elastically non-deformable and rigid. As the air particles cannot penetrate the reflecting surface, the velocity at $x = 0$ can be assumed as $v = 0$. Therefore, the reflection factor ρ is assigned $\rho = 1$. The location and time progressions then can be assumed to be as indicated in formulas 2.16 and 2.17 for pressure and velocity as:

$$p(x) = 2p_0 \cdot \cos kx \cdot \cos \omega t \quad (2.18)$$

⁶ “Es ist ersichtlich, dass für den Anpassungsfall $Z_a = Dc$ der Verlustfaktor maximal, $\beta = 1$, wird. Außerdem lässt sich erkennen, dass der Imaginärteil der Impedanz den Verlustfaktor verringert und damit die Absorption verschlechtert.” [Original text]

and

$$v(x) = \frac{2p_0}{D_0c} \cdot \sin kx \cdot \sin \omega t \quad (2.19)$$

and the location progressions are visualized in figure 2.4.

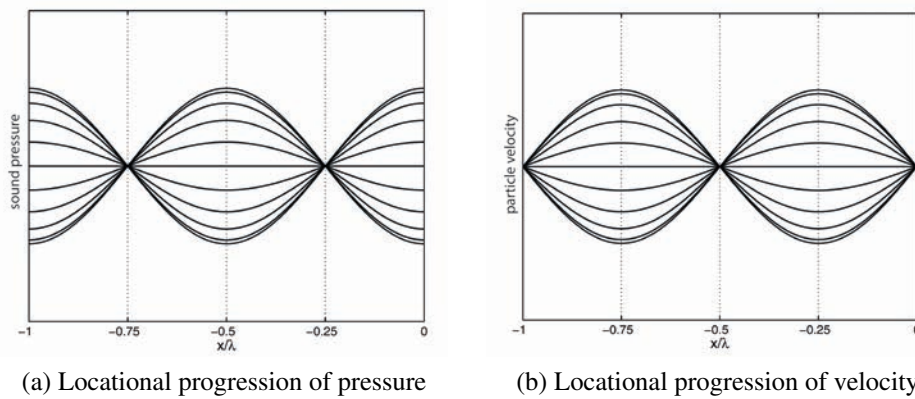


Fig. 2.4: Locational progressions of a standing waves' pressure and velocity with sinusoid signal pattern (Moeser 2015: 41)

The figures clearly show that there is no shift over time of pressure and velocity but rather the amplitudes change. There is also a phase difference of $\varphi = 90^\circ$ between the two values when comparing the values at the same values x . This can easily be traced back to the cosine and sine functions used, as visible in equations 2.18 and 2.19 (cf. Deter 2013: 12).

2.4 The Kundt impedance tube

The physicist August Kundt (1839-1894) created an experiment to determine the velocity of sound in different materials. He “dusted the interior of a tube with a finely divided powder to show the position of the nodes of the sound waves, thereby determining their wavelength” (cf. Encyclopaedia Britannica; Kundt 2020). Based on his experiments, the tube was then further developed and can now be used to observe and determine wave propagation and acoustic impedance. The version of the impedance tube we know today, as is shown in Figure 2.5, consists of a loudspeaker at one end of the hollow cylindrical tube and a sound-proof, hard-to-excite boundary surface at the opposite end. At the latter, a material probe can be introduced to the environment. The outer boundary of the tube is sound-reflecting so that the sound only propagates as a plane wave perpendicularly

to the tube's end. Furthermore, sensors can be put into place to determine the looked-for characteristics of the probe, such as the acoustic impedance. To complete the experimental setup, a signal generator is connected to the loudspeaker. The test signals are created and played back and in turn get picked up by the sensors again. Subsequently, the data is being transmitted to an analyzation unit able to compare all input information of the sensors, as well as the original signal(s).

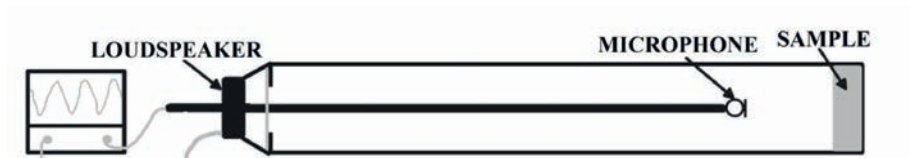


Fig. 2.5: Kundt's impedance tube (Macho-Stadler; Elejalde-Garcia 2019: 1)

When a sound wave travels as a plane-wave from the loudspeaker through the tube it is then reflected from the tube's end. The incident and reflected waves form standing waves that can be observed. "If a sample of absorbing material is placed at the end of the tube, some of the incident sound energy is absorbed by the sample, then the incident and reflected waves have different amplitudes. The total sound field in the pipe is the superposition of a standing wave and a wave travelling in the tube-axis direction" (Macho-Stadler; Elejalde-Garcia 2019: 1).

The measurement techniques that are generally used have been standardized in norm *EN ISO 10534*. It is composed of two sub-standards, both measuring uni-dimensional plane-wavefronts in the incident and reflecting directions. They differ in the measuring methods applied. *EN ISO 10534-1* uses the standing wave method and *EN ISO 10534-2* applies the transfer function method.

With the transfer function method applied in this thesis and explained in chapter 2.5 it is important to also summarize how *EN ISO 10534-1* works. When utilizing the standing wave method a sinusoidal sound wave is played back within the tube. When a standing wave forms pressure minimums and pressure maximums, it can be measured by the sensor and the material's reflection coefficient can be defined (cf. Brunnader 2002: 3).

2.5 EN ISO 10534-2

EN ISO 10534-2 is not only an alternative measuring method but also much faster than the method described in *EN ISO 10534-1*. The information presented in this chapter and its subchapters has been largely adopted and consolidated from the ISO standard (cf. ISO 10534-2:2001) and its corrigendum (cf. ISO 10534-2:2007).

“In this test method, plane waves are generated in a tube by a noise source, and the decomposition of the interference field is achieved by the measurement of acoustic pressures at two fixed locations using wall-mounted microphones or an in-tube traversing microphone, and subsequent calculation of the complex acoustic transfer function, the normal incidence absorption and the impedance ratios of the acoustic material” (ISO 10534-2:1998: 3). The method only allows parametric examinations at perpendicular sound incidence. For information about the behavior in the diffuse sound field, a conversion step is necessary. The measurements can be carried out using either an impedance tube with a round cylindrical or square cylindrical cross-section.

For better understanding, it is compulsory to introduce a few terms used within the standard that have not yet been used within this thesis.

- The term *reference plane* describes the “cross-section of the impedance tube for which the reflection factor ρ or the impedance Z or the admittance G are determined and which is usually the surface of the test object. [...] The reference plane is assumed to be at $x = 0$ ” (ISO 10534-2:1998: 3).
- The *normal surface admittance* G is defined as the reciprocal value of the normal surface impedance Z as $G = \frac{1}{Z}$.
- The *wave number* k_0 is defined as assumably complex variable

$$k_0 = \frac{\omega}{c_0} = \frac{2\pi f}{c_0} = \text{Re}\{k_0\} - j\text{Im}\{k_0\}.$$
- The *cross spectrum* $S_{12} = p_2 \cdot \bar{p}_1$ is “determined from the complex sound pressures p_1 and p_2 at two microphone positions” (ISO 10534-2:1998: 2).
- The *auto spectrum* $S_{11} = p_1 \cdot \bar{p}_1$ is “determined from the complex sound pressure p_1 at microphone position one” (ISO 10534-2:1998: 3).
- H_{12} is the “transfer function from microphone positions one to two, defined by the complex ratio $\frac{p_2}{p_1} = \frac{S_{12}}{S_{11}} = \frac{S_{22}}{S_{21}} = \left(\frac{S_{12}}{S_{11}} \cdot \frac{S_{22}}{S_{21}}\right)^{\frac{1}{2}}$ ” (ISO 10534-2:1998: 3).
- The *calibration factor* H_c is the factor used for compensating amplitude and phase divergence between the microphones in use.

The standard facilitates two measurement options. The one-microphone method requires much more time and signal processing. Yet, it excludes phase mismatches of different microphones for it only uses one microphone. It also allows for optimal positioning of the microphone for different frequencies. The two-microphone wave separation method requires a preliminary check or correction during experimentation to determine the amplitude and phase differences between the two microphones. It combines time efficiency

with precise and straightforward execution. It is recommended for general testing purposes and therefore applied in this thesis.

2.5.1 Structural parameters of the impedance tube

The ISO has defined the structural parameters of the tube. This information is collated hereafter (cf. ISO 10534-2:2001: 5-6). It must be straight and may not have any cross-sectional deformations. The tolerance for the diameter or transverse dimension has been set at $\leq \pm 0.2\%$. The tube's outer boundary surface must be a rigid, smooth, non-porous wall. For round metal impedance tubes, a wall thickness of about 5 % of the diameter d is recommended. If a rectangular tube is used, its corners must be sturdy enough to avoid deformation of the side plates. A side plate thickness of about 10 % of the pipe's transverse expansion is recommended. Tubes that are made of different materials than metal need to follow specific guidelines to conform to *EN ISO 10534-2*.

The tube length needs to be sufficiently long enough, so plane-waves can develop between loudspeaker and specimen. The microphones as sensors need to be in a plane-wave sound field. The ideal length of an impedance tube varies with the frequencies that want to be observed. The standard asks for the microphones to at least have a distance of the diameter to the sound source, ideally more and up to 3 times the diameter of the tube. Generally put: the greater the distance the more conclusive the observations for low frequencies will be. As the specimen cause near-field distortions, recommendations have been put in place on minimal distances x_l of the microphones to the probe. These consist of $x_l \geq \frac{1}{2}d$ for non-structured test specimens, $x_l \geq d$ for semi-laterally structured probes and $x_l \geq 2d$ for highly asymmetric specimens.

2.5.2 Operating frequency range

To determine the operating frequency range $f_l < f_{operation} < f_u$, as defined in chapter 4.2 of ISO 10534-2:2001: 5-6, the lower cut-off frequency f_l and upper cut-off frequency f_u need to be identified. f_u for round impedance tubes must comply with:

$$f_u < \frac{0,58 \cdot c_0}{d} \quad (2.20)$$

and for rectangular tubes comply with:

$$f_u < \frac{0,5 \cdot c_0}{d} \quad (2.21)$$

The distance between the two microphones s , measured at the center of the capsule, must be set accordingly:

$$s < \frac{0.45 \cdot c_0}{f_u}. \quad (2.22)$$

The greater the distance between the microphones, the more accurate the measurement results will be.

While f_l is determined through the limit by the measurement uncertainty of the signal processor, it can also be calculated using equation 2.22. If it is assumed that s , if compliant with 2.22, “is 5 % of the wavelength of the corresponding lower frequency of interest”⁷ (ISO 10534-2:2001: 6), the following correlation can be made based on the simple formula $f = \frac{c}{\lambda}$:

$$f_l = \frac{c_0}{\left(\frac{s}{0,05}\right)} = \frac{c_0}{20s}. \quad (2.23)$$

If now 2.22 is inserted into equation 2.23, a relation to f_u can be made visible:

$$f_l = \frac{c_0}{20 \left(\frac{0.45 \cdot c_0}{f_u}\right)} = \frac{c_0 \cdot f_u}{9c_0} = \frac{1}{9} f_u. \quad (2.24)$$

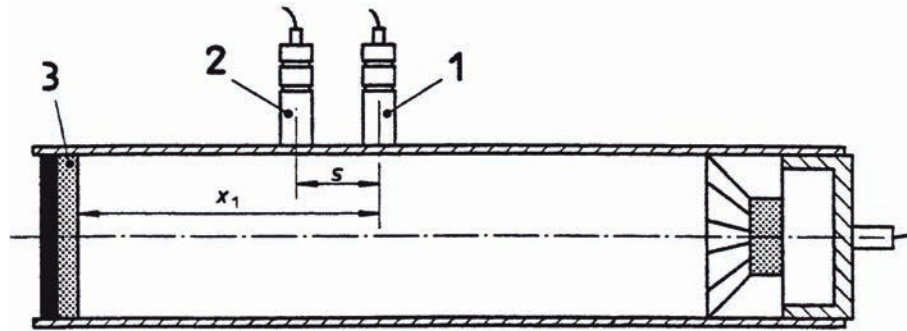
2.5.3 Microphones

It is compulsory to use two identical microphone types. They are mounted to the tube as illustrated in figure 2.6. Their capsules diameter should be smaller than $\frac{c_0}{f_u}$ and the capsules' diameters should be $< \frac{s}{5}$. When being mounted, the microphones' capsules need to be sealed within the microphone holder and flush with the inside of the impedance tube. It is important to check for leakages and while usually a small keyway is necessary to be able to mount the microphones in the first place, it should be kept as small and as contained as possible. (cf. ISO 10534-2:2001: 6-7)

2.5.4 Sample Holder

The sample holder may be either a separate unit, that can be attached to the tube or built right into the tube. If rectangular tubes are used the latter are recommended. Then, a cap

⁷ “[...dass der Mikrofonabstand] 5 % der Wellenlänge der interessierenden entsprechenden niedrigeren Frequenz beträgt.” [Original text]



legend

- 1 Microphone A at position 1
- 2 Microphone B at position 2
- 3 probe/specimen

Fig. 2.6: Drawing of the impedance tube (ISO 10534-2:2001: 7)

is used that can be attached and detached from the tube, sealing the sample holder so that no unwanted sound bypaths occur. Should the sample holder itself be detachable it needs to share the same properties as the rest of the tube. The structural parameters must be the same as the tubes with a 0.2 % tolerance. The attachment should be resulting in a flush, sealed experimental setup. To avoid small leakages and to seal all possible byways shut, the use of petroleum jelly or vaseline is recommended. No elastic seals of any kind should be used. The sample holder's back wall must be inflexible and attached firmly to the impedance tube. For most measurements, it is employed as a soundproof end of the tube from which the sound waves are reflected. There are, however, cases in which no soundproof closure is needed. Then an air volume is left behind the sample. The air layer between the probe and back wall then must have the length of $\frac{\lambda_0}{4}$ for the frequency under examination. For further information confer with ISO 10534-2:2001: 7-8.

2.5.5 Signal generation and processing

To successfully complete the measurement, a signal generator is needed that can produce a test signal with constant spectral density. The test signal may be either “a random, pseudo-random, periodic pseudo-random or chirp excitation”⁸ (ISO 10534-2:2001: 8). Usually, white noise is used. For calibration, an extra step needs to be taken. The generation of a discrete frequency and its visual representation and evaluation is necessary. The generated single frequency and measured frequency shall have an inaccuracy of less than $\pm 2\%$ (cf. ISO 10534-2:2001: 8).

⁸ “zufällige, pseudo-zufällige, periodische pseudo-zufällige oder Piep-Anregung” [Original text]

The signal processing unit must be able to work with two signals simultaneously and must be capable of performing Fast Fourier Transformation (FFT). The device is responsible for the computation of the transfer function H_{12} . “Its dynamic range should be greater than 65 dB. Errors in the transfer function estimation due to non-linearities, resolution, instability and temperature sensitivity of the signal processing equipment shall be less than 0.2 dB”⁹ (ISO 10534-2:2001: 8).

2.5.6 Loudspeaker

The loudspeaker, usually a membrane speaker, needs to be attached to the tube’s end. While “its surface should be at least two-thirds of the cross-sectional area of the impedance tube”¹⁰ it also needs to be fitted in a sound-absorbing housing to avoid airborne sound transmission byways to the microphones (ISO 10534-2:2001: 8). The loudspeaker must furthermore be elastically suspended to minimize sound transmissions through impedance tube resonances as far as possible (cf. ISO 10534-2:2001: 8).

As resonances of the air will always occur in a tube, they need to be suppressed. To accomplish that a sound-absorbent covering should be placed inside the impedance tube near the speaker. The sound-absorbent lining should have a length of at least 200 mm (cf. ISO 10534-2:2001: 8).

2.5.7 Temperature and air pressure

Both temperature and air pressure must be measured before and after each measurement using a thermometer and a barometer. The temperature must be kept steady during the measurement with a maximum tolerance of $\pm 1 K$ and the measuring inaccuracy of the thermometer has to be $\pm 0,5 K$ or better. Additionally, the maximum permissible deviation of the air pressure is $\pm 0,5 kPa$ (cf. ISO 10534-2:2001: 8).

2.5.8 Before the measurement

In order to be able to perform the impedance measurement following *EN ISO 10534-2*, a few preliminary steps need to be taken (cf. ISO 10534-2:2001: 9-12; ISO 10534-2:2007: 2):

⁹ “Der Dynamikbereich des Analysators sollte größer als 65 dB sein. Fehler in der geschätzten Übertragungsfunktion H_{12} infolge Nichtlinearitäten, Auflösung, Instabilität und Temperaturempfindlichkeit der Signalverarbeitungseinrichtung müssen kleiner als 0,2 dB sein.” [Original text]

¹⁰ “Die Oberfläche der Lautsprechermembrane muss mindestens zwei Drittel der Querschnittsfläche des Impedanzrohres abdecken.” [Original text]

Firstly the plane of reference $x = 0$ needs to be set. Its position is usually on the surface of the specimen. Should the probe have a rough surface x is to be set a little distant from the surface, keeping in mind that it needs to be compliant with the guidelines specified in 2.5.1.

Then the following values are being calculated after measuring the temperature and air pressure:

- The sound velocity in air dependent on the temperature T in Kelvin:

$$c_0 = 343,2 \cdot \sqrt{\frac{T}{293}} \frac{m}{s}. \quad (2.25)$$

- The air density D tributary to the measured temperature T (in K) and air pressure p_a (in kPa):

$$D = D_0 \cdot \frac{p_a \cdot T_0}{p_0 \cdot T} = 1,186 \frac{kg}{m^3} \cdot \frac{p_a \cdot 293 K}{101,325 kPa \cdot T}. \quad (2.26)$$

This process is being repeated after each measurement to be able to compare the values before and after the measurement for compliance with the requirements in 2.5.7.

When multiple microphones are used it is necessary to compensate for microphone maladjustments. This is usually being done by repetitive measurements with swapped channels. Both use the same principle of measuring and calculating the transfer function H_{12}^I for the microphones in their original position and H_{12}^{II} with their positions swapped. For both measurements, the probe needs to be in place. The transfer function H_{12} then can be calculated using

$$H_{12} = (H_{12}^I \cdot H_{12}^{II})^{\frac{1}{2}} = |H_{12}| e^{j\varphi}. \quad (2.27)$$

It is also possible to calculate a calibration factor using a calibration probe. This is especially useful when experimenting on a higher count of specimens. The formula for determination of the calibration factor is described in chapter 7.5.2 of ISO 10534-2:2001. The objective of both calibration methods is to equalize differences in frequency and phase response of both microphones, so their unique parameters do not falsify the results.

2.5.9 Performing Measurements in compliance with *EN ISO 10534-2*

The after listed information on the measurement procedure was gathered from the ISO standard and its corrigendum (cf. ISO 10534-2:2001: 10-14, 22-23 & ISO 10534-2:2007: 2).

Figure 2.6 visualizes the impedance tube with two microphones A and B in their relative positions x_1 and x_2 . These microphones measure the pressure gradients on the tube wall. When the loudspeaker plays back the random noise the microphones pick up the incident and reflected sound pressures.

The transfer function is defined by the pressure quotient of the pressures at the microphone positions x_1 and $x_2 = x_1 - s$. The pressure gradients $p_1(x_1)$ and $p_2(x_2)$ can be equated with (cf. Deter 2013: 19)

$$p_1 = e^{jkx_1} + \rho e^{-jkx_1} \quad (2.28)$$

$$p_2 = e^{jkx_2} + \rho e^{-jkx_2} = e^{jk(x_1-s)} + \rho e^{-jk(x_1-s)}. \quad (2.29)$$

Based on the above equations H_{12} can be equated

$$H_{12} = \frac{p_2}{p_1} = \frac{e^{jk(x_1-s)} + \rho e^{-jk(x_1-s)}}{e^{jkx_1} + \rho e^{-jkx_1}}. \quad (2.30)$$

Within ISO 10534-2:2001 and ISO 10534-2:2007 more possibilities of determining H_{12} have been presented :

$$H_{12} = \frac{S_{12}}{S_{11}} = \frac{S_{22}}{S_{21}} = |H_{12}| e^{j\varphi} = \left(\frac{S_{12}}{S_{11}} \cdot \frac{S_{22}}{S_{21}} \right)^{\frac{1}{2}}. \quad (2.31)$$

The reflection coefficient which is a complex value consisting of a real and an imaginary part $\rho = Re\{\rho\} + jIm\{\rho\}$ can be equated (cf. ISO 10534-2:2001: 13-14, 22-23 and ISO 10534-2:2007: 2):

$$\rho = \frac{H_{12} - e^{-jk_0s}}{e^{jk_0s} - H_{12}} \cdot e^{2jk_0x_1}. \quad (2.32)$$

This takes into account the complex wave number k , as first introduced in chapter 2.5. It is calculated using the formula $k_0 = k'_0 - jk''_0$, “where k'_0 is the real component ($k'_0 = \frac{2\pi}{\lambda_0}$); λ_0 is the wavelength; k''_0 is the imaginary component which is the attenuation constant, in nepers per metre” (ISO 10534-2:1998: 4). Using equation A.18 of ISO 10534-2:2001:18 to calculate $k''_0 = 1,94 \cdot 10^{-2} \sqrt{f}/c_0d$, where d is the tube’s inner diameter, the complex wave number’s formula reads:

$$k_0 = \frac{2\pi f}{c_0} - j \left(1,94 \cdot 10^{-2} \frac{\sqrt{f}}{c_0} \cdot d \right). \quad (2.33)$$

From the results of equation 2.32 it is easy to calculate the following values:

- The absorption coefficient α is equated as:

$$\alpha = 1 - |\rho|^2 = 1 - R^2, \quad (2.34)$$

- and the specific acoustic impedance Z_a :

$$Z_a = \frac{1 + \rho}{1 - \rho} \cdot Dc_0. \quad (2.35)$$

3 Application of the theory

Having established the theoretical basis for further observations, it is now appropriate to implement them. In the following chapters, the measurement system will be developed and evaluated first and then the measurement steps will be adapted and adopted.

3.1 The Measurement System

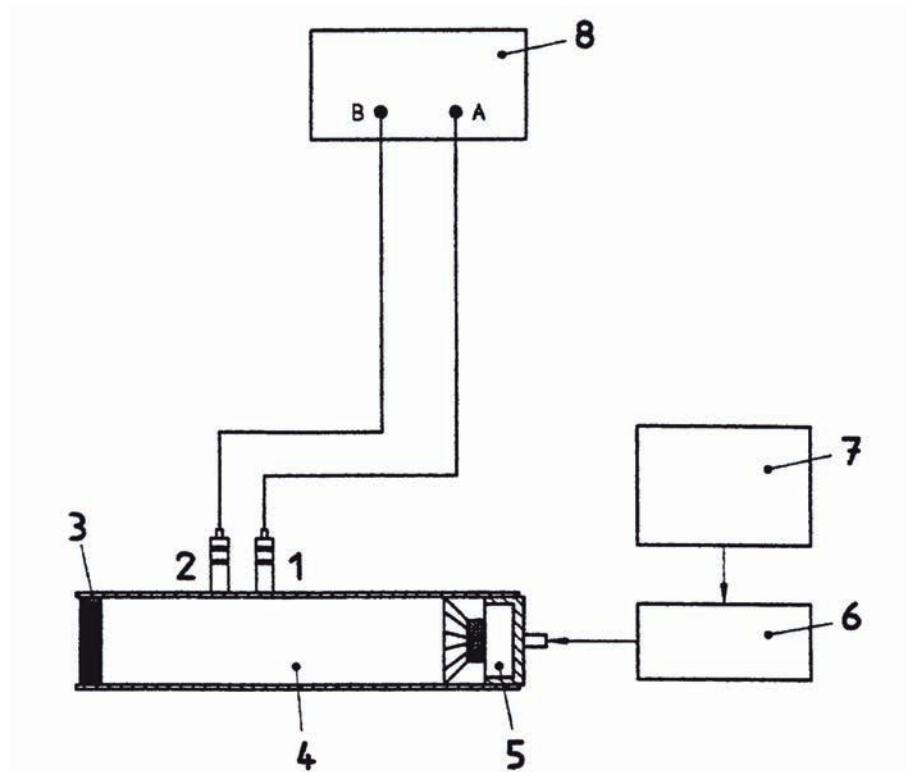
Subsequently, the measurement system itself will be developed. While full commercial systems, like the Brüel & Kjær Type 4206 (B&K 4206) or the AED AcoustiTube® exist, it is the objective of this thesis to build on their developments and enable a more accessible setup with more widely available commercial components to not be bound by proprietary solutions. Therefore, in the following subchapters, every component will be evaluated and improvements suggested in order to optimize and enable impedance measurements with individual pre-existing equipment. This is, in part, motivated by the often very high price of integrated systems, which may mean that not all interested individuals are able to actually have access to such a system, as well as the interest not to be dependent on predefined modules, but rather to be able to use components that are known and have been proven efficient in individual applications.

3.1.1 Design drawing

As shown in figure 3.1 the measurement system generally consists of eight components.

- The two microphones A and B, described under 3.1.3,
- the probe under investigation,
- the impedance tube, as per description in 3.1.2,
- the sound source/loudspeaker used for excitation and its amplifier outlined in 3.1.3,
- and the system for generation of the test signal, as well as analyzation of the measured microphone responses. As generation and analyzation are done in the digital domain and the speaker and microphones work in the analog domain, a device for signal conversion is necessary. These are being addressed in 3.1.4.

Whilst components one through six are necessarily needed separately as they are shown, components seven and eight can and will be unified in one “black box system” running on a computer. It is not contemporary to use multiple devices for these procedures nowadays, as any basic computer has enough computing power to process the measurement. It is additionally accompanied by the signal conversion unit.



- | | |
|------------------|-----------------------------|
| 1 microphone A | 5 sound source |
| 2 microphone B | 6 amplifier |
| 3 probe/specimen | 7 signal generator |
| 4 impedance tube | 8 frequency analyzer system |

Fig. 3.1: Design drawing of the impedance measurement system (ISO 10534-2:2001: 9)

3.1.2 The impedance tube

The heart-piece for the measurement is the impedance tube. It is also, with a high probability the component that is hardest to acquire. That leaves two main options to procure a pipe:

1. Using an existing or purchased impedance tube, or
2. building an own impedance tube.

While option 1 is the more expensive way, if a new impedance tube needs to be bought, it is also much easier and more convenient than option 2. When using an impedance tube, like the B&K 4206, the user does not need to be cautious to build and test an own tube in accordance to *EN ISO 10534*, as outlined in 2.5.1. All the engineering and testing has already been taken off the user's hands who can then start using it straight away. It minimizes the room for errors, as the industrial production process is optimized for maximum efficiency and is followed by extensive quality checks before being shipped out to the customer. Therefore this is the recommended procedure.

For the experimental setup used in this thesis option 1 has been chosen and a B&K 4206, as displayed in figure 3.2, will be used. As the tube is already owned, compliant with



Fig. 3.2: The Brüel & Kjær Type 4206 Impedance Tube (Brüel Kjaer 2019: 1)

standards *EN ISO 10534-2* and *ASTM E1050-12* and used around the world it is the obvious choice for this thesis. The following information about the dimensions and properties of the B&K 4206 has been adopted from Brüel Kjaer 2019.

As a component of a comprehensive commercial acoustic material examination and analysis unit, the B&K 4206 consists of:

- a large tube ($d = 100\text{ mm}$)
- a small tube ($d = 29\text{ mm}$)
- sample holders ($d = 29\text{ mm}$ and $d = 100\text{ mm}$)
- tube extensions ($d = 29\text{ mm}$ and $d = 100\text{ mm}$)

The exact dimensions can be found in figure 3.3. The tube can be assembled in “a large

	Inner Diameter mm (in)	Max. Sample Length mm (in)		
Small Meas. Tube	29 (1.1)	200 (7.9)	Small Tube (length)	1050 mm (41.3")*
Medium Meas. Tube	63.5 (2.5)	200 (7.9)	Medium Tube (length)	910 mm (36")
Large Meas. Tube	100 (3.9)	440 (17.4)	Large Tube (length)	900 mm (35.4")*
Small Sample Holder	29 (1.1)	200 (7.9)	TL Small Tube (length)	1280 mm (50.4")
Medium Sample Holder	63.5 (2.5)	200 (7.9)	TL Large Tube (length)	1370 mm (53.9")
Large Sample Holder	100 (3.9)	200 (7.9)	Total Width	140 mm (5.5")
Small Ext. Tubes	29 (1.1)	200 (7.9)	Total Height	240 mm (9.5")
Large Ext. Tubes	100 (3.9)	200 (7.9)		
Small TL Tube	29 (1.1)	190 (7.4)		
Large TL Tube	100 (3.9)	260 (10.2)		
Small TL Sample Holder	29 (1.1)	65 (2.9)		
Large TL Sample Holder	100 (3.9)	150 (5.9)		

* Add 200 mm for each extension tube used

(a) Tube dimensions

(b) Assembled tube dimensions

Fig. 3.3: Information on the dimensions of the B&K 4206 (Brüel Kjaer 2019: 6)

tube set-up to measure parameters in the frequency range from 50 Hz to 1.6 kHz and a

small tube set-up to measure parameters in the frequency range from 500 Hz to 6.4 kHz” (Bruel Kjaer 2019: 2).

The recesses for the sensors are designed for microphones with a capsule diameter of ¼”. The B&K 4206 has a loudspeaker built right in at one end of the tube. It is a 3.2” (81.28 mm) circular driver with $P_{maxRMS} = 10 W @ 4 \Omega$. Over a period of two seconds, it can withstand a peak in power of 50 W which is limited by a protection circuit to avoid accidental breakdown. On the input side of the loudspeaker, a frequency weighting unit is included. A choice between “High-pass, for high-frequency measurements in the small tube, Linear, for measurements in the large tube [, and] Low-pass, for extra measurement accuracy below 100 Hz” can be made right on the tube, making further settings within the software unnecessary (Bruel Kjaer 2019: 2).

3.1.3 Electroacoustic transducers

Microphones

The microphones are an integral part of the measurement process. As sensors, they are picking up the pressure gradients at their individual positions.

As the B&K 4206 is part of a complete measurement setup, of course, designated microphones are recommended. The standard setup of the Brüel & Kjær tube envisages ¼” condenser microphones of Type 4187. Obviously, these are the manufacturer’s own products.

In light of trying to design an easily accessible setup, one step is to swap out the original microphones for microphones that are already available and / or commercially available. Though, the B&K 4206 requires ¼” microphones it is important to first calculate which microphone types can be used before determining the specific microphones. For that reason, it is important to look back on the microphone requirements for compliance with *EN ISO 10534–2* as described in 2.5.3. The capsules maximum diameter can be equated as follows:

$$\frac{s}{5} > d_{capsule} < \frac{c_0}{f_u}. \quad (3.1)$$

When calculating $d_{capsule}$ in dependence on s , the smallest possible distance between the microphones needs to be taken into account. With the B&K 4206 large tube setup the distances s can measure 50 mm or 100 mm. When measuring with the small tube setup the distance s measures 25 mm. If you now assign this smallest value $s = 25 mm$ in the equation you can calculate

$$d_{capsule} < \frac{s}{5} = \frac{25 \text{ mm}}{5} = 5 \text{ mm}. \quad (3.2)$$

If also accounting for $c_0 = 343.2 \frac{m}{s}$ (sound velocity in air at 20 °C) and $f_u = 6.4 \text{ kHz}$ (the highest measurable frequency with the B&K 4206 small tube setup, cf. 3.1.2) the diameters can be calculated according to equation 3.1 as

$$d_{capsule} < \frac{c_0}{f_u} = \frac{343.2 \frac{m}{s}}{6400 \text{ Hz}} = 0.053625 \text{ m} = 5.3625 \text{ mm}. \quad (3.3)$$

The diameter of the microphone capsules needs to be smaller than the smallest value calculated in equations 3.2 and 3.3. Consequently, it is possible to conclude:

$$d_{capsule} < 5 \text{ mm}.$$

As capsule diameters are usually indicated using inches it can be converted to:

$$d_{capsule} < \frac{13''}{64} = 0.1968503937''.$$

The smallest usual capsule size for measuring microphones is $\frac{1}{4}$ ". This means that the capsule diameter is larger than the calculated diameter. However, since the capsule diameter is only about 1.35 mm larger than the calculated value, this is tolerable, as it should not or only slightly influence the results at high frequencies. Furthermore the formula provides a reference value and is not a strict requirement.

After having evaluated that $\frac{1}{4}$ " measurement microphones, while not optimal, are the best option for measurements in the impedance tube the microphones can be selected and defined. As it is the objective of this thesis to make measurements possible with any $\frac{1}{4}$ " pressure transducer condenser microphone two types of measurement microphones will be used for the thesis' experiments. Firstly, state-of-the-art microphones will be used. These are Microtech Gefell MK301E capsules on MV220 measuring microphone amplifiers, which were generously provided by the manufacturer from Gefell. Another set of microphones that will be used are the low-cost measurement microphones Superlux ECM-888B. In chapter 4 the two pairs of microphones will be directly compared and the measurement system tested for its ability to take the different microphone's characteristics in frequency and phase response out of the equation. It is the goal to achieve the same or similar results using a very well produced high-end microphone pair, like the Microtech Gefell MK301E, which has very well-documented and stable characteristics, and a cost-effective microphone, like the Superlux ECM-888B, which assumably has much worse characteristics and parameter stability. This is being done to create a much more accessible measurement option while not having to spend a lot of money on expensive state-of-the-art microphones.

Speaker

The speaker used for excitation of the air in the impedance tube should have at least the areal size of two-thirds of the cross-sectional area of the impedance tube, as stated previously in 2.5.6.

In the case of the B&K 4206, the loudspeaker is placed on one end of a tube with an inner diameter of 100 mm. Therefore the loudspeaker's diameter can be calculated using the following equation:

$$A_{speaker_{min}} = \frac{2}{3}A_{tube}. \quad (3.4)$$

The tube's area can be calculated from its diameter using the formula

$$A_{tube} = \frac{\pi d_{tube}^2}{4}. \quad (3.5)$$

To make the calculation process easier the speaker's area is also assumed as a flat surface, so the same formula to determine a circle's area value can be used. This can be done as the speaker's conical design makes its actual area value greater than that of a circle. As a minimal surface area needs to be calculated and it is better if the speaker's area value is as great as possible this does not pose an issue. Accordingly, the speaker's area can be equated with the speaker's diameter as follows:

$$A_{speaker_{min}} = \frac{\pi d_{speaker_{min}}^2}{4}. \quad (3.6)$$

If equations 3.5 and 3.6 are now substituted into equation 3.4 and rearranged for $d_{speaker}$, the following equation is obtained to calculate the minimum loudspeaker diameter:

$$d_{speaker_{min}} = \sqrt{\frac{2}{3}d_{tube}^2}. \quad (3.7)$$

The speaker diameter can therefore lie between $d_{speaker_{min}}$ and d_{tube} .

In the case of the B&K 4206 where $d_{tube} = 100 \text{ mm}$ the minimum speaker diameter can be equated as $d_{speaker_{min}} \approx 81.65 \text{ mm}$. As mentioned in 3.1.2, the built-in speaker of the B&K 4206 has a 3.2" (81.28 mm) circular driver. While it is theoretically 0.37 mm too small in diameter this value is so low it should not pose a problem, whatsoever. The bead of the loudspeaker should make up the difference.

To be able to use the B&K 4206 correctly it is compulsory to take a deeper look into the three operating modes which are changed via a filter and controlled with a poti. As

no sufficient documentation on the filter properties could be found, a measurement has been performed and documented in Appendix A to find out the influence of the respective poti positions. The “Linear” mode with the middle poti position does not filter the signal. “Low-Pass” mode uses a shelf filter with a decrease in amplitude of around 15 dB in the frequency range from 300 Hz to 800-1000 Hz. This mode is to be used for low-frequency measurements in the large tube. The third option, the “High-Pass” mode, performs a 6 dB/octave low-cut filtering with a cut-off frequency around 250 Hz. This mode is intended to be used for measurements with the small tube setup. A more profound and detailed examination of the filter characteristics, including graphical visualizations of the filter properties, can be found in appendix A.

Concomitantly with the loudspeaker, its amplification needs to be considered. To properly operate the speaker it must be run by a fitting power amplifier. It should be able to supply enough power to create a loud enough output, although without distorting the signal. The equipment piece used for the experiments of this thesis is a Wangine WPA-600PRO, a standard Hifi Stereo-Amplifier. This leveling must be performed manually by the user.

Another theoretical possibility for the output level adjustment, which could eliminate the human component through an automated method, involves a sound pressure limit method. The amplifier would be set to its maximum level.¹¹ Via a program (module) a test signal would be played back, iteratively increasing in volume. Via constant parallel evaluation of the signals, it could be determined exactly at which point the loudspeaker starts to distort. From this measured point, at which the system should no longer be operated, the signal volume can be lowered by, i.e. -6 dB , stored and used repeatedly as a gain factor for all signals reproduced during measurement. With this method, it could be ensured that the system is always operated below the overload limit, whilst maintaining a high volume and simplifying the process for the operator.

3.1.4 Processing Hardware

The hardware used for signal processing and analysis with the B&K 4206 is either the Multichannel Analysis System 3550 (cf. Bruel Kjaer 1995: 2), or a PC enabled system using an IEEE-488 interface and the application software BZ 5050 (cf. Bruel Kjaer 1995: 3). Both have since been updated but are still using proprietary hard- and software. This is not compatible with the objective of creating a system independent, open-source option. For that reason, the components for signal conversion and computing need to be rethought.

¹¹ Attention should be paid to the fact that the power amplifier has to be dimensioned for use with the driver. It must not be able to produce a multiple of the maximum input power of the driver in order to avoid possible destruction of the loudspeaker due to excessive amplitudes.

Signal Conversion D/A - A/D

As the measurement cannot stay only in either the analog or digital domain it is necessary to convert signals between the two domains. This does not seem like much anymore, as quality audio-interfaces have become widely available and affordable nowadays.

For the audio output, an instance of D/A-conversion is necessary. The mono signal containing the measurement's testing signals needs to be converted to an analog signal stream before being able to be amplified and played back.

Two mono A/D-conversions are necessary, as well. These are needed to convert the analog signal streams from the microphones to digital data streams to be able to be processed in the analyzer software on the computer.

This adds up to a total of three signal paths that need to be processed in real-time. This can be done using any basic modern audio interface with two or more inputs and one or more outputs.

Because operating systems need drivers to process audio in real-time, different audio drivers have established themselves as most used and therefore also widely supported by computer component and audio hardware manufacturers. For the different operating systems they can be narrowed down to ASIO (Audio Stream Input/Output) on Windows, Core Audio on Mac OS, and JACK on Linux Unix Systems. They all enable audio processing on a deeper operating system level software usually can not run at, therefore setting the basis for sophisticated audio processing, including real-time audio. As most users of audio equipment work on Windows and Mac OS platforms, manufacturers usually choose to support ASIO and Core Audio drivers and shipping out modifications tailored to the equipment piece's needs with the product. Unfortunately, support for Unix-based Linux systems is oftentimes not natively enabled. Therefore, the Linux platforms are not going to be further considered, as it is not as easily possible to make all components run on those systems, subsequently possibly causing multiple errors. As this thesis is rather a proof of concept than a fully developed, stand-alone program/system, it is not the purport of the paper. To be able to support all operating systems, an extensive development process would need to follow.

ASIO is a driver or rather transfer protocol, developed by pro-audio manufacturer Steinberg, to vastly expand a computer's native audio processing capabilities. While most soundcards natively only support two channels in either input and output directions, audio professionals and consumers oftentimes need much higher channel count capabilities. The protocol has quickly rooted itself in standard manufacturing with almost every hardware and software manufacturer supporting and providing ASIO drivers. Over the years, ASIO capabilities have far advanced improving performance and reducing laten-

cies rapidly. Today, it enables even the most basic CPUs to be able to perform multitrack audio processing in real-time with minimal latency.

While ASIO runs on most platforms, Apple has developed its own counterpart running even smoother on Mac devices. “Core Audio is tightly integrated into iOS and OS X for high performance and low latency. In OS X, the majority of Core Audio services are layered on top of the Hardware Abstraction Layer (HAL) [...]. Audio signals pass to and from hardware through the HAL. You can access the HAL using Audio Hardware Services in the Core Audio framework when you require real-time audio” (Apple 2017).

The biggest impediment when converting the signals and trying to work in real-time is latency. While a digital system’s latency depends on various factors including CPU capabilities, CPU load, and up-to-date drivers an important factor is the Buffer or Frame Size. During the conversion process, an analog signal’s amplitude is being sampled at a fixed speed, called the sampling rate. Each sample needs to be scanned individually. When working with the audio in real-time, blocks of audio are processed at any given time. The size of these data blocks is set by the Buffer Size. Latencies are incurred, as each block needs to be processed first before being able to be passed on to further processing. A system’s latency (in seconds) can easily be calculated if sampling rate fs (in Hz) and buffer size $bufferSize$ (in samples) are known:

$$latency = \frac{bufferSize}{fs}. \quad (3.8)$$

Using this formula it can be concluded that the latency declines as the buffer size decreases.

As the buffer size is a value the user can set manually, using a modern audio interface running either ASIO or Core Audio drivers, it enables the utilization of these interfaces for acoustic measurements in the impedance tube. Because most audio interfaces also can amplify a signal and provide phantom power, if needed, they render a separate microphone pre-amplifier unnecessary. Higher quality audio interfaces have become very affordable and commercially wide available, also, making individual components and setups possible. Therefore, the original proprietary solution provided by Brüel & Kjær is not necessarily needed anymore. For the thesis, a Tascam US 16x08 audio interface will be used.

Computing unit

The choice of computer, doing the actual data processing, should be free. Depending on the software that is run, as described in chapter 3.1.5, the user should be able to choose

whichever system they feel most comfortable with or have available. As the software developed and used in this thesis is a Matlab script, the choice is narrowed down to any computer capable of running the Matlab host software. For the subsequent observations, a MacBook Pro 2018 running OS X is selected as the computing unit for this thesis, due to availability.

3.1.5 Software

As integral to the observations of impedance measuring as the tube and microphones were, so is the software processing and evaluating the data. A complete overview of the software created for this purpose and its modules can be found in appendix chapter B. The applied methods used within the program modules will be described in the subsequent chapters.

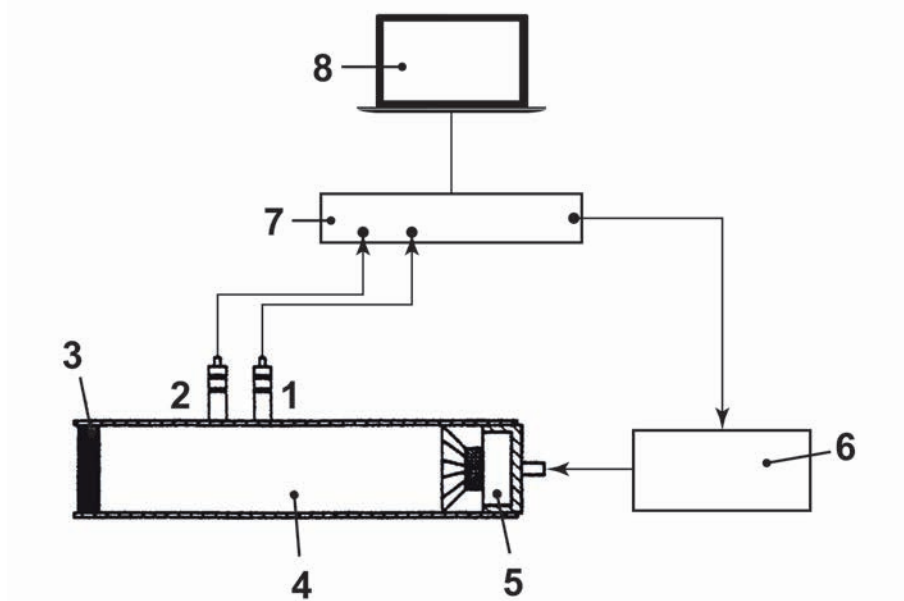
The principal tasks of the software consist of:

- The signal generator, creating the needed test signals,
- modules for signal transmission accessing and controlling the signal conversion unit,
- the analysis unit, that evaluates and further processes the signals, at the end of which the searched-for results are displayed,
- and a module for the compilation of the test protocol.

As mentioned before, the software has been created using the host software Matlab, using built-in functionalities, as well as code by Dr. Roland Kruse of the University of Oldenburg and the ITA-Toolbox of the Institute of Technical Acoustics of the RWTH Aachen (cf. Berzborn et al. 2017).

3.1.6 Subsumption of the individual setup used in this thesis

As elaborated in the previous chapters, the following setup, illustrated in figure 3.4, is used for the successive measurements of this bachelor thesis.



legend

1 Microphone A Microtech Gefell MK301E Superlux ECM-888B	5 loudspeaker B&K 4206 built-in speaker
2 Microphone B Microtech Gefell MK301E Superlux ECM-888B	6 power amplifier Wangine WPA-600PRO
3 probe/specimen	7 audio interface Tascam US 16x08
4 impedance tube Brüel & Kjær Type 4206	8 computing unit MacBook Pro 2018 running Matlab 2018b

Fig. 3.4: Individual setup for measuring acoustical impedance

3.2 Determination of the transfer function

As already outlined in chapter 2.5.9, the transfer function can be determined by relating the pressure gradients at the microphones as shown in equation 2.30.

For the practical application, this means that a transfer function needs to be calculated from the recorded signals of the microphones. To accomplish that Matlab has a built-in function that takes most of the work off of the programmer's hands. Using `tfestimate`, Matlab "finds a transfer function estimate, `txy`, given an input signal, `x`, and an output signal, `y`" (MathWorks; `tfestimate` n.d.):

$$[TF_norm, xsNorm] = tfestimate(ref_channelNorm, sig_channelNorm, [], [], nfft, fs) \quad (3.9)$$

This function, as exemplarily taken from the calibration-script of the Matlab-Code, returns the estimated transfer function `TF_norm` and the frequencies `xsNorm`, at which the transfer function has been estimated. Input values to the function are the microphone signals `ref_channel` (channel 1) and `sig_channel` (channel 2), as well as the number of DFT points `nfft` and the sampling rate `fs`.

Inside the Matlab `ImpedanceMeasurement` program, `tfestimate` is used within two modules for a total of three times: twice in the calibration module

```
ImpedanceMeasurement_Calibration
```

and once in the measurement module

```
ImpedanceMeasurement_Measurement.
```

3.3 Calibrating the system

Before being able to perform the actual measurement process itself the system requires calibration, both to be able to produce accurate and conclusive results as well as being compliant with the requirements of *EN ISO 10534-2*. This can be organized into three calibration sub-modules. The entire calibration and measurement processes should be performed for each probe/specimen individually.

3.3.1 Calibration of speaker and microphone levels

The first step of calibration is to set the levels of all input and output devices, which is being done in the module

```
ImpedanceMeasurement_levelCalibration.mlapp.
```

First up, the output volume needs to be set. To allow for that to happen, the user can play back a signal from the output by pushing the corresponding button in the program. Then the signal is produced and the user can set the optimal volume manually on the amplifying device.

After this process has been completed, the second part is unlocked. This is to set the input gain levels of the microphones. When pushing the corresponding button another signal is being played back within the impedance tube. A graphical display then shows the input levels numerically and visually, for the user to set the microphones' gain levels to an adequate amount and adjust for equality. Only if the microphones' signal volumes

are within the tolerance boundary of ± 0.3 dB, as required by the ISO standard, the user can complete the setup process and move on to the next calibration step.

Ideally, this last step of calibrating the input levels would be done using a pistonphone. In service of ease-of-use and accessibility, this has been adapted to be done within the impedance tube setup using the tube's speaker. The same results should be attained.

3.3.2 Tube component calibration

As evaluated in chapter 2.5.5, the tube's signal transmission equipment needs to be tested for accuracy. For that purpose the module

```
ImpedanceMeasurement_Calibration_tubeCalibration
```

has been created. From the module's figure

```
ImpedanceMeasurement_Calibration_tubeCalibrationFigure.mlapp
```

the calibration process is started with the push of a button. Then a pure sine signal is being generated, played back in the tube and recorded by the microphones. The recorded signal is then being examined for the frequency of its loudest recorded signal using FFT. As only the sine signal is being played back and not much noise should be able to get into the tube it should be the loudest part of the signal. If the recorded frequency matches the originally generated frequency within a tolerance of ± 2 % the components can be assumed intact and working. Therefore the user can then continue to the last calibration component - the frequency and phase calibration of the microphones.

3.3.3 System calibration using the sensor-switching-method

In order to be able to compensate for distortions of the measurement results by the differences in the microphones' levels, amplitude frequency responses and phase frequency responses this third and arguably most important step of the calibration process is necessary.

Using the module

`ImpedanceMeasurement_Calibration`

a function to calibrate the two microphones using the sensor-switching-method is called. It consists of four steps that need to be taken before being able to move on to the measurement itself. A specimen or a calibration probe must already be in place during this step. However, this shall not be the specimen under investigation but ideally a special calibration sample.

In the beginning, the user must choose which kind of tube setup will be used. The choices are the large or small impedance tube setups.

Once the choice for the tube setup has been made the user can move on to the first calibration recording. While it is possible to begin with either the calibration in the switched or normal positions, it is advisable to begin with the step where the microphone positions have been switched, so the microphones will only need to be switched in their places once. This starts a process to produce the first transfer function. During this process, a random noise signal is being played back in the impedance tube. The microphones then pick up the pressure gradients and for each microphone, an audio channel is being recorded. Using the function `tfestimate`, as described in chapter 3.2, the transfer function for the inverse microphone position `TF_inv` is estimated and saved.

After this step has been completed the microphones need to be switched in their positions and the same process repeated using the second button. This produces the transfer function for the microphones in their normal positions `TF_norm`.

Once both transfer functions have been estimated the calibration factor `H` is calculated using

$$H = \text{sqrt}(\text{TF_norm./TF_inv}) \quad (3.10)$$

and graphically displayed. The equation obtains the square root value of the point-wise division of the previously determined transfer functions, as determined previously in equation 2.27. The calibration factor `H` can then later on, during the measurement process, be loaded in to compensate for the actual measurement's transfer function and enables the correct computation and presentation of the analysis results. It is important to note that `H` is returned as a vector with the calibration factors for each frequency specified within `xs`.

It is therefore important to keep in mind that when referring to the calibration factor in the following, a dataset of calibration factors at certain fixed frequencies is being referred to. Following this step the user can and needs to save the calibration to a file, so it can be used in the measurement process which the user can initiate after successful calibration file export.

3.4 Determination of acoustic parameters

As soon as the system is fully calibrated the actual measurement can be performed. For this purpose, the module `ImpedanceMeasurement_Measurement` has been made available. At this point, the specimen under investigation should be introduced to the tube testing environment.

Once the measurement's transfer function `TFMeas` has been estimated, again using `tfestimate`, as previously utilized during the calibration steps, the looked-for parameters can be calculated using the measurement's transfer function `TF`. The following code snippets have been taken from the above-mentioned script which is largely based on the code of Dr. Kruse (cf. Kruse 2006).

First, the error compensation using the calibration factor `H` is being done, in order to return a conclusive transfer function `TF`:

$$TF = TFMeas./H \quad (3.11)$$

Then the reflection coefficient is being calculated using the following formulas that have been derived from equation 2.32.

For this step it is necessary to adopt the wave number formula as presented in equation 2.33 as

$$k = (2 * pi * xs) ./ soundVelocity - 1j * 1.94e - 2 * sqrt(xs) ./ (soundVelocity * tubeDiameter) \quad (3.12)$$

The equation includes the information about the frequencies the transfer function has been estimated at `xs`, the velocity of sound `soundVelocity`, and the tube's inner diameter `tubeDiameter`. `k` is a factor necessary to calculate the phase shift φ by individually

multiplying k with micDistance and $(\text{micDistance} + \text{probeToMicDistance})$, respectively.

$$R = ((TF - \exp(-1j * k * \text{micDistance})) ./ (\exp(1j * k * \text{micDistance}) - TF)) .* \exp(2 * 1j * k * (\text{micDistance} + \text{probeToMicDistance})) \quad (3.13)$$

From the values of R the acoustical impedance Z can easily be calculated, according to equation 2.35:

$$Z = ((1 + R) ./ (1 - R)) \quad (3.14)$$

Equation 2.35 contains a multiplication step with Dc_0 . This would additionally multiply the characteristic impedance of the medium Z_c with equation 3.14. During testing of the developed Matlab code, both variations with and without this multiplication step have been tested. As the characteristic impedance is a static value it affects all values in the frequency domain to the same extent. This could be noticed as the scaling of the y-axis containing the impedance values changed drastically. The re-scale on the y-axis makes the values more difficult to interpret. For this reason, the pragmatic decision was incidental to omit multiplication and work with the more interpretable values for impedance in the graphical representation of the results. The value calculated with equation 3.14 in Matlab therefore represents the normalized acoustic impedance instead of the specific acoustic impedance.

The value α , as shown in equation 2.34, can just as easily be derived:

$$\alpha = 1 - (\text{abs}(R).^2) \quad (3.15)$$

These parameters then can be plotted for visualization and later on be used during the preparation of the test protocol. For usage with the latter, an additional step is taken smoothing the absorption coefficient α by a $\frac{1}{n}$ octave smoothing unit. The user determines the smoothing bandwidth from which n is being extracted as variable `smooth`. The

smoothing process is being performed by the `smoothSpectrum` function of the IOSR-Toolbox returning the value `absorptionSmooth`:

$$\text{absorptionSmooth} = \text{smoothSpectrum}(\alpha, \text{xs}, \text{smooth}) \quad (3.16)$$

The calculated vector variable is subsequently used for determining the $\frac{1}{3}$ octave band values printed on the measurement protocol and as input data for the figure graphically displaying the results on said protocol.

3.5 Retrieval of important data for evaluation

As needed for the evaluation process and preparation of the test protocol, some data must be queried by the user. This includes some information that is immediately used for further computational processes, as well as raw information that will later appear on the test protocol. The requested information, being asked for by pop-up GUIs within the measurement module, includes:

- language - a choice can be made between German and English,
- the experimentation date, location and testing station,
- the name of the tester performing the experiment,
- probe name, description, and thickness,
- number of repetitions the measurement should perform - values between 1 and 6 times,
- the choice, whether multiple repetitions should be averaged during evaluation over samples or repetition count,
- information about the sound source, sound card, microphones and microphone preamp,
- temperature, air pressure, humidity,
- distance between the microphones and the distance of the microphones to the specimen.

3.6 Error analysis for measurements in the impedance tube

As with any experiment in the field of physics, although the tester always tries to avoid all possible causes of error and constant innovation steadily improves technical equipment, the impedance measurement is still subject to errors. Generally, the error analysis is divided into three categories: systematic errors, random errors, and gross errors. For this evaluation another category is introduced: preparatory and preconception errors.

The following observations and elements of the error analysis were collated from the research work of Mr. Brunnader (cf. Brunnader 2002: 28-32), Mr. Deter (cf. Deter 2013: 66), Seybert and Soekarno (cf. Seybert; Soenarko 1981: 1190-1198), as well as Hans Bodén and Mats Åbom (cf. Boden; Abom 1986: 543-549), of course taking into consideration the error analysis provided within the applied ISO standard, itself (cf. ISO 10534-2:2001: 23-24).

3.6.1 Systematic errors

“The systematic errors predominantly comprise the errors that may occur during the measurement or its analysis or post-processing”¹² (ISO 10534-2:2001: 23). They occur mainly in the engineering process of the system and have been minimized to a large extent by the manufacturer (cf. Brunnader 2002: 28).

Most systematic errors can be attributed to the tube geometry. Therefore, the impedance tube’s length should not exceed a value of 5-10 times the inner tube diameter, otherwise an unnecessarily high proportion of dissipation must be expected during wave propagation (cf. Brunnader 2002: 28). Another length value that might cause grave errors is the distance between the microphones s . When measuring all distance values in millimeters an accuracy of $\pm 0.5\text{ mm}$ can be assumed. As this theoretical value is exceeded quickly in the field the distance between the two microphones should be $s > 50\text{ mm}$ for large tube measurements. This allows for the relative corresponding error of to be $s_{error} < 1\%$ (cf. Boden; Abom 1986: 548). Furthermore, it is hard to delineate the precise location of the cross-sectional area the acoustic impedance shall be measured at (cf. Boden; Abom 1986: 545). When observing the tube’s geometry it is crucial to note that both, the first and the second part of the tube show resonance frequencies. As very small tolerances during the fabrication process cause a minuscule alteration on the tube’s inner surface which then, in turn, may influence the sound-wave propagation (cf. Deter 2013: 66).

The design of the impedance tube introduces a few more sources of error. Not only is it not possible to accurately place the microphones as sensors flush with the tube’s inner

¹² “Systematische Fehler beinhalten mögliche Fehler entweder durch die Messung oder die Analyse [...]” [Original text]

surface, due to the microphone holders and their drill holes, but the probe holder can be the cause of a jumping point. This is caused by the edges of the holder, where it closes off with the wall and may result in diffraction and reflection phenomena (cf. Deter 2013: 66).

Furthermore, the tube mount influences the resonance curve of the tube. This support can therefore influence and change the structure-borne sound vibrations, which cannot be completely avoided. The tube end and sample holder with their rigid properties and in most cases metallic composition can also transmit structure-borne sound between parts of the tube. The inner wall of the duct is also not completely sound-reflecting and therefore allows for some transmission and structure-borne sound excitation (cf. Deter 2013: 66). Thus it is necessary to further counteract the transmission of structure-borne and transmitted interference sound (cf. Brunnader 2002: 29).

To perform a conclusive measurement it is not necessary to have more than the incident and reflected sound waves within the tube. To avoid multiple reflections and therefore a change of the sound field within the tube, the sound source should have non-reflective properties (cf. Brunnader 2002: 28).

Due to the geometry of the used tube not always being entirely reconcilable with the requirements of the standard, a few minor adjustments may need to be made in terms of the microphones' and probe's placement (cf. Deter 2013: 66).

For the formation of the power density spectra a narrow band frequency analysis method, i.e. FFT, should be applied. The minimum frequency resolution should be $\geq 3 \frac{\text{points}}{\text{Hz}}$ (cf. Brunnader 2002: 29).

Another systematic error lies within time distorted sampling errors. Therefore, the duration of each recording pass should be equal to or greater than the length of the impulse response of the system. If not, falsifications due to crosstalk during signal processing are possible (cf. ISO 10534-2:2001: 23).

The errors due to maladjustments of amplitude or phase response of the microphones in use are being compensated by the calibration process. The calibration factor produced during this process counteracts errors in phase and amplitude of the measurement system (cf. ISO 10534-2:2001: 23-24, Brunnader 2002: 29).

Lastly, errors due to faulty programming in the evaluation system can be categorized as both systematic and preconception errors.

3.6.2 Random errors

The contingent of the only partially avoidable random errors occurs during the measurement of the material parameters (cf. Brunnader 2002: 30).

First, random errors are introduced by an insufficient signal to noise ratio and the test signal (white noise) itself. As the test signal has a random amplitude and phase response it is unpredictable and may falsify the results (cf. Brunnader 2002: 30). Generally, disruptive sources of noise should be kept at a minimum (cf. Boden; Abom 1986: 548).

“In order to keep the random error small, we must have a high coherence between the microphones” (Boden; Abom 1986: 545). This means that the smaller the microphone spacing s , the higher the coherence of the microphones. If the spacing is too small the system breaks down causing even more errors (cf. Boden; Abom 1986: 545). However, this negatively affects the sensitivity of the measuring system in the low-frequency range, where the accuracy is then lowered as a result (cf. Brunnader 2002: 30).

By asserting a high coherence between the loudspeaker and the overall pressure in the tube the random error is also kept small. This can be accomplished through the previously described minimization of noise disruption and the usage of smaller microphone spacing (cf. Seybert; Soenarko 1981: 1197).

Random errors can further be minimized through an averaging process of multiple spectra datasets. As the ISO standard recommends the minimum number of datasets to be calculated using the following formula, “where n is the the number of averaged independent (non-overlapping) spectra and σ is the standard error”¹³ (ISO 10534-2:2001: 24):

$$n = \left(\frac{1}{2\sigma} \right)^2 \quad (3.17)$$

To get beneath a wanted threshold of $\sigma \leq 0.1$, formula 3.17 equates to $n \geq 25$ (cf. ISO 10534-2:2001: 24, Brunnader 2002: 30).

If the value of the product of the frequency bandwidth and the total averaging time returns equated for a number between 50 and 100, the random errors are usually held to a minimum, too (cf. ISO 10534-2:2001: 24).

“The constraints mentioned above are not normally severe and can usually be accommodated” (Seybert; Soenarko 1981: 1197).

3.6.3 Gross errors

The gross errors include general errors and avoidable mistakes of the tester.

These errors include, but are not limited to, incorrect or negligent readings, the use of unsuitable measurement or evaluation procedures and equipment, and significant external perturbations.

¹³ “Dabei ist n die Anzahl der gemittelten unabhängigen (sich nicht überschneidenden) Spektren; σ der Standardfehler.” [Original text]

To counteract these errors, only careful monitoring and inspections during the measurement process, as well as critical reflection on the results obtained, can help. Gross errors can usually be avoided and a measurement should therefore not contain any gross errors in the measurement uncertainties.

3.6.4 Preparatory and preconception errors

This last category of errors can be traced back to the faulty installation of the probes and errors during preconception, also called bias errors.

To avoid the preparatory errors it is crucial to thoroughly prepare the test specimen. Therefore the diameters of the tube and probe need to match. The probe's surface should also be as plane and even as possible. Heavily structured surface textures may cause irregular wavefronts to form which then in turn can falsify the measurement results. Also, only specimens can be experimented on, whose mode of action is not altered by cutting out a sample. This limits the selection of probes mostly to porous absorber materials (cf. Brunnader 2002: 30).

To avoid or at least minimize the error of inadequate spectral resolution, “the overall length of the duct (L) should be kept small, in practice (say) $L \simeq 5 - 10$ duct diameters; the source end of the duct should be as non-reflective ($\xi_i \approx 1$) as possible; and microphone 1 should be placed as close as possible to the duct end (the sample)” (Boden; Abom 1986: 548).

The microphone closest to the specimen should also be as close to this probe as possible. The minimum distance between the microphone and probe should be equal or greater than 10 mm (cf. Brunnader 2002: 29). As Seybert and Soekarno point out “the bias errors can be reduced [...] by selecting a small analysis bandwidth” (Seybert; Soenarko 1981: 1197).

4 Examination of the phase response of different measurement microphone pairs

Of particular importance for the measurement and observation of acoustic parameters is the phase frequency response of the microphones used for measurement. Especially for the impedance wave separation method, apart from more evident errors due to different amplitude frequency responses¹⁴, the different phase responses of the microphones can be principal sources of error. The following chapter therefore focuses in more detail on the importance of phase compensation and its effects on the measurement results.

4.1 Importance of phase information for the 2-microphone method

To be able to conduct an experiment about phase and its importance it is necessary to define the term first.

The phase shift φ describes how the phase-angle of a signal is changed or affected between input and output. When observing microphones, the phase of the original acoustic signal and the electrical signal converted by the microphone are considered.

The phase influences the delay time Δt of a signal passing through the system depending on the frequency. As a delay in the output from the input can be assumed, the phase angle is negative. It should be noted that due to the periodicity of sinusoidal oscillations, $-180^\circ = +180^\circ$ applies, *e.g.* $-90^\circ = +240^\circ$.

A linear shift of the phase response can be spoken of when the delay time Δt is the same for all frequencies. If this is not the case and frequencies with different delay times pass through the system, it is referred to as dispersion. In that case, phase distortions can occur, causing the waveform to appear different at the output from the waveform at the input. Lerch, Sessler, and Wolf illustrate the effect of distortion using an impulse: “The pulse widens temporally on the transmission path, i.e. it diverges in time and is thereby deformed”¹⁵ (Lerch et al. 2009: 186), as visualized in figure 4.1 with the black-box transmission system at the top being non-dispersive and the system below causing dispersion.

¹⁴ The errors due to differences in amplitude frequency response are usually kept to a minimum due to the microphones in use. 1/4” measurement microphones are typically used which, ideally, have a flat amplitude frequency response. Therefore only minor deviations between two microphones of the same model should occur, especially if a matched pair is used.

¹⁵ “[... ,] dass sich der Puls auf dem Übertragungsweg zeitlich verbreitert, d. h. er läuft zeitlich auseinander und wird dabei verformt.” [Original text]

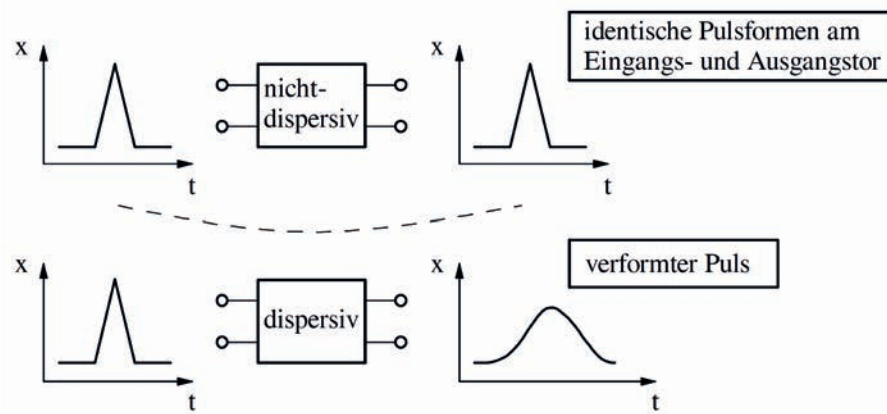


Fig. 4.1: Dispersion in transmission systems (Lerch et al. 2009: 186)

They furthermore point out that in a tube on the occurrence of dispersion a “frequency dependence exists and with regard to the propagation velocity of the wave, a distinction must be made between phase velocity c_p and group velocity c_g ”¹⁶ (Lerch et al. 2009: 187-188):

$$c_p = \frac{\omega}{k_x} = \frac{c}{\sqrt{1 - \left(\frac{f_{m(n)}}{f}\right)^2}}, \quad (4.1)$$

$$c_g = \frac{d\omega}{dk_x} = c \sqrt{1 - \left(\frac{f_{m(n)}}{f}\right)^2}. \quad (4.2)$$

The context can also be formulated as:

$$c_p c_g = c^2 = \frac{p_0}{D_0} \cdot \kappa. \quad (4.3)$$

It is also important to recall that the particle velocity can also be calculated with respect to the phase:

$$v = v_0 \cdot \cos(\omega t + \varphi). \quad (4.4)$$

As described above, the phase has a large impact on time and is, therefore, necessary to be observed when capturing time-relevant signals. In the impedance tube wave-separation method the incident and returning wavefronts are evaluated based on their relative positions to each other and to the specimen, as reflected for instance in equations 2.31 and

¹⁶ “[Im dispersiven Fall hingegen] existiert diese Frequenzabhängigkeit und man muss bezüglich der Ausbreitungsgeschwindigkeit der Welle zwischen *Phasengeschwindigkeit* c_p und *Gruppengeschwindigkeit* c_g unterscheiden.” [Original text]

2.32. Therefore, it is important to be aware of possible distortions due to different phase responses of the used microphones. Possible phase differences could then result in temporal deferrals or even cancellation effects, which in turn could lead to great errors in the measurement's evaluation calculations.

4.2 Taking differences in phase alignment out of the equation

Building on the theoretical framework of phase in signal processing and the methods used by the wave separation method, it is of great importance to compensate for different phase responses. Very different phase responses should, in theory, lead to strong distortions of the result.

To counteract this, as standardized in *EN ISO 10534-2*, the sensor-switching method is used to compensate for differences in amplitude frequency response and phase frequency response and render the measurement results conclusive.

On closer consideration, this method would not be necessary if the two microphones in use had an identical or insignificantly different phase response. If the amplitude frequency responses are also identical and the microphone input levels can be perfectly adjusted to the same value, then the results should be the same without a calibration process as if the measurement had been performed using sensor-switching calibration. To be able to assess whether this is the case, it is of paramount importance to have the amplitude frequency response and phase frequency response data of both microphones available for comparison and evaluation.

It would also theoretically be possible to achieve this compensation employing calibration data for the individual microphones. If the amplitude frequency responses and phase differences between the microphones are known, a correction curve could be applied to both and only the input volume setting would be required. However, this is difficult to implement, as most measurement microphones are provided with amplitude frequency responses from the manufacturer for the respective serial numbers, but not with phase frequency responses or comparative curves of both phase frequency responses. The effort to produce these measurements and to convert them into calibration data is not proportionate to the benefit of these measurements if they can be substituted or rendered void, as the sensor-switching method can be used without much additional effort.

4.3 Testing the theory

To evaluate if the above-mentioned theory is right and different phase responses distort the result, the following experiment is proposed.

Using the experimental setup described in chapter 4.3.1, two different measurements will be performed.

Firstly the different phase responses of the microphones will be measured to be able to estimate the probable results of the impedance measurement in the second experiment. This is of great importance to be able to draw comparisons, as the phase must always be observed with relativity (e.g. with regard to the object in question). Thus it would not be feasible to seriously compare measurements from different laboratories. More conclusive and comparable results are obtained from measurements in the identical situation and on the same object.

The second experiment will then be subdivided into two parts, using different microphone combinations:

1. Performing the impedance measurement without any calibration and therefore no compensation applied,
2. and performing the same measurement, using the same microphone combinations applying the calibration, and compensating for phase differences.

This will illustrate the true significance of the phase for conclusive results and justify the calibration process. Furthermore, it will also be used for evaluating whether two identical microphones can, in fact, effectively be used without the calibration process as proposed earlier.

As mentioned before in chapter 3.1.3, two different pairs of microphones will be used to exemplify the effects of different microphones, their respective phase responses, and manufacturing qualities. These are:

1. Microtech Gefell MK301E capsules on MV220 measuring microphone amplifiers, the manufacturer from Gefell generously provided. The microphone capsules are a matched pair with serial numbers 0556 and 0557. The measurement data provided by Microtech Gefell can be found in appendix C.1. Both microphones, as expected of high-end products like these, are almost a perfect match in frequency and phase responses, at least in the frequency range that is being evaluated topping off at 6.4 kHz. The greatest phase disparity only measures 0.372° at 6.3 kHz which is so low it should not cause much of a difference in the results when measuring with or without prior calibration.

2. Two Superlux ECM-888B with serial numbers E888B5A0528 and E888B5A0530 represent the second pair used in this exemplary comparison. The microphones' specifications can be found in appendix C.2. As the microphones represent products from the low-cost category they are expected to have much more different amplitude and phase frequency responses when directly compared to one another. As they are "cost-effective" only an averaged curve for the amplitude frequency response is available and the precise data traces for each microphone must be determined.

4.3.1 Experimental setup

Both parts of the experiment will be performed in the impedance tube.

Phase frequency response measurement

For the first experiment of measuring all microphones' phase frequency responses, the tube will be set up as follows. This is to be able to compare them and make an educated prediction on how they might affect the second measurement.

To get as much direct signal as possible of the loudspeaker in the B&K 4206 impedance tube the extension for the small tube setup is being placed at the end of the large tube. This is done because of the large absorbent cushioning around the small tube part that is being inserted to the large tube so that during small tube measurements no unwanted reflections and distortions can appear in the large tube affecting the small tube measurement. Another highly absorbent sample is placed in the small tube for as few as possible reflections to be thrown back into the large tube. This probe is a sample of Cellofoam CELLO[®] 521. Each microphone is then placed in the large tube's second or middle microphone position. Subsequently, using the software Room EQ Wizard, a sweep is being played back in the tube and then processed as impulse response (IR). Within the software itself, the measurements may provide information on both amplitude frequency response and phase frequency response of each microphone which can then be evaluated and graphically compared. This method, although not optimal for the measurement of phase responses, is capable of providing the desired comparisons between microphones. In the spirit of this thesis, to get the desired measurement results in an uncomplicated way and to extract the procedures from the laboratory environment, this target-oriented, pragmatic method is proposed and subsequently used. Due to the imperfect conditions for this measurement in the impedance tube, mainly due to the tube's geometry and the loudspeaker not being designed for the reproduction of that signal over the entire frequency range, the measured curves will probably appear as very dynamic graphs. Nonetheless, these will be easily graphically comparable.

Impedance measurement using different microphone pairs with and without using the calibration process

The main measurement consists of measuring the acoustic impedance with different microphone combinations.

In the small tube, a 20 mm thick probe of Cellofoam CELLO[®] 521 is being placed in the sample holder. This material was chosen because of its availability and absorption data specified on its datasheet¹⁷. The 20 mm thick sample should show some characteristic frequency ranges where it shows clear signs of excellent absorption properties and other frequency ranges where it absorbs less well. The corresponding curve should be recognizable in the impedance tube as well. To achieve optimal comparability between measurements, it is advisable to use a distinctive graph instead of a plane plot of a completely absorbent sample's values over the entire frequency range under observation.

The impedance measurement process is then being performed with the following microphone combinations specified in table 4.1.

	Microphone A	+	Microphone B
1	Microtech Gefell MK301E ser. 0556	+	Microtech Gefell MK301E ser. 0557
2	Superlux ECM-888B ser. E888B5A0528	+	Superlux ECM-888B ser. E888B5A0530
3	Microtech Gefell MK301E ser. 0557	+	Superlux ECM-888B ser. E888B5A0530

Tab. 4.1: Microphone combinations for impedance measurements

The measurements for each microphone combination are carried out, utilizing the sensor-switching calibration. All data from the different steps of the procedure are collected and saved separately. Using the exported data, the calculation of the measurement results can be repeated retrospectively. For the best comparability of the results, this is employed. To avoid unnecessary causes of error, the measurement results without compensation are extracted and calculated a posteriori. Therefore, the same recorded audio data is used for each combination's variations with versus without calibration. It provides changes in the results only to be caused by the differences in computation. These results can then be compared for each microphone combination with versus without prior calibration.

With this information, it is possible to compare the deviations of the two absorption coefficients. The more similar the phase frequency responses of the microphones used are, the smaller the deviations should be. In the case of the Microtech Gefell MK301E, which, according to the manufacturer's measurements, show almost no deviation in amplitude and phase frequency response, the two measurements should in theory hardly differ.

¹⁷ For further information on this sample please refer to the datasheet in appendix D.1.2.

As the calibration process is designed to compensate for all differences in level, amplitude frequency response, and phase frequency response all calibrated measurements should return the same or very similar results. If so, it would also show that it is not necessary to use the best microphones the testers can get their hands on but any measurement microphone of this type will do.

4.3.2 Measuring phase frequency response of different microphones at the same position

All four microphones were subjected to the measurement procedure proposed in chapter 4.3.1 and impulse responses were generated utilizing a logarithmic sweep. Each microphone underwent several test runs with single sweep impulse responses as well as averaged results from eight successively measured results. The sweep used covered the frequency range from 20 Hz to 20 kHz, with a digital output level of -12 dBFS and a length of 1 million samples at a sampling rate of 48 kHz.

The complete measurement results and comparisons of each microphone can be found in appendix C. Based upon those observations predictions can be made about how the microphone pairs might behave.

Microphone pair 1: The Microtech Gefell MK301E

As can be seen in figure 4.2, the MK301E again show what was to be expected from the knowledge of the manufacturer's data addended in C.1.

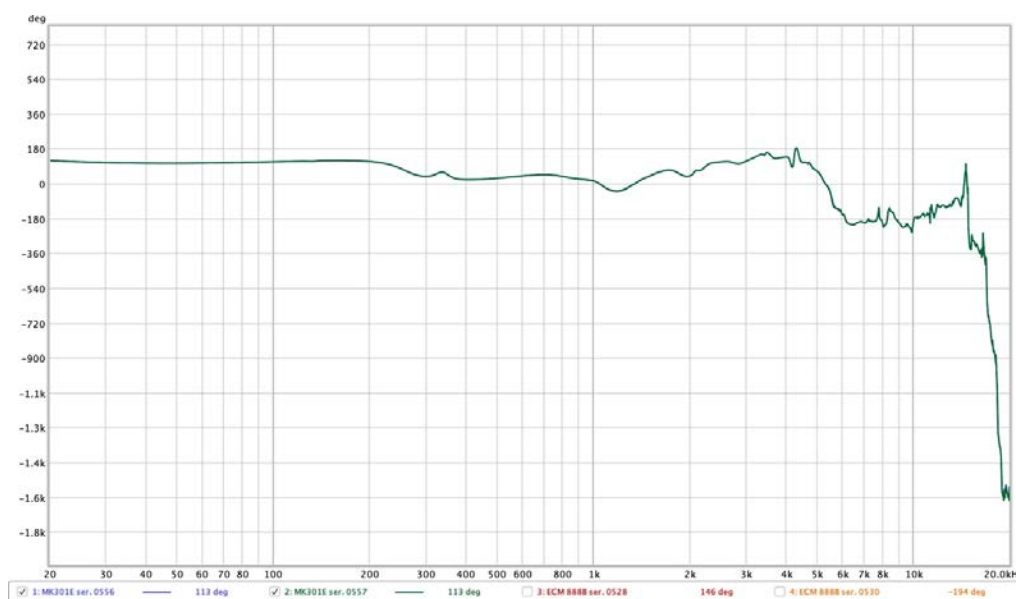


Fig. 4.2: Comparison of phase frequency responses of both Microtech Gefell MK301E

In the frequency range up to 6.4 kHz to be observed, only at approximately 1.2 kHz and between 5.5 kHz and 6 kHz minimal deviations in the phase response of the two microphones are noticeable. These deviations are of very small values. Therefore, it can be assumed that, provided the microphone gain levels are set to the same value, the results of the measurements using these two microphones without and with the calibration process should return very similar and possibly the same results. If so, it will be proving the theory of not needing the calibration process at all, if the microphones are well-built high-quality products with almost identical attributes concerning amplitude frequency response and phase frequency response.

Microphone pair 2: The Superlux ECM888B

Visualized in figure 4.3 it is easily visible to the naked eye that the “bang-for-the-buck”

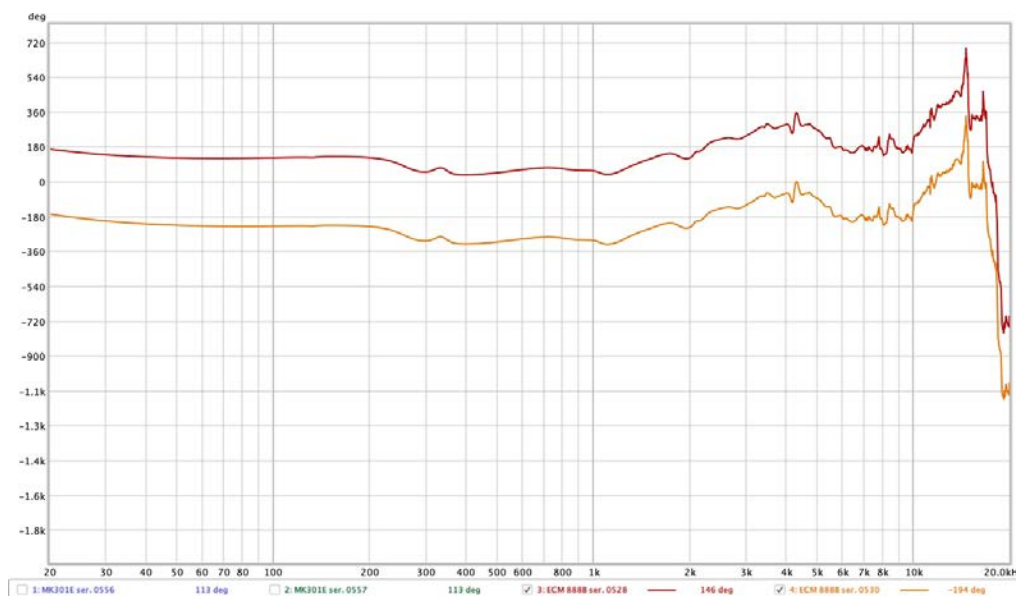


Fig. 4.3: Comparison of phase frequency responses of both Superlux ECM888B

products differ more from each other than the laboratory-grade microphones.

Over the entire observed spectrum, the phase responses are misaligned. Their phase responses seem to parallelize each other. The two curves are shifted almost 360° to each other. On closer look a few minor deviations can be noticed, as i.e. between 1 kHz and 2 kHz, thus rendering the seemingly parallel path divergent. Yet, the deviations are of relatively small value which should therefore not cause as great measurement result distortions as previously expected. As phase is of great importance for the impedance tube measurement with two microphones the results of measuring without calibration should show visible disparities from measuring with calibrating the system first.

Microphone pair 3: The Gefell MK301E with serial number 0557 and the Superlux ECM888B with serial number E888B5A0530

The most interesting combination should be made up of two completely different microphones as visualized in figure 4.4.

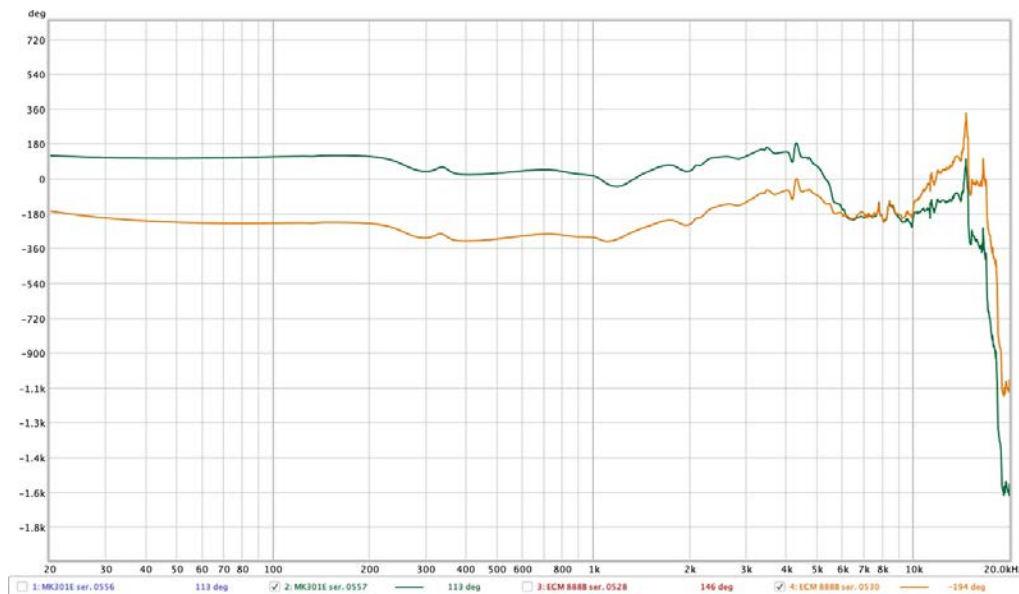


Fig. 4.4: Comparison of phase frequency responses of Microtech Gefell MK301E ser. 0557 and Superlux ECM888B ser. E888B5A0530

As can be expected, two completely different microphones show no common phase frequency response data. This combination of microphones poses as the greatest difference in phase frequency response. If used without calibrating the system first the usage of these two microphones should distort the results vastly. Therefore, it will be interesting and informative to compare the calibrated measurement of these two completely different microphones with the measurements of the other two combinations. If the calibrated measurement results are consistent with those of the other combinations, the efficiency and importance of the sensor-switching calibration will be proven. A combination of those two different microphones is not compliant with *EN ISO 10534-2*, nor recommended practice. At all times, two microphones of the same model and make should be used. It is interesting, nonetheless, to observe the behavior of this mix-match. It should provide the most information about the influence of the phase responses.

4.3.3 Measurements with different microphone pairs

All measurement procedures proposed in chapter 4.3.1 were carried out. For optimal comparability of the results, the three measurements with calibration were carried out,

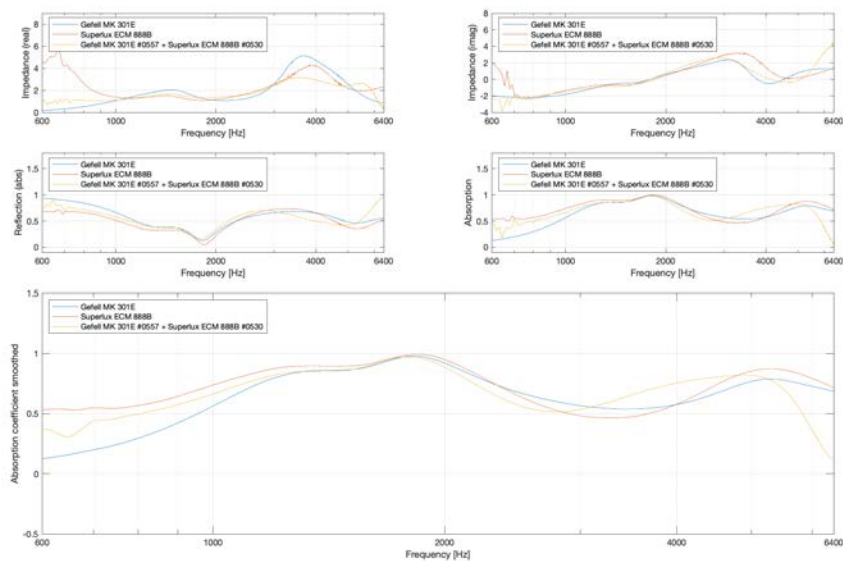
and retrospectively the measurements without compensation by the calibration factor were extracted, generated, and evaluated from these measurement data sets.

Each measurement, as well as a complete list of comparisons of the different measurements, can be found in appendix D. In the following, the microphone combinations without calibration, as in figure 4.5a, and with calibration, as in figure 4.5b, are compared.

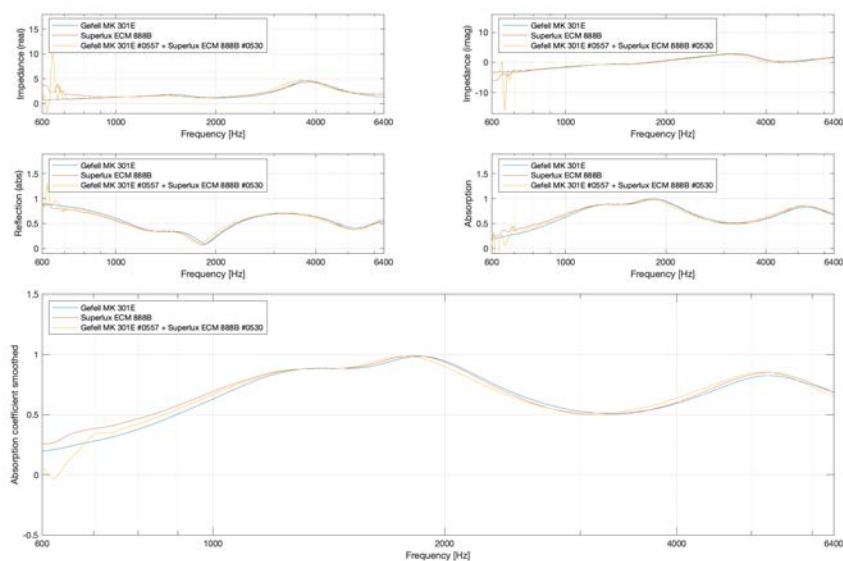
The clearest indication on the different microphones' phase response influences is presented through the calculated calibration factor data. When the compensation is applied during the measurement process, as specified in equation 3.11, the measured transfer function TF is divided by the calibration factor H. Therefore it can be assumed that for very similar characteristics of two microphones¹⁸, the values of the calibration factor approach 1 along the frequency axis. This would imply that a calibration factor H_c at a certain frequency f with the value $H_{cf} = 1$ would not influence the measurement, because no compensation is necessary. Therefore, it can be concluded that a microphone pair, of which the calibration factors are equal or close to 1, is (approximately) equivalent and can be operated without a preceding calibration process. Due to this importance of the calibration factor, its resulting values will be evaluated for each microphone combination.

All measurements were performed on a sample of Cellofoam CELLO[®] 521. The specified absorption coefficients on the material's datasheet, as displayed in Appendix D.1.2, have been measured with the reverberant room method as specified in ISO 354:2003. Since the measurements in the impedance tube were carried out with a different measuring method, the manufacturer's specified values must be observed in a more differentiated way. Some values of the datasheet for the 20 mm thick test specimen are above the value 1, which is not possible with a coefficient as the values can typically only contain values between 0 and 1. Furthermore, the reverberation chamber accommodates a significantly larger specimen. There are also considerably more reflected components as, in contrast to the impedance tube, the sound cannot propagate on one axis only, which is terminated on one side by the test specimen. Therefore it is to be expected that the data obtained in the impedance tube will show smaller values than the data on the specification sheet. Furthermore, small displacements, elongations, and/or compressions of the obtained data may occur along the frequency axis.

¹⁸ The most important parameters are: amplitude frequency response, phase frequency response and equal input levels/gain staging.



(a) Comparison of the microphone combinations' measurement results without calibration



(b) Comparison of the microphone combinations' measurement results with calibration

Fig. 4.5: Comparison of the microphone combinations' measurement results without and with calibration

Microphone pair 1: The Microtech Gefell MK301E

As visible in figure 4.6 the MK301E returned a fairly flat calibration factor.

The values for H_c approach $H_c = 1.1$ across the entirety of the inspected frequency band. The values are all very close to each other and form a continuous graph in the absence

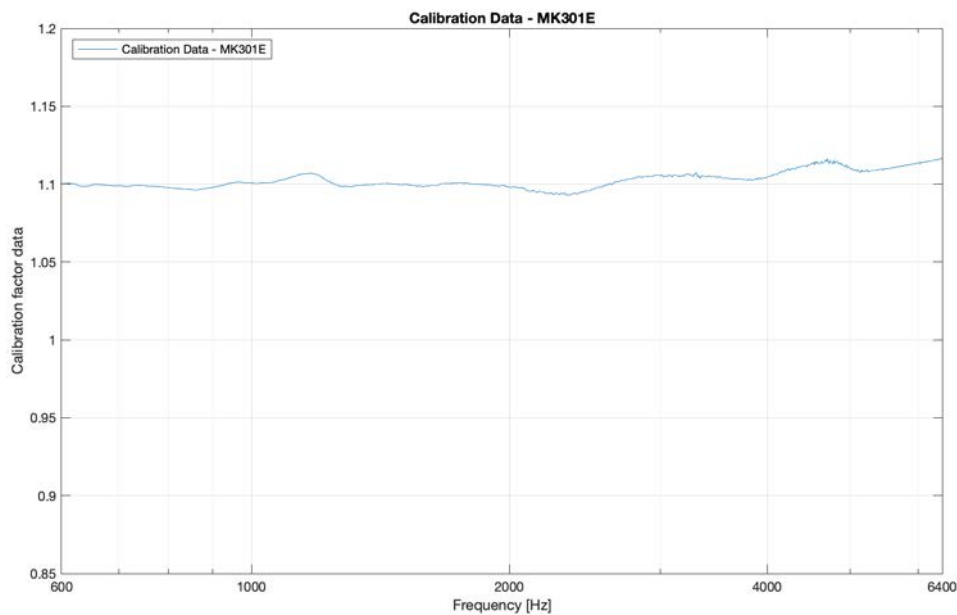


Fig. 4.6: Calibration data from measurement with Microtech Gefell MK301E

of graphical smoothing. At a few points, relatively clearly recognizable deviations can be detected. When comparing with figure 4.2 of the phase differences of both microphones two of those deviations can be linked to differences in the microphones' phase frequency responses. The small increase in values around 1.2 kHz could be attributed to the respective slight phase shift of both microphones. The small phase deviations between 5 kHz and 6 kHz probably cause the increasing slope of the calibration factors in this frequency range. Despite these smallest deviations, the graph of the calibration factors appears very flat and continuous. This testifies to the excellent similarity of the two microphones. Due to this linear characteristic, it can be assumed that both microphones could be used without calibration. The shift of the graphs from $H_c = 1$ to $H_c = 1.1$ is probably attributable to an imperfect adjustment of the microphone input levels, shifting the graph in parallel. If the shift was caused by amplitude or phase differences it would cause a more distinct curving. If both microphones were perfectly leveled, the calibration curve could be expected to be centered around $H_c = 1$.

These conclusions can be further elaborated when comparing the results of the measurements without versus with calibrating the system first in figure 4.7. Both measurements with this combination of microphones show very similar results. However, due to the similarity of the microphones, the expectation of almost identical results gets disappointed. The graphs show clear deviations from each other. This also disproves the assumption of the calibration factor's shift in value to solely being attributable to differences in the

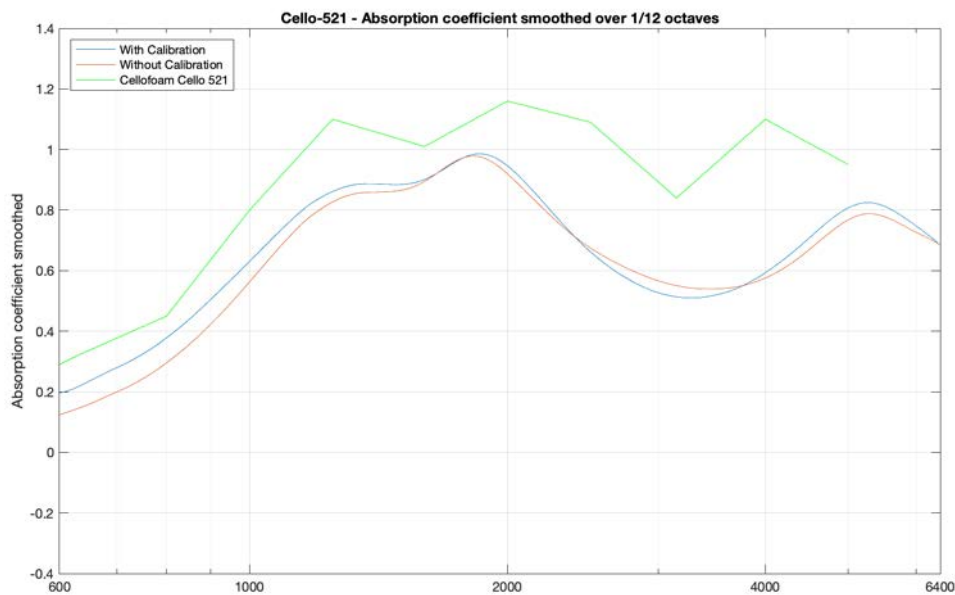


Fig. 4.7: Comparison of measured absorption data using Microtech Gefell MK301E

levels of the microphones. If that was the case the two graphs would run parallel to each other. Therefore the deviations must have additional causes.

In comparing the results to the data points of the specimen's datasheet the measurement results are rendered valid. Up to around 3 kHz, the graphs are parallel to the data from the reverberant room measurement. Above this frequency, the sample in the impedance tube seems to stretch its values slightly towards higher frequencies as compared to the datasheet. Both graphs from the measurements without versus with calibration could reconfirm the specification sheet data if the values were parallel shifted and overlapped.

It can therefore be concluded that the utilization of these two Microtech Gefell MK301E without compensating the measurement results through sensor-switching calibration returns valid results. The projection made in chapter 4.3.2 on the behavior of these microphones is supported and substantiated by the measurement results. Both measurement procedures yield very similar, albeit not identical, results. It should also be noted that the microphones are so well built so that the results from the measurements have very smooth and even resulting graphs. For these microphones, an additional step of smoothing is not necessary.

Microphone pair 2: The Superlux ECM888B

In contrast to the measurements with the MK301E, the Superlux ECM 888B returned a very different calibration factor, as visualized in figure 4.8. The calibration data has a

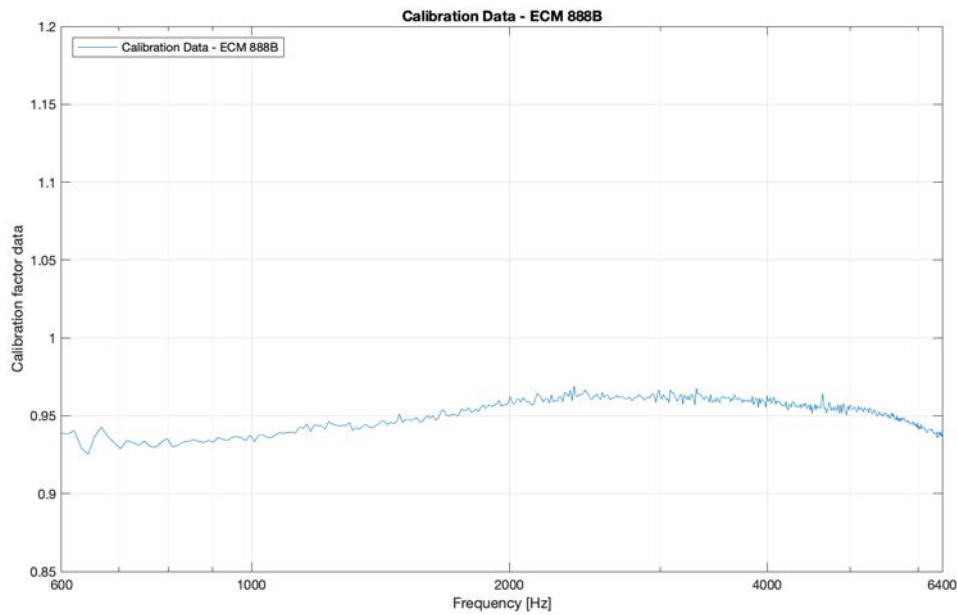


Fig. 4.8: Calibration data from measurement with Superlux ECM 888B

very uneven, almost noisy graph. The graph, which shifts around $H_c = 0.95$, additionally shows significant bends, with a value minimum between 600 Hz and 700 Hz and a maximum at approximately 3 kHz. It is much less flat than of the MK301E. Unexpectedly, this calibration data is much closer to the value of no compensation $H_c = 1$ in comparison to the MK301E.

The strongly varying adjacent values, which make the graph appear noisy, indicate relatively strong disparities between the two microphones in small frequency bands. Even if the phase frequency responses of the two microphones seem to parallelize with a small phase shift, as shown in figure 4.3, many small deviations are distributed over the entire frequency band. From these observations, the following effects on the measurement results can be assumed. Due to the proximity of the calibration values to $H = 1$ it can be expected that the results without and with calibration should be quite similar. The greatest disparities, however, could be assumed below 1 kHz as the calibration data shows the greatest divergences in that frequency range. Furthermore, it can be assumed that the results could show equally noisy visualizations of the results. It is unlikely that the compensation by calibration will smooth out all unevenness.

To elaborate on this a comparison of the measurement results is in order, as visualized in figure 4.9. The measurements without and with compensation are largely similar. As was expected the greatest deviation of the measurement without calibration can be observed below 1 kHz. The values at around 600 Hz show a difference in value of about $\Delta\alpha = 0.3$. From this observation, it can be assumed that the divergence below this frequency may

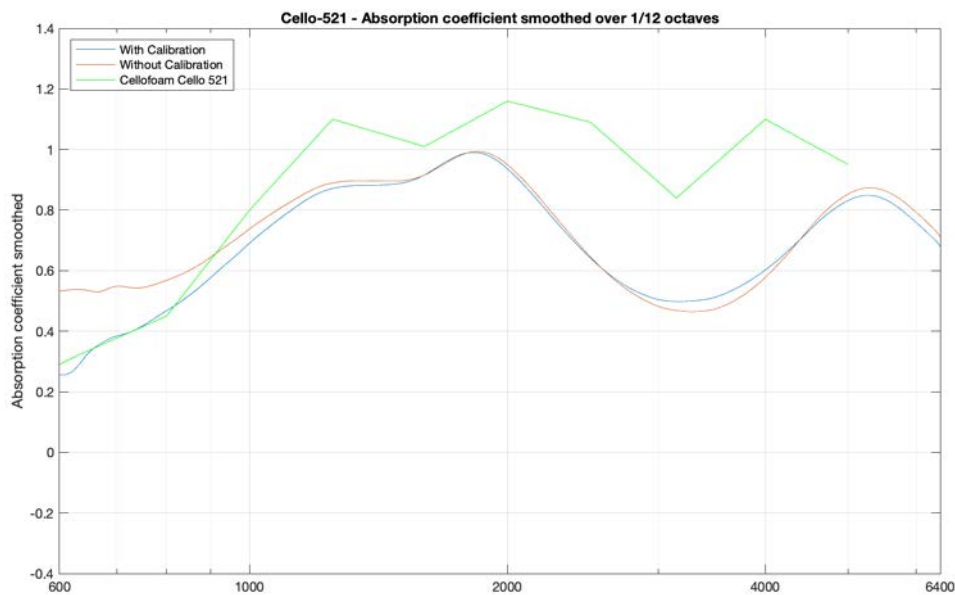


Fig. 4.9: Comparison of measured absorption data using Superlux ECM 888B

increase the lower the frequency. Above the frequency of around 1.2 kHz, the results of both measurements show very similar values with minor deviations. Despite much greater deviations of the phase frequency responses over the entire spectrum, when compared to the MK301E, the returned results are very consistent.

Similar to the measurement with the MK301E the calibrated measurement is rendered valid by the data points of the specimen's datasheet.

As the results plotted in figure 4.9 show smoothed result values it is necessary to refer to the comparison data in appendix D.3.2 to be able to assert a conclusion about the corrugation of the results. All shown parameters that have not been smoothed show clear unevenness and noisy behavior along the entire frequency range and for both variations of the measurement. Therefore the assertion can be incurred that the microphone pair clearly shows more disparities in the entire frequency spectrum. In contrast to the MK301E, smoothing is essential to obtain an averaged curve and to be able to provide information about the overall behavior in the frequency domain.

Recapitulatory can be said that the measurement with the Superlux microphones returns valid results. Even without applying the sensor-switching compensation, the microphone combination could be used for measurements in the frequency range above 1 kHz. The supposition from chapter 4.3.2, that the phase shift should have a significant effect on the measurement without calibration, has not been confirmed. Unexpectedly, the measurement results without applied calibration are largely satisfactory and in concurrence with the calibrated measurements.

Microphone pair 3: The Gefell MK301E with serial number 0557 and the Superlux ECM888B with serial number E888B5A0530

The third microphone combination promised to be very interesting in chapter 4.3.2. This was supported by the calibration factor, as visualized in figure 4.10. As could be ex-

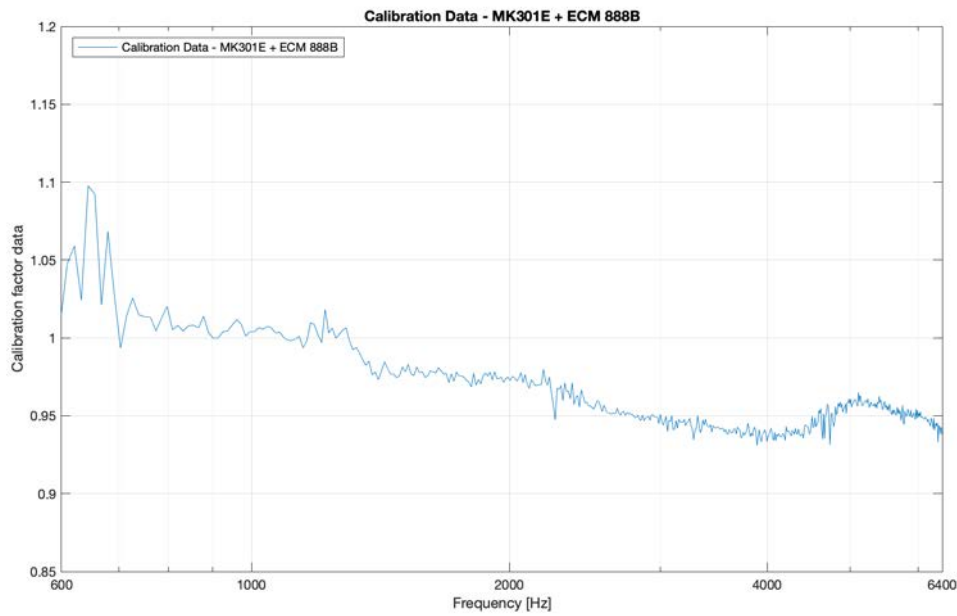


Fig. 4.10: Calibration data from measurement with Microtech Gefell MK301E + Superlux ECM 888B

pected, a very uneven, noisy curve with many alterations along the frequency axis can be observed. As is known from figure 4.4 the two microphones provide very different phase frequency responses. Although both microphones have a very flat and consistent amplitude frequency response and were leveled to the same gains during the measurement process, the differences in phase should have vast effects on the measurements when comparing without vs. with calibration process and compensation. The calibration factor data supports that. It shows the greatest value range of all three microphone combinations, with values between $H_c \approx 0.93$ and $H_c \approx 1.1$. Similar to the Superlux microphones the greatest changes in value occur below 700 Hz. Further significant visible changes in the values for H_c are noticeable around 5 kHz. This is also the frequency range where the phase responses of both microphones are incident and intercross each other. This distinct alteration in the phase frequency responses can be detected in the calibration factor. From these observations of the calibration data, it can be assumed that the measurements without compensation should differ vastly from those with calibrating the system first. This however excludes the frequency range around 800 Hz to 1.2 kHz. In that frequency band,

the values for the calibration factor lie around $H_c \approx 1$, thus the two curves for calibrated and uncalibrated measurements should coincide in this frequency range.

This is supported by the measurement results displayed in figure 4.11. As predicted the

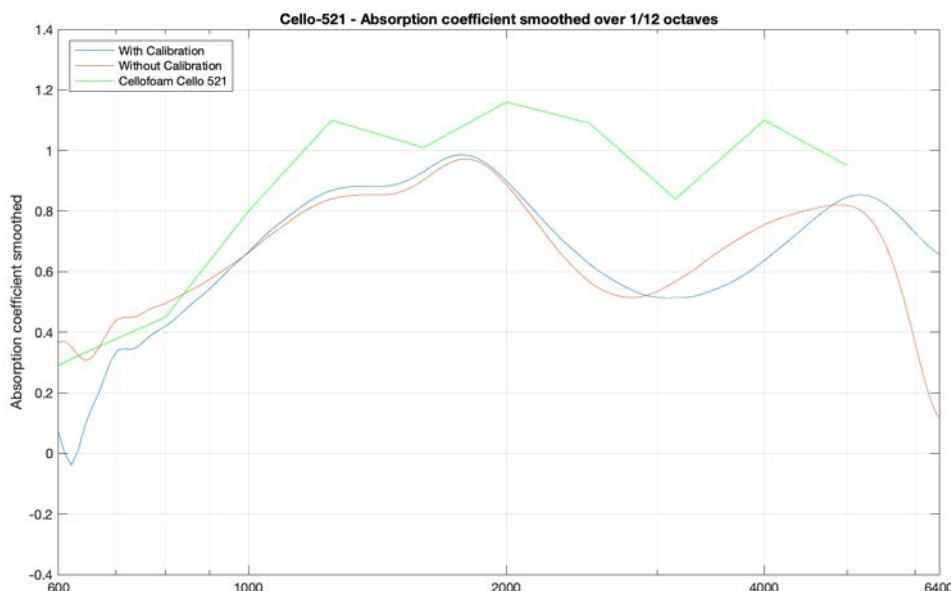


Fig. 4.11: Comparison of measured absorption data using Microtech Gefell MK301E + Superlux ECM 888B

different measurements show very distinctly different results. While the results show relatively similar results and are almost identical in the frequency range where $H_c \approx 1$; in this comparison the greatest deviations are noticeable. Similar to the Superlux comparison, below 1 kHz the values vastly deviate and assumably do so below the 600 Hz mark, as well. The other easily noticeable divergence occurs above approximately 3 kHz. Above this frequency the graphs start to become completely uncorrelated and around 5 kHz, noticed before in the calibration factor dataset and comparison of phase frequency responses, the differences in value start to incrementally increase.

Interestingly, the observed roughness and noisy graphs of the Superlux measurements are not as pronounced for these measurements, which can be observed in more detail in appendix D.3.3. This is probably due to the second microphone. The combination of the MK301E, which produced very clear values, and the ECM 888B, which showed much rougher readings, seems to reduce the noisiness, albeit not eliminate it.

Summarizing it can be noted that this mix-match microphone combination as expected shows the greatest deviations between the uncalibrated and calibrated measurements. However, the calibrated measurement results are validated by the datasheet, also. As predicted in chapter 4.3.2 the vast differences of the mix-matched microphones caused

great distortions of the uncalibrated measurement results. Yet, the sensor-switching calibration was able to compensate for all differences and return a plausible, conclusive, and valid measurement result.

4.4 Evaluation of results

All three measurements that underwent the calibration process first are arguably similar, as visible in figure 4.12. The compensation can correct for differences in levels, amplitude

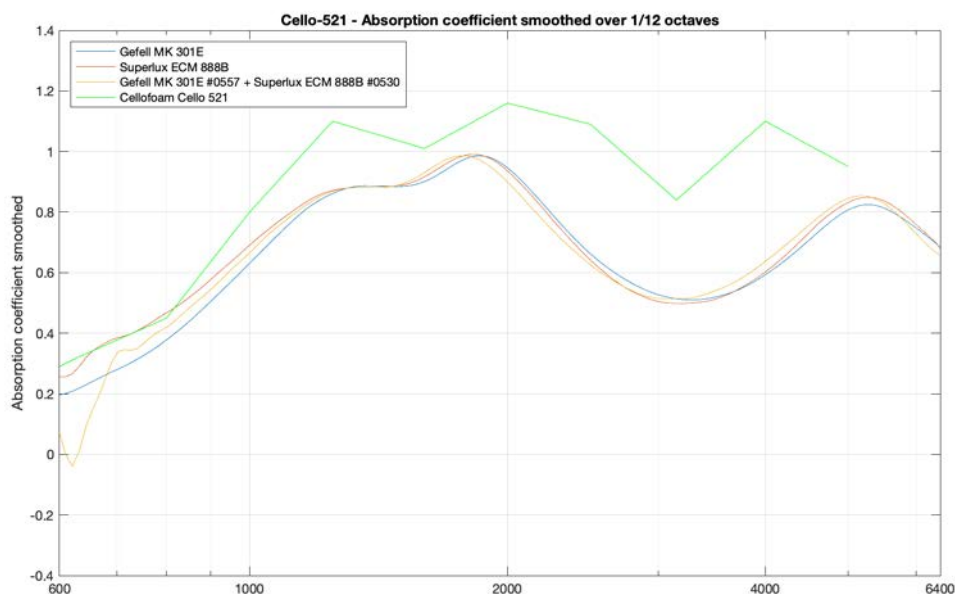


Fig. 4.12: Comparison of measured absorption data from the three microphone combinations

frequency response, as well as phase frequency response in the time domain. If very large compensation values occur or the compensation values H_c in the frequency domain suddenly fluctuate heavily, it can be assumed that either something is not working properly in compensation or indicates an error in the calibration measurements. The microphone pairs in use must exhibit a certain similarity and shall not leave this similarity range to exclude such errors. This was the case with the measurements made here¹⁹. Even the mix-match pair has no implausible correction values. The roughness of the correction curves for the Superlux ECM 888B measurements and the mix-match combination should not be interpreted as an insufficient similarity. Especially in the case of the combination of MK301E and ECM 888B, there are no major jumps to be found that would indicate too great a dissimilarity. This can be attributed to the very similar flat amplitude frequency

¹⁹ The calibration data from all three microphone combinations has been compared in appendix D.4.4.

response of both microphones so that only the phase angles and differences thereof determine the values to be calibrated. These results of the calibrated measurements can be compared with the results of the uncompensated measurements, which show very large deviations compared to each other and the dataset from the datasheet of the test sample, as can be observed in Appendix D.3.5. Hence, it can be concluded that the compensated measurements are all similar and yield conclusive results. The calibration process was capable of compensating even for the pair of MK301E and ECM 888B. This speaks for a highly efficient and powerful procedure when executed precisely. It can therefore be concluded that the calibration process should be used in all circumstances. To ensure compliance with *ISO 10534-2* this is obligatory as well.

With the help of the calibration process, the same conclusive results could be achieved with all combinations. It was proven that with the appropriate compensation each microphone pair can be used and achieve similar results. One of the objectives of this thesis was therefore fulfilled, as no laboratory-grade microphones like the Microtech Gefell MK301E have to be used. Instead, equally conclusive results can be obtained with a pair of microphones that require only a fraction of the acquisition cost of the MK301E, as in the case of this work the Superlux ECM 888B.

The assumption that the measurements without calibration for Microtech Gefell microphones do not show much difference from the measurements with calibration was confirmed. Yet, the deviations of both graphs show greater deviations than previously expected. As a result, these microphones could in theory be used even without calibration to obtain very similar results. Consequently, it would also be possible but not recommended for other very well produced microphones with known phase and amplitude frequency responses. This should not be done, however, as there still are some minor deviations between the curves without versus with previous calibration. Furthermore, it would not grant compliance with the ISO standard anymore.

Unexpectedly, the Superlux measurements returned comparison results that would also allow for these microphones to be used without calibration for frequencies higher than approximately 1 kHz. Above this frequency, no increased distortion of the results would need to be expected. However, this is only true for the specific microphone pair used within this thesis. This is because the manufacturing process of these low-cost microphones is not expected to produce the same consistent characteristics across a large number of products. For each pair, the amplitude and phase frequency responses would first have to be determined and it would have to be determined whether the calibration factor H_c yields as good results as for the pair used in this case.

The evaluation of the measurements allows further conclusions to be drawn about the relationship between the unevenness of the result plots and the microphone quality. It

can be concluded that the more continuous the visualized graphs of the measured values appear, the better the microphones. In this respect, the noisy nature of the results could be classified as a quality feature. The superb Microtech Gefell MK301E microphones have shown their results to be very consistent, smooth, and without noise. This speaks to the excellent quality of the transducers. The Superlux, on the other hand, produced very corrugated and noisy curves, which suggests that the quality of the capsules is likely to be lower. The fact that the measurements with the combination of MK301E and ECM 888B showed an intermediate unevenness between the other two results illustrates this correlation. Typically, measurements of this kind produce a certain amount of ripple or noisiness in their results. To be able to assess the overall behavior of the system, a smoothing of the results is usually necessary. The laboratory-grade microphones used in the measurements evaluated here yielded results that made smoothing superfluous.

4.5 Error analysis

In chapter 3.6 possible errors in measurements in the impedance tube have already been discussed in detail. Nonetheless, it is indispensable to account for some specific sources of error that could have affected the measurements of the last chapters. These might have occurred in addition to or amplifying the sources of error previously recognized.

Initially, the evident difference in the measured values of the material sample compared to the values of the datasheet should be observed. In the frequency range above approximately 3 kHz, all three measured values appear stretched to the curve on the datasheet. Below this frequency, all results appear in clear similarity to the values on the specification sheet. The deviation of both data sets could be narrowed down to a few possible sources of error. One of which is the difference in measurement techniques. The data from the datasheet was measured in accordance with *ISO 354* in the reverberant room. As that method requires much larger samples and evaluates a completely different set of captured data, differences are to be expected when comparing to results from a different measurement process. Another reason might be the specimen under investigation. The material tested, Cellofoam CELLO[®] 521, is a studded foam with a rubber-like surface coating. Due to the small burls, it is difficult to cut out an optimal test specimen. In the best case, it should also have a flat surface. For the measurement in the small impedance tube, an area between the studs was therefore punched out, which has a mostly plane surface. This can only be compared with the measurement in the reverberation chamber in a differentiated matter, as the larger test specimen naturally retains its studded structure in the reverberation chamber and no plane test specimens are cut from the test object. If a studded probe was sampled from the material the measurement results might have matched the data from the reverberant room more closely and/or shown more deviations.

The best comparability would have been provided by comparison with other measurement results from an impedance tube. Furthermore, the deviations could also originate from the manufacturing process of the respective test specimens. In all likelihood, they do not originate from the same foam mat.

For the measurements performed a major source of error might lie within the microphone leveling. To be able to have the best results and comparability, the respective levels of the microphones would need to be set in perfect unison. Given that the levels are adjusted by human hand, this cannot be completely guaranteed. For the evaluated measurements this is of vital importance, especially when comparing the uncalibrated measurements with the measurements that underwent compensation. During a normal impedance measurement process, minor maladjustments are equalized and compensated for through the sensor-switching calibration. As during the previous evaluation the calibration data itself was closely considered, it is compulsory to note that errors may have been introduced through imperfect gain staging.

Other gross or preparatory errors might include: imperfect placement of the probe, so that a small air gap behind the test specimen or byways on the tube walls have been created, despite the use of vaseline for sealing; errors during the preparation of the test specimen; and minor measurement deviations.

Some additional systematic errors might have been introduced by the evaluation software that was created for this thesis. Those errors might lie within data processing, the mathematics used, incorrect allocation of data sets, or in the averaging of the values.

5 Conclusion and prospects

Building on pre-existing impedance measurement systems and in strict compliance with *EN ISO 10534-2*, a two-microphone wave separation measurement system has been adapted to determine the acoustic impedance of materials. It is capable of determining the coefficients for absorption α and reflection ρ properties, as well as the acoustic impedance Z . The system was developed through the implementation of four steps:

- Theoretically elaborating and gaining an understanding of the necessary fundamentals;
- The design of a novel measurement system via evaluation of a pre-existing, proprietary system manufactured by Brüel & Kjær;
- Programming an easy-to-use, uncomplicated, and streamlined software system that helps the operator to quickly obtain the sought-after results and to autonomously generate a measurement protocol;
- Additionally, a more in-depth examination of the phase influence of different microphone pairs on the measurement results was conducted. This revealed the importance and efficiency of the compensation of differences in level, amplitude and phase frequency response through the sensor-switching method.

With the objective to realize an accessible and affordable system, all components on the hardware and software side have been revised. It was the aim to extract the impedance measurement method from the laboratory environment and to become system and component independent. The proprietary hardware environment has been dissolved so that the impedance tube, the transducer, the microphones and microphone preamplifier, the audio interface, and the computer can be freely selected. Utilizing software in a Matlab host environment, the measurement data obtained with the help of the hardware components previously mentioned can be collated and analyzed irrespective of the operating system. The results can be obtained relatively quickly and a protocol is compiled via a simple operation.

The preceding examinations in previous chapters yielded conclusive results and supported most of the assumptions made. Although the results presented were plausible and valid, further observations, involving a large number of different test specimens, are required to ultimately assess the viability of the system. Also, component independence can be further improved and the cost efficiency can be optimized as well. This can be achieved primarily by not using a prefabricated impedance tube, and in its place using an in-house design like the ones developed in the works of Brunnader 2002 and Palella; Binkley

2018. The further exploration of this subject necessitates the construction of a self-made impedance tube and its comparison with a standard B&K 4206 device.

Due to missing components, observations in the large tube, unfortunately, were not possible. Accordingly, follow-up observations are necessary.

Prospects for the future

Although already relatively aged and time-consuming, procedures such as the impedance tube measurement used in this thesis have become of great importance for acoustics and present a reference procedure. However, it is now time to further develop and rethink them. The basis for this is to break open and understand the proprietary methods more precisely. This can already be seen in Microflown and its novel approaches, which have already been presented in chapter 1. Thus it can be considered a favorable indication that, at the time of this work, standard ISO 10534-2:1998 is under review by the ISO²⁰. Although no new techniques and procedures should be anticipated, corrections and improvements of the procedure could be consequential to this review.

The exemplary experimental observations in chapter 4 could and should be substantiated by quantitative experimental observation. This was not possible in the context of this thesis, because there were only two pairs of microphones available and also not enough test specimens. The quantitative investigation of a high number of measurement results would have exceeded the scope of this work.

The Matlab code could be compiled as a standalone application using an add-on to the software. This would allow for native operation on the operating system without the need to use the Matlab host. The software can also be further improved. For example, an "expert mode" with more functions and control options would be possible, should this be desired by the user. Likewise, the GUI environments can be further unified and, ideally, merged into a common host window. However, this was beyond the scope of the proof-of-concept approach of the software developed for the thesis.

It is very interesting to examine and further develop the measuring procedure in the impedance tube for in-situ capabilities. If the test objects could be tested for their parameters directly in the installed condition this would mean faster and easier results without having to go through the difficult process of specimen preparation. It would also make it possible to measure test objects that cannot be employed without destroying them or because they would have completely different properties in a small format. To make this possible, an adaptation of the system would be necessary, for many materials to be

²⁰ The life cycle status of the standard is defined by the ISO as "Now under review" and has the stage code: "90.92 International Standard to be revised" (ISO/TC 43/SC 2 2020).

examined, such as specific wall environments, rarely have porous surfaces and the tight fitting of the measuring system to the surface of the object would have to be clarified. Presumably, the calculations would also have to be reviewed for their suitability for such a procedure.

Finally, research could be done on a more advanced calibration method. The sensor-switching method could be replaced by a simpler and more efficient method. Ideally, this method would permit a static mounting of the microphones. When the microphones no longer need to be interchanged for calibration purposes, the potential errors caused by the position switching could be eliminated. Furthermore, it would make the procedure much easier if no manual intervention in the hardware would be required, except for setting levels and introducing the probes under investigation to the experimental setup.

References

- [Apple 2017] Apple Inc., 2017, October 30. *Core Audio Overview*. Available at: <https://developer.apple.com/library/archive/documentation/MusicAudio/Conceptual/CoreAudioOverview/WhatisCoreAudio/WhatisCoreAudio.html> [Accessed: August 09, 2020].
- [Berzborn et al. 2017] Berzborn, M. et al., 2017. DAGA 2017: 43rd Annual German Congress on Acoustics. *The ITA-Toolbox: An Open Source MATLAB Toolbox for Acoustic Measurements and Signal Processing*. pp. 222-225. Available at: https://www.researchgate.net/publication/317256502_The_ITA-Toolbox_An_Open_Source_MATLAB_Toolbox_for_Acoustic_Measurements_and_Signal_Processing [Accessed: August 05, 2020].
- [Boden; Abom 1986] Bodén, H. & Åbom, M., 1986. *Influence of errors on the two-microphone method for measuring acoustic properties in ducts*. The Journal of the Acoustical Society of America, 79(2), pp. 541-549.
- [Bree 2003] Bree, H., 2003. *An Overview of Microflow Technologies*. Acta Acustica united with Acustica. 89. pp. 163-172. Available at: https://www.researchgate.net/publication/233697735_An_Overview_of_Microflow_Technologies [Accessed: August 08, 2020].

- [Briel Kjaer 1995] Brüel & Kjær, 1995. *Product Data. Two-microphone Impedance Measurement Tube — Type 4206.*
- [Briel Kjaer 2019] Brüel & Kjær Sound & Vibration Measurement A/S, 2019. *PRODUCT DATA Impedance Tube Kit (50 Hz – 6.4 kHz) Type 4206, Impedance Tube Kit (100 Hz – 3.2 kHz) Type 4206-A, Transmission Loss Tube Kit (50 Hz – 6.4 kHz) Type 4206-T.* Available at: <https://www.bksv.com/media/doc/bp1039.pdf> [Accessed: August 05, 2020].
- [Brunnader 2002] Brunnader, R., 2002. *Aufbau und Programmierung der 2p Messmethode im Impedanzrohr für die Messung akustischer Materialparameter.* diploma thesis. Technische Universität Graz.
- [Deter 2013] Deter, S., 2013. *Erstellen eines Versuchsaufbaus zur Bestimmung von Transmissionsgraden poröser Materialien mit einem Impedanzrohr.* bachelor's thesis. Technische Universität Berlin.
- [Encyclopaedia Britannica; Huygens 2016] Encyclopaedia Britannica, 2016. *Huygens' principle.* Available at: <https://www.britannica.com/science/Huygens-principle> [Accessed: September 06, 2020].
- [Encyclopaedia Britannica; Kundt 2020] Encyclopaedia Britannica, 2020. *August Kundt.* Available at: <https://www.britannica.com/biography/August-Adolph-Eduard-Eber>

- hard-Kundt [Accessed: September 06, 2020].
- [Hobohm 2018-2019] Prof. Dr.-Ing. Hobohm, Klaus, WS 2018-2019. *Grundlagen der Akustik*. Lecture.
- [ISO 354:2003] International Organization for Standardization, 2003. *Measurement of sound absorption in a reverberation room (ISO standard no. 354:2003)*.
- [ISO 10534-1:2001] International Organization for Standardization, 2001. *Bestimmung des Schallabsorptionsgrades und der Impedanz in Impedanzrohren Teil 1: Verfahren mit Stehwellenverhältnis (ISO standard no. 10534-1:1996)*. Deutsche Fassung EN ISO 10534-1:2001.
- [ISO 10534-2:1998] International Organization for Standardization, 1998. *Determination of sound absorption coefficient and impedance in impedance tubes — Part 2: Transfer-function method (ISO standard no. 10534-2:1998)*. English version.
- [ISO 10534-2:2001] International Organization for Standardization, 2001. *Bestimmung des Schallabsorptionsgrades und der Impedanz in Impedanzrohren Teil 2: Verfahren mit Übertragungsfunktion (ISO standard no. 10534-2:1998)*. Deutsche Fassung EN ISO 10534-2:2001.
- [ISO 10534-2:2007] International Organization for Standardization, 2007. *Bestimmung des Schallabsorptionsgrades und der*

- Impedanz in Impedanzrohren – Teil 2: Verfahren mit Übertragungsfunktion (ISO standard no. 10534-2:1998). Deutsche Fassung EN ISO 10534-2:2001, Berichtigungen zu DIN EN ISO 10534-2:2001-10.*
- [ISO/TC 43/SC 2 2020] ISO/TC 43/SC 2, Building acoustics, 2020. *ISO 10534-2:1998*. Available at: <https://www.iso.org/standard/22851.html> [Accessed: August 31, 2020].
- [Kruse 2006] Dr. Kruse, Roland, 2006. *Two microphone impedance tube*. Matlab Code. University of Oldenburg.
- [Lerch et al. 2009] Lerch, R., Sessler, G. & Wolf, D., 2009. *Technische Akustik*. Berlin, Heidelberg, Germany: Springer-Verlag Berlin Heidelberg.
- [MathWorks; tfestimate n.d.] MathWorks, n.d. *tfestimate*. Available at: https://de.mathworks.com/help/signal/ref/tfestimate.html?s_tid=srchtitle [Accessed: August 06, 2020].
- [Meier 2000] Meier, A., 2000. *Die Bedeutung des Verlustfaktors bei der Bestimmung der Schalldämmung im Prüfstand*. doctoral dissertation. Rheinisch-Westfälische Technische Hochschule Aachen.
- [Microtech Gefell n.d.] Microtech Gefell GmbH, n.d. *Condenser Measuring Microphone Cartridge Type MK 301 E*. datasheet. Available at: <https://www.microtechgefell.de/d>

- atei/477/MK-301-E_vYDsT.pdf
[Accessed: August 20, 2020].
- [Moeser 2015] Möser, M., 2015. *Technische Akustik*. 10th edition. Berlin, Germany: Springer-Verlag Berlin Heidelberg.
- [Rodriguez-Fernandez; Fernandez-Comesana 2017] Rodríguez-Fernández, C. & Fernández-Comesaña, D., 2017. *In-situ estimation of sound transmission loss using a scanning sound intensity P-U probe*.
- [Russell 1998] Dr. Russell, D., 1998. *Acoustics and Vibration Animations*. Available at: <https://www.acs.psu.edu/drussel1/Demos/waves/wavemotion.html> [Accessed: August 04, 2020].
- [Seybert; Soenarko 1981] Seybert, A. F., & Soenarko, B., 1981. *Error analysis of spectral estimates with application to the measurement of acoustic parameters using random sound fields in ducts*. The Journal of the Acoustical Society of America, 69(4), pp. 1190-1199.
- [Superlux 2018] Superlux, 2018. *Superlux ECM888B 1/4" MEASUREMENT MICROPHONE*. datasheet. Available at: http://www.superlux.com.tw/upload/function.product.info/7d26cb23-94da-45cc-8ffc-001f1238d415/resource/20180718-ECM888B_ug_TC_SC_EN.pdf [Accessed: August 20, 2020].
- [Tijs 2013] Tijs, E., 2013. *Study and development of an in situ acoustic absorp-*

tion measurement method. doctoral dissertation. University of Twente.

[Tikander 2002]

Tikander, M., 2002. *Model-based curvefitting for in-situ impedance measurements.* master's thesis. Helsinki University of Technology.

Appendix

A Measuring the filter responses of the Brüel & Kjær Type 4206

The documentation of the B&K 4206 impedance tube does not provide further insights into the built-in filtering unit. As a choice need to be made to be able to use the loudspeaker with different tube setups the following measurement was performed. Conclusions about the filters behind the three poti positions have been drawn subsequently. The choices that can be made on the tube are: Low-Pass, Linear, High-Pass.

A.1 Measurement Setup

To get as much direct signal as possible of the loudspeaker and minimize unwanted alterations in the sound field in the B&K 4206 impedance tube the extension for the small tube setup was placed at the end of the large tube. This has been done because of the large absorbent cushioning around the small tube part that is being inserted to the large tube so that during small tube measurements no unwanted reflections and distortions can appear in the large tube ultimately affecting the measurement. Another highly absorbent sample was placed in the small tube for as few as possible reflections to be thrown back into the large tube. This probe was a sample of Cellofoam CELLO® 521. The microphone, a Microtech Gefell MK301E with serial number 0556, has been placed in the large tube's second or middle microphone position.

Subsequently, using the software Room EQ Wizard (REW) a sweep has been played back in the tube and then processed as impulse response (IR). This measurement process was repeated three times using the same test signal and settings: once for each poti position, each using different filters.

Within REW the measurements provided information on the amplitude frequency responses of each filter. These are evaluated and graphically compared hereafter.

A.2 Graphical comparison of all filters



Fig. A.1: Comparison of amplitude frequency response of the three filter settings on the B&K 4206 impedance tube

A.3 Middle poti position: Linear

The poti position in the center is *Linear mode*. This mode is supposed to not have any filter stages interposed in its signal chain. The amplitude frequency response of the unfiltered signal is displayed below:

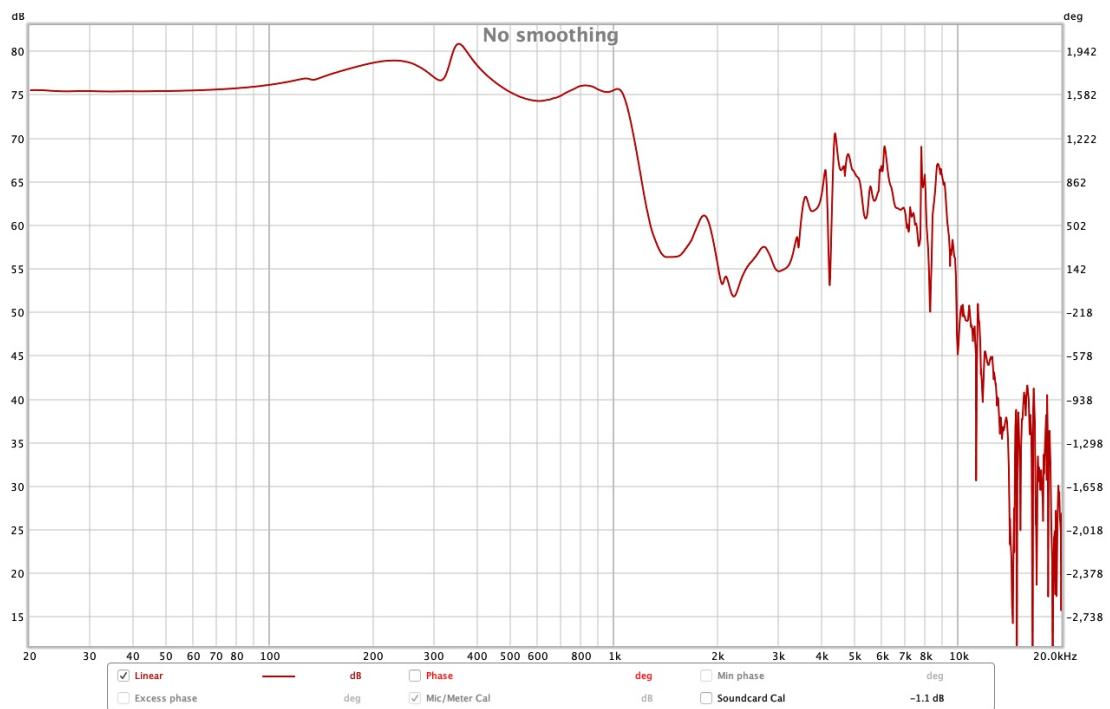


Fig. A.2: Amplitude frequency response of the 'Linear' filter setting on the B&K 4206 impedance tube

A.4 Left poti position: Low-Pass

The amplitude frequency response of the low-pass filtered audio signal has been visualized below:

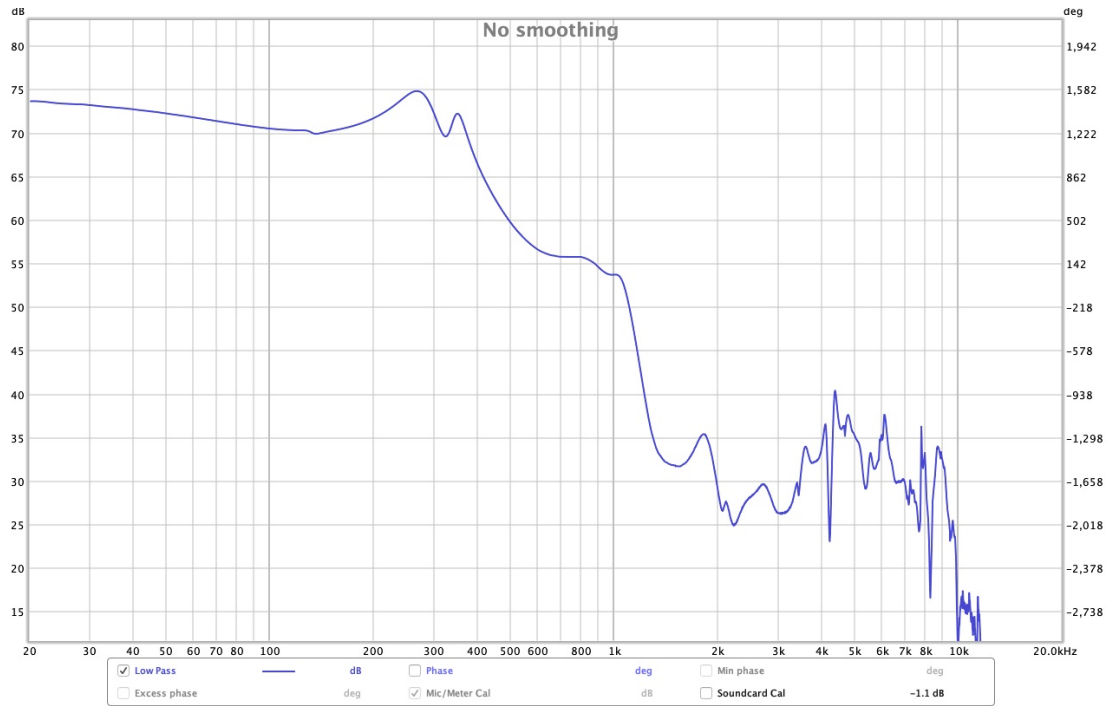


Fig. A.3: Amplitude frequency response of the 'Low-Pass' filter setting on the B&K 4206 impedance tube

If the low-passed amplitude frequency response is compared to the unfiltered linear frequency response the following table can be derived:

Frequency [Hz]	100	200	300	500	800	1027	1480	2700	3000	5380	11750
amplitude linear mode [dB _{SPL}]	76.1	78.5	77.0	75.3	76	75.7	56.3	57.6	54.7	60.6	39.7
amplitude low-pass mode [dB _{SPL}]	70.5	71.7	72.1	59.8	55.7	53.8	31.8	29.5	26.3	29.1	4.4
amplitude difference Δ [dB _{SPL}]	5.6	6.8	4.9	15.5	20.3	21.9	23.5	28.1	28.4	31.5	35.3

Tab. A.1: Frequency value data of B&K 4206 'Low-Pass' filter

It can be concluded that the output signal is generally lowered by the filter stage. However, it is not as easy to find clear indicators of a simple low-pass filter. While at around 300 Hz a cut-off frequency can be assumed it is not of a low-pass filter but rather of a shelf filter. It lowers the output amplitude of the higher frequencies by around 15 dB. This is supported by the values shown for the frequency range from 300 Hz to 800 - 1000 Hz. Over this range of a little less than two octaves, the amplitude is being drastically reduced and then stabilizes towards higher frequencies. In the frequency range above 1 kHz, only small amplitude reductions can be observed and a low-pass filter with a 3 dB/octave characteristic could be assumed. However, due to the age and individualism of the observed speaker, this might only be a subsidiary or spillover effect from the unambiguous shelf filtering and can therefore be neglected.

This estimation has been visualized in the following graphic:

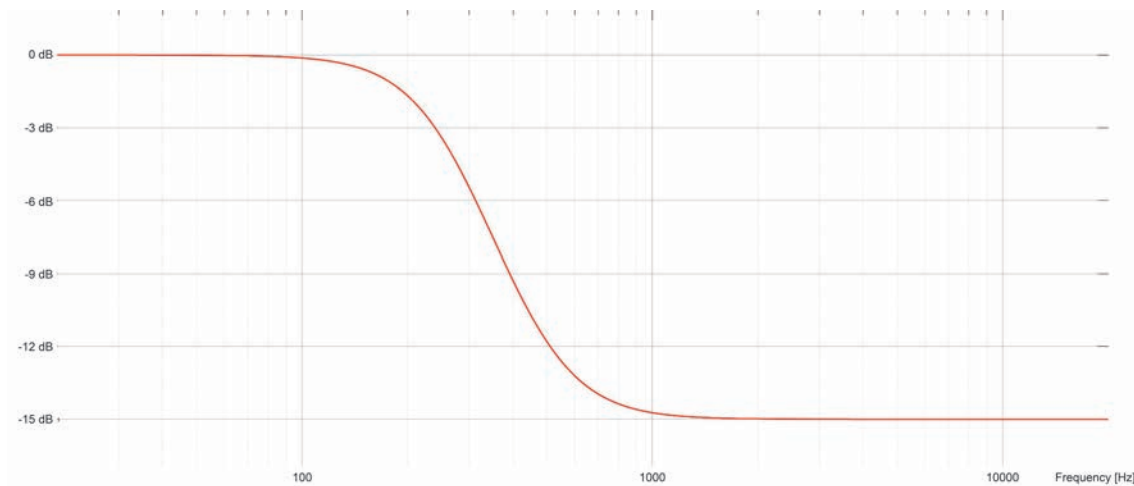


Fig. A.4: Filter estimation of the 'Low-Pass' filter on the B&K 4206 impedance tube

A.5 Right poti position: High-Pass

The third option to choose from is posed by the High-Pass option, as shown below:

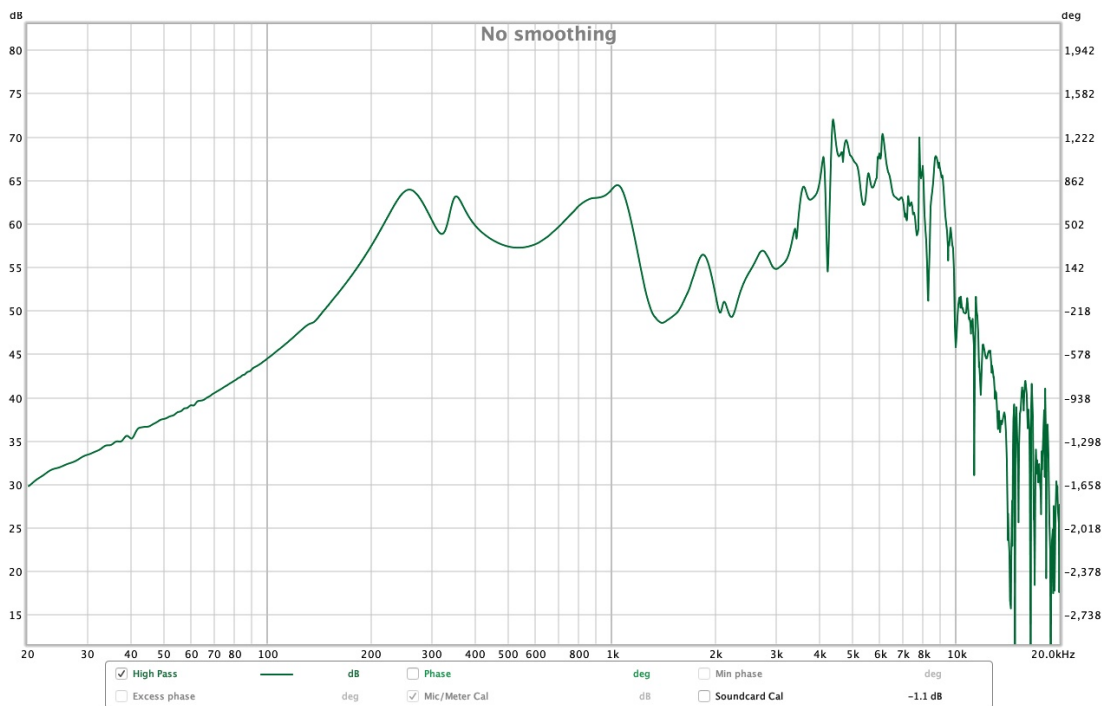


Fig. A.5: Amplitude frequency response of the 'High-Pass' filter setting on the B&K 4206 impedance tube

The amplitude frequency response of the high-pass filtered signal appears much more linear than the unfiltered “linear” signal above the cut-off frequency up to around 2.5 kHz where they start to match. With this option, it is much easier to find clear filtering. Assuming the cut-off frequency at around 250 Hz a high-pass filter is distinctly recognizable. If amplitude values of “linear” and “high-passed” signals are compared up to that frequency the following table can be arranged:

Frequency [Hz]	30	50	60	100	125	250
amplitude linear mode [dB_{SPL}]	75.5	75.5	75.5	76.0	76.9	78.8
amplitude high-pass mode [dB_{SPL}]	33.5	37.5	39.0	44.5	48.0	63.8
amplitude difference Δ [dB_{SPL}]	42.0	38.0	36.5	31.5	28.9	15.0

Tab. A.2: Frequency value data of B&K 4206 'High-Pass' filter

If now the amplitude differences Δ are compared in octave frequency pairs the slope of the filter can be determined:

$$\begin{aligned}\Delta_{30Hz} - \Delta_{60Hz} &= 42dB_{SPL} - 36.5dB_{SPL} = 5.5dB, \\ \Delta_{50Hz} - \Delta_{100Hz} &= 38dB_{SPL} - 31.5dB_{SPL} = 6.5dB, \\ \Delta_{60Hz} - \Delta_{125Hz} &= 36.5dB_{SPL} - 28.9dB_{SPL} = 7.6dB, \\ \Delta_{125Hz} - \Delta_{250Hz} &= 28.9dB_{SPL} - 15dB_{SPL} = 13.9dB.\end{aligned}$$

Based on these equations and supported by the visual graphs the slope of the filter can be assumed at around 6 dB/octave. This does not consider the obvious higher value in the octave from 125 Hz to 250 Hz, which has a calculated slope of ca. 14 dB/octave. This steeper slope can be attributed to the analog signal processing and a steeper slope towards the cut-off frequency, being more consistent in the filter's cut-off range. This tendency is supported by the above-calculated values and the visual curve of the amplitude frequency response. A visualization of this estimation can be found in the graphic below:

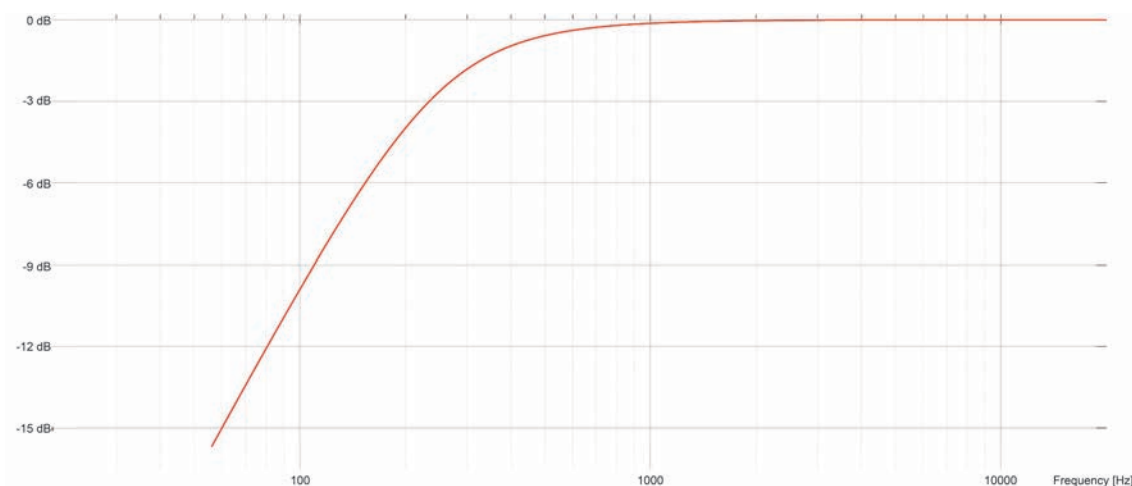


Fig. A.6: Filter estimation of the 'High-Pass' filter on the B&K 4206 impedance tube

B Software Overview and Module Description

Subsequently, the software will be introduced and a short overview of its modules is given.

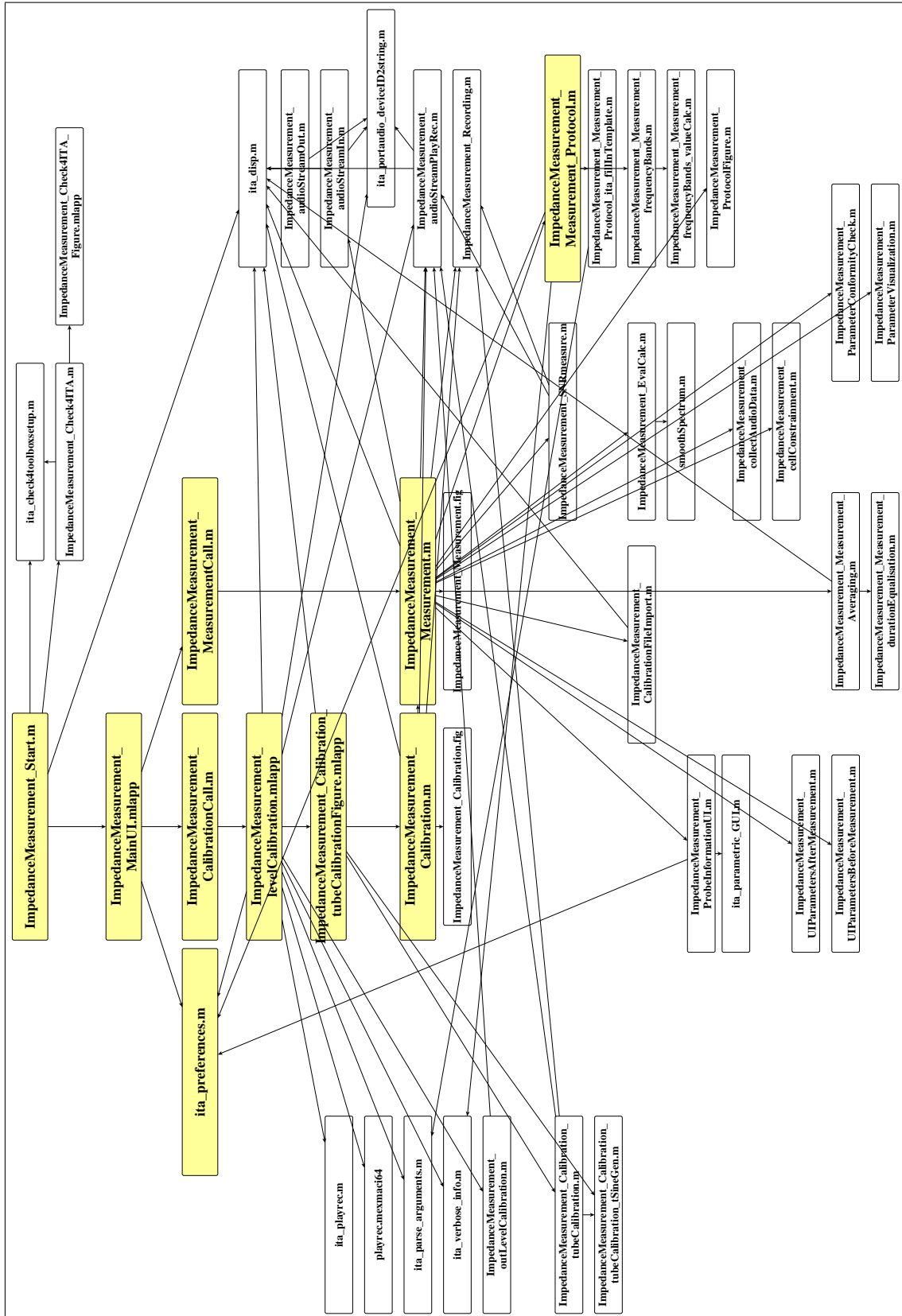
The entire program has been created and tested on Matlab R2018b (9.5.0.944444) maci64 on a MacBook Pro (15-inch, 2018) running macOS Mojave Version 10.14.6 (18G103). It was also tested on Windows. A HP 350 G2-Notebook running Windows 10 Pro Version 1909 (Build 18363.1016), successfully ran the software in a Matlab R2018b host environment.

Modules and functions of the following Matlab toolboxes have been used:


- Matlab toolboxes:
 - Audio Toolbox
 - Communications Toolbox
 - Data Acquisition Toolbox
 - Simulink Control Design
 - Wavelet Toolbox
- Third-party toolboxes:
 - ITA-Toolbox
 - IOSR-Toolbox

B.1 Call Graph











The following call graph illustrates the software's function dependencies and procedures.






















B.2 Directory Tree - Overview of all required files

 ImpedanceMeasurementFile Listing
Page 1

Name

-  ImpedanceMeasurement_Start.m
-  **Protocols**
-  **run**
 -  **calibrations**
 -  **components**
 -  **graphics**
 -  filmuni_logo_black_positiv_preview.jpg
 -  filmuni_logo_black_positiv_preview.png
 -  FUB-Logo-rgb.ai
 -  FUB-Logo-rgb.png

-  ImpedanceMeasurement_audioStreamIn.m
-  ImpedanceMeasurement_audioStreamOut.m
-  ImpedanceMeasurement_audioStreamPlayRec.m
-  ImpedanceMeasurement_Calibration.fig
-  ImpedanceMeasurement_Calibration.m
-  ImpedanceMeasurement_Calibration.m~
-  ImpedanceMeasurement_CalibrationCall.m
-  ImpedanceMeasurement_CalibrationFileImport.m
-  ImpedanceMeasurement_Calibration_tubeCalibration.m
-  ImpedanceMeasurement_Calibration_tubeCalibrationFigure.mlapp
-  ImpedanceMeasurement_Calibration_tubeCalibration_tSineGen.m
-  ImpedanceMeasurement_cellConstrainment.m
-  ImpedanceMeasurement_Check4ITA.m
-  ImpedanceMeasurement_Check4ITA_Figure.mlapp
-  ImpedanceMeasurement_collectAudioData.m
-  ImpedanceMeasurement_EvalCalc.m
-  ImpedanceMeasurement_EvalCalc.m~
-  ImpedanceMeasurement_levelCalibration.mlapp
-  ImpedanceMeasurement_levelCalibrations.m



ImpedanceMeasurement

File Listing
Page 2**Name**

- ImpedanceMeasurement_Measurement.fig
- ImpedanceMeasurement_Measurement.m
- ImpedanceMeasurement_MeasurementCall.m
- ImpedanceMeasurement_Measurement_Averaging.m
- ImpedanceMeasurement_Measurement_durationEqualisation.m
- ImpedanceMeasurement_Measurement_frequencyBands.m
- ImpedanceMeasurement_Measure...t_frequencyBands_valueCalc.m
- ImpedanceMeasurement_Measurement_Protocol.m
- ImpedanceMeasurement_Measure...rotocol_ita_fillInTemplate.m
- ImpedanceMeasurement_outLevelCalibration.m
- ImpedanceMeasurement_ParameterConformityCheck.m
- ImpedanceMeasurement_ParameterVisualization.m
- ImpedanceMeasurement_ProbeInformationUI.m
- ImpedanceMeasurement_ProtocolFigure.m
- ImpedanceMeasurement_Recording.m
- ImpedanceMeasurement_SNRmeasure.m
- ImpedanceMeasurement_UIParametersAfterMeasurement.m
- ImpedanceMeasurement_UIParametersBeforeMeasurement.m
- IoSR-Surrey-MatlabToolbox-4bff1bb**
 - smoothSpectrum.m
- ITA_Toolbox**
 - applications**
 - contents.m
 - CONTRIBUTING.md
 - debug**
 - external_packages**
 - Getting_Started.txt
 - HTML**
 - ita_toolbox_license.m



ImpedanceMeasurement

File Listing
Page 3**Name**

- ita_toolbox_setup.m
- ita_toolbox_uninstall.m
- kernel**
- license.txt
- pics**
- README.md
- tutorials**
- ita_toolbox_logo_wbg.png
- protocolTemplates**
- ImpedanceMeasurement_ProtocolTemplate_English.tex
- ImpedanceMeasurement_ProtocolTemplate_German.tex
- FUB-Logo-black.png
- FUB-Logo-white.png
- ImpedanceMeasurement_MainUI.mlapp
- measurements**
- recordings**
- settings**
- absorptionSmooth.mat
- CalibrationSignal.wav
- calibrationVarExport.mat
- completeUserParameters.mat
- emptyAudio.wav
- levelCalibrationSignal.wav
- measurementAllVarExport.mat
- measurementSaveBtnVarExport.mat
- UIParameters.mat
- UIParametersAfterMeasurement.mat
- UIParametersBeforeMeasurement.mat
- varsForProtocol.mat

B.4 Graphical User Interfaces (GUI-Modules)

ImpedanceMeasurement_MainUI

App Designer - Object

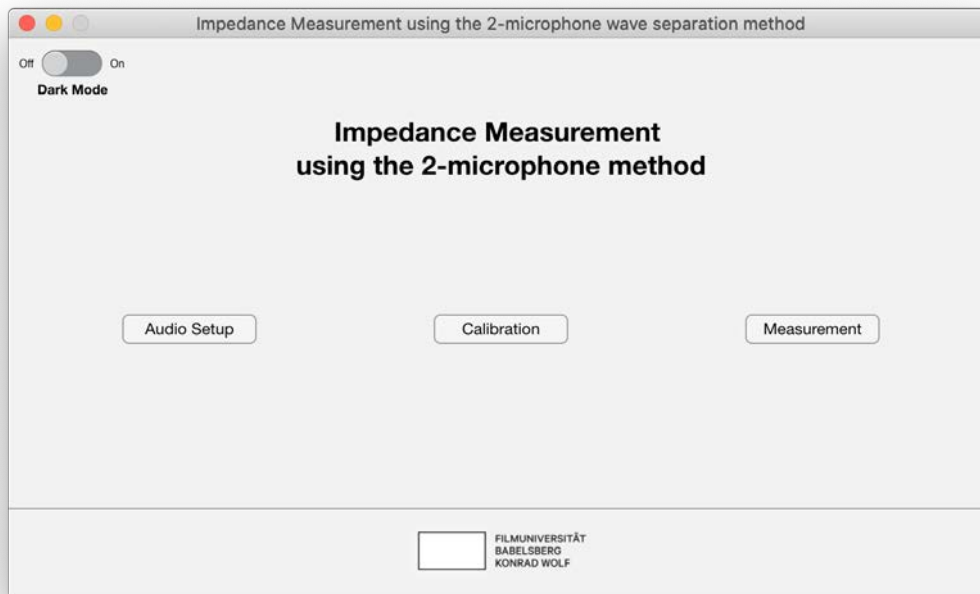


Fig. B.1: Main User Interface of 'ImpedanceMeasurement' program

function ita_preferences

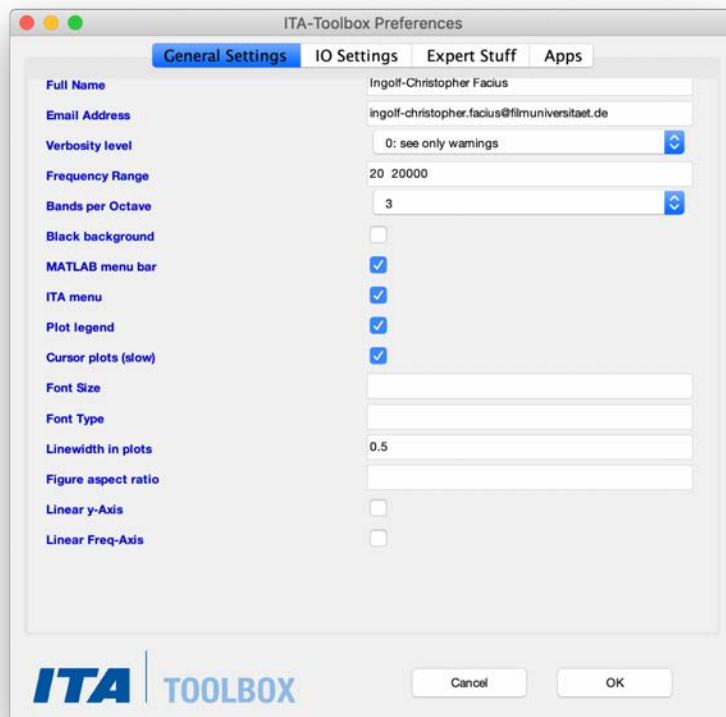


Fig. B.2: Preference UI of 'ImpedanceMeasurement' program

```

function varargout = ita_preferences(varargin)
%ITA_PREFERENCES - Switch Preference Mode Flag
% This function switches the flag of the preference mode requested.
% 0 means off and 1 means on. In case no preference exists, it simply
% returns all the RWTH_ITA_Toolbox preferences, together with their
% values.
%
% struct = ita_preferences() - return all existing preferences
% ita_preferences() - show GUI
% ita_preferences(struct) - set all fields specified in struct, can be used to restore/load settings (e.g. from another computer)
% ita_preferences('reset') - reset all preferences to default
%
%
% Call: ita_preferences('pref_name') - returns the value of the preference named pref_name.
% Call: [pref1, pref2] = ita_preferences({'pref1','pref2'}) - returns the values of all preferences in the argument cell
% Call: s = ita_preferences('s*') - returns all preferences starting with s
%
% Call: ita_preferences('pref_name',value) - Set preference pref_name to
% the given value;
%
% Remarks: ita_preferences_verbose(preference,value) - If preference
% doesn't exist yet, add it to the preferences and set it to value
% (value -> 'on'/'off')
%
% See also ita_toolbox_setup
%
% Reference page in Help browser
% <a href="matlab:doc ita_preferences">doc ita_preferences</a>
%
% <ITA-Toolbox>
% This file is part of the ITA-Toolbox. Some rights reserved.
% You can find the license for this m-file in the license.txt file in the ITA-Toolbox folder.
% </ITA-Toolbox>
%
% pdi: this function only takes care about the settings itself and how they
% are stored. The GUI is nested in a separate function as a graphical
% frontend only

```

ImpedanceMeasurement_Calibration

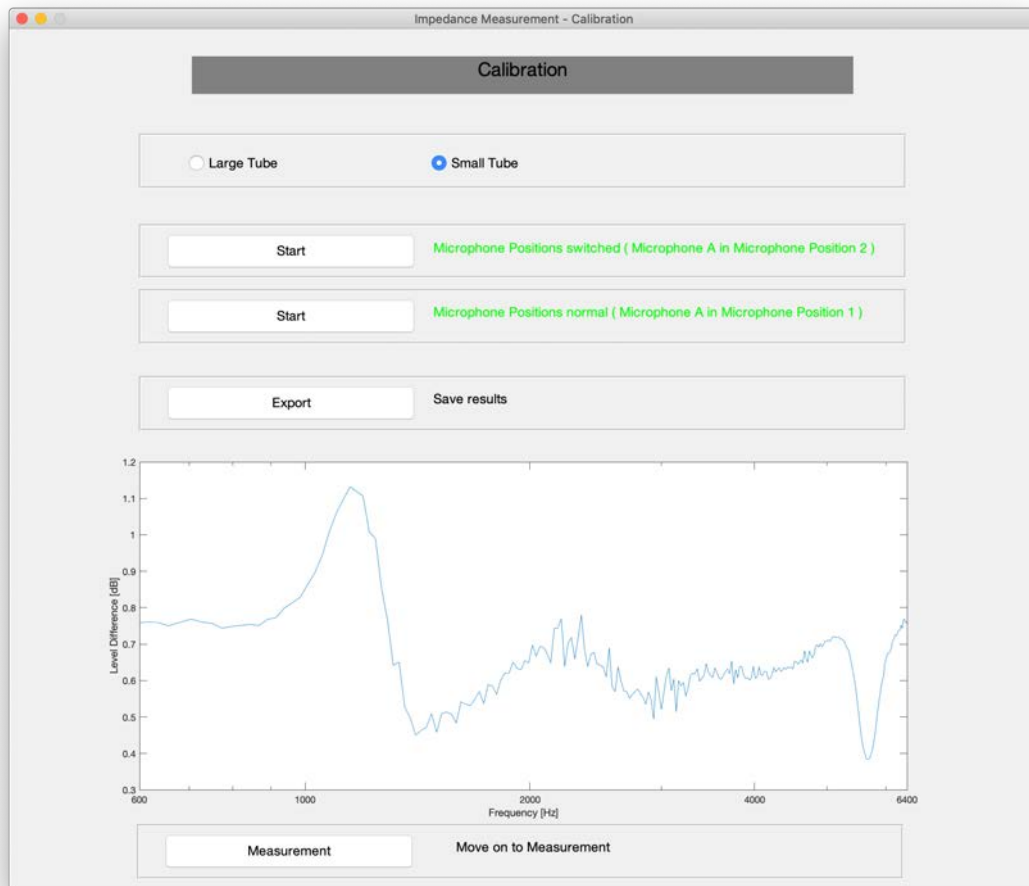


Fig. B.3: UI of 'ImpedanceMeasurement' Calibration module

ImpedanceMeasurement_Measurement

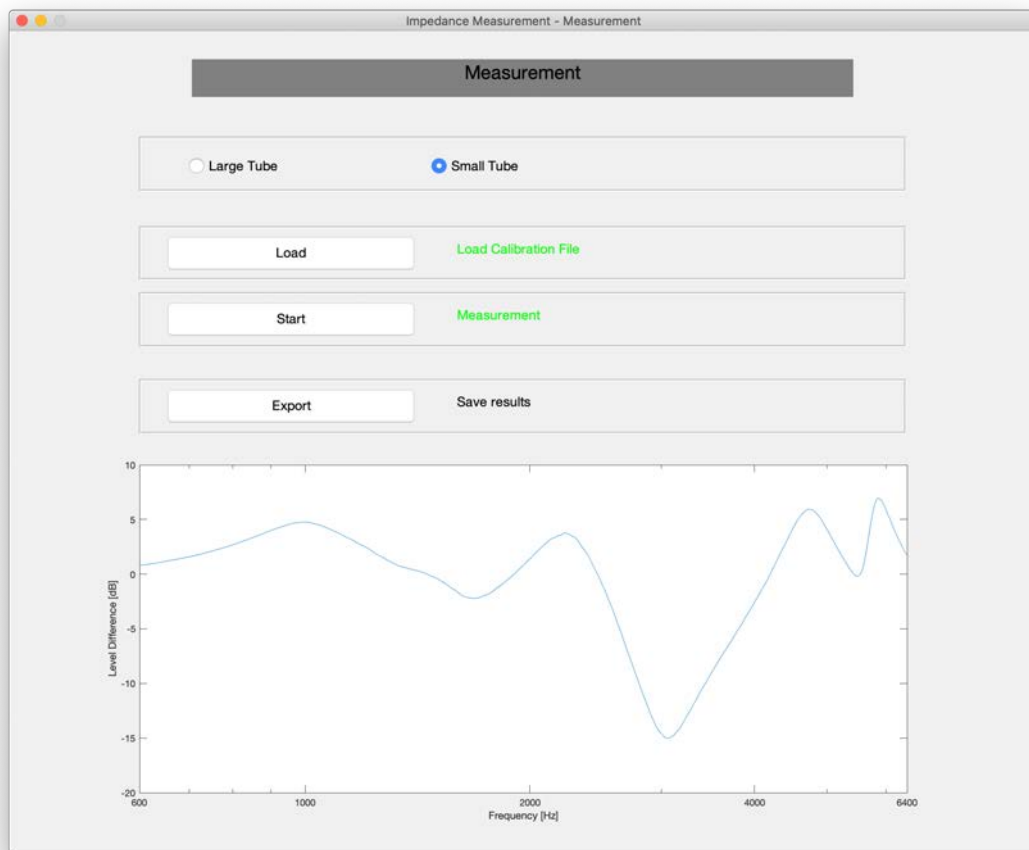


Fig. B.4: UI of 'ImpedanceMeasurement' Measurement module

ImpedanceMeasurement_Calibration_tubeCalibrationFigure

App Designer - Object

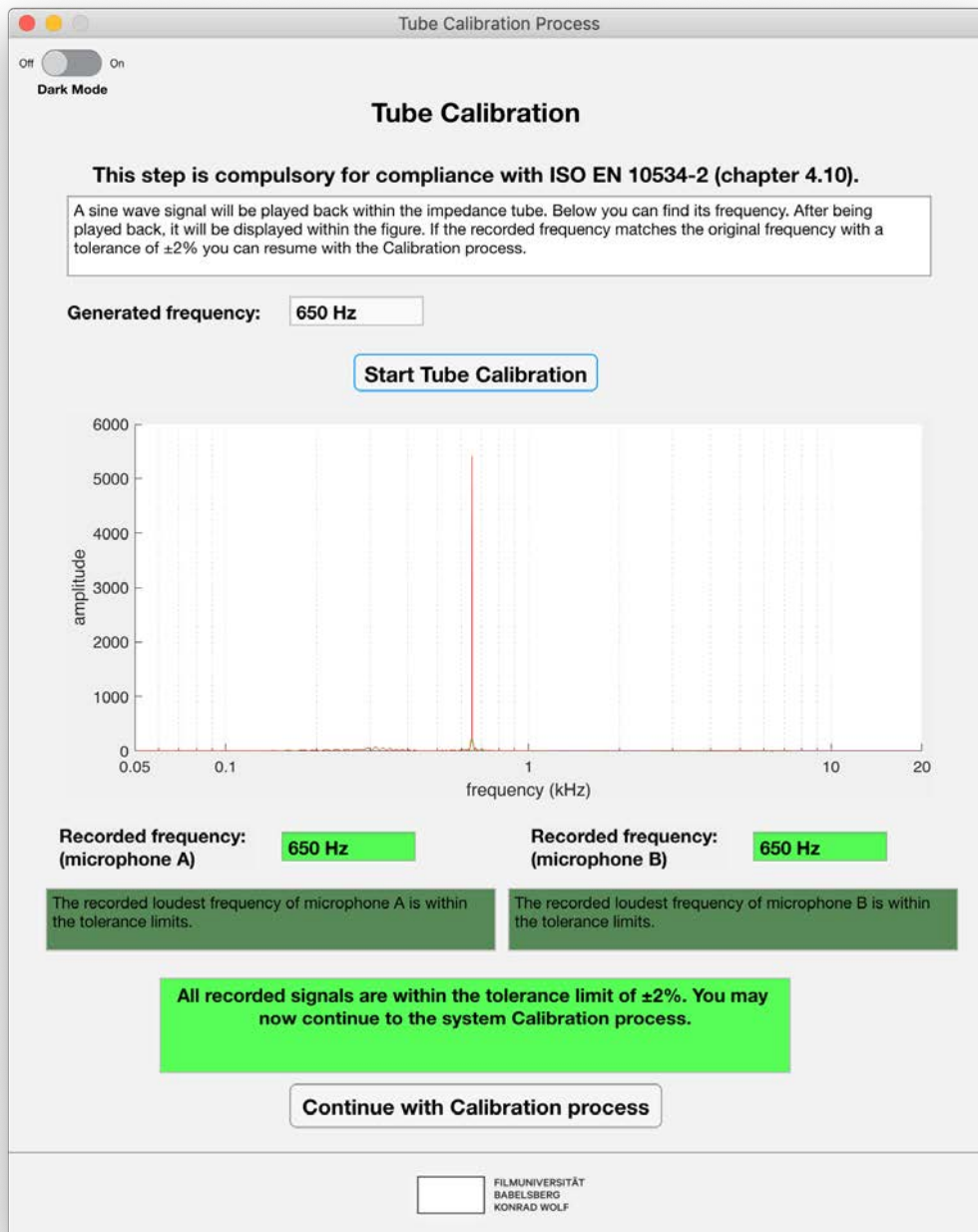


Fig. B.5: Impedance tube calibration UI of 'ImpedanceMeasurement' program

ImpedanceMeasurement_levelCalibration

App Designer - Object

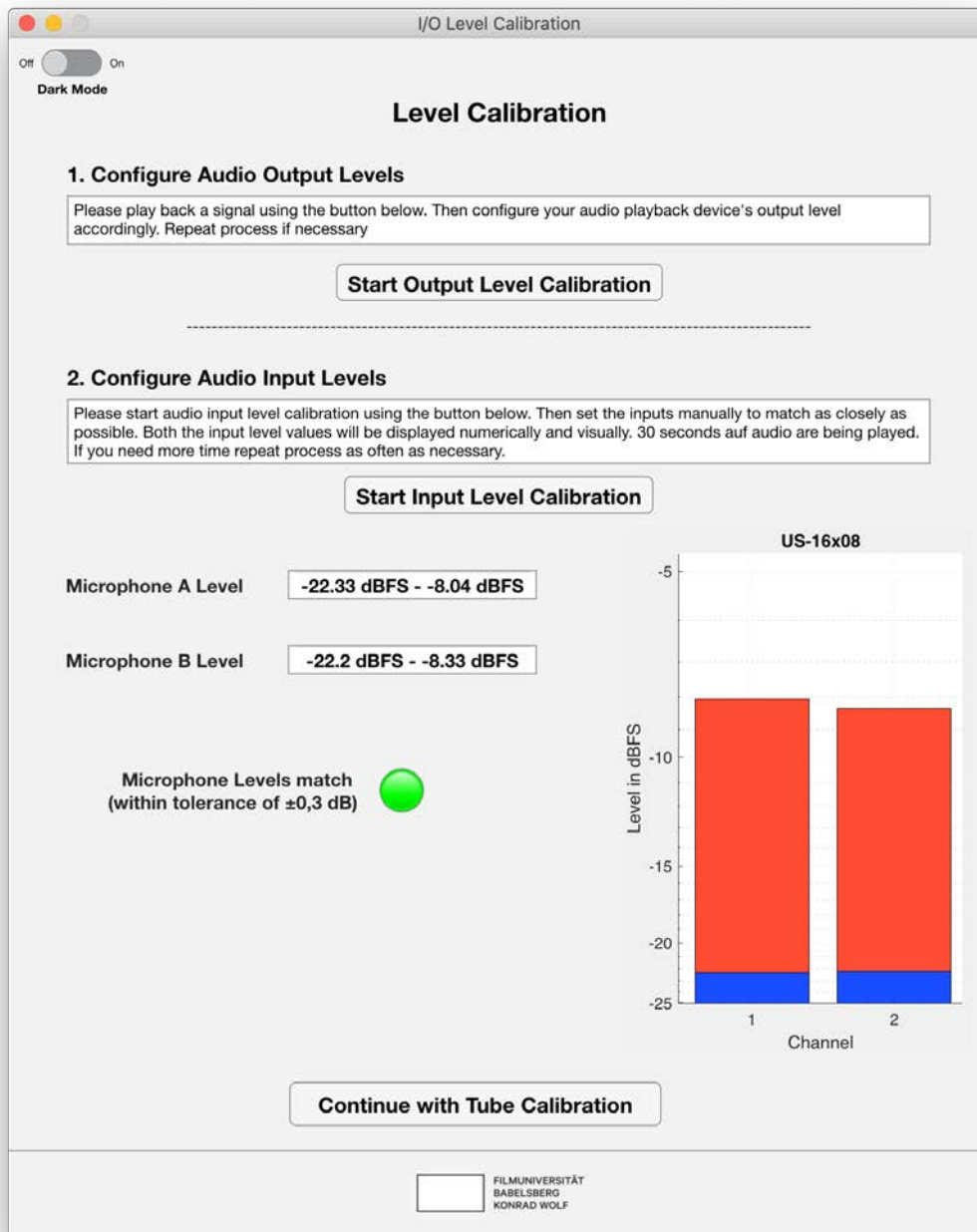
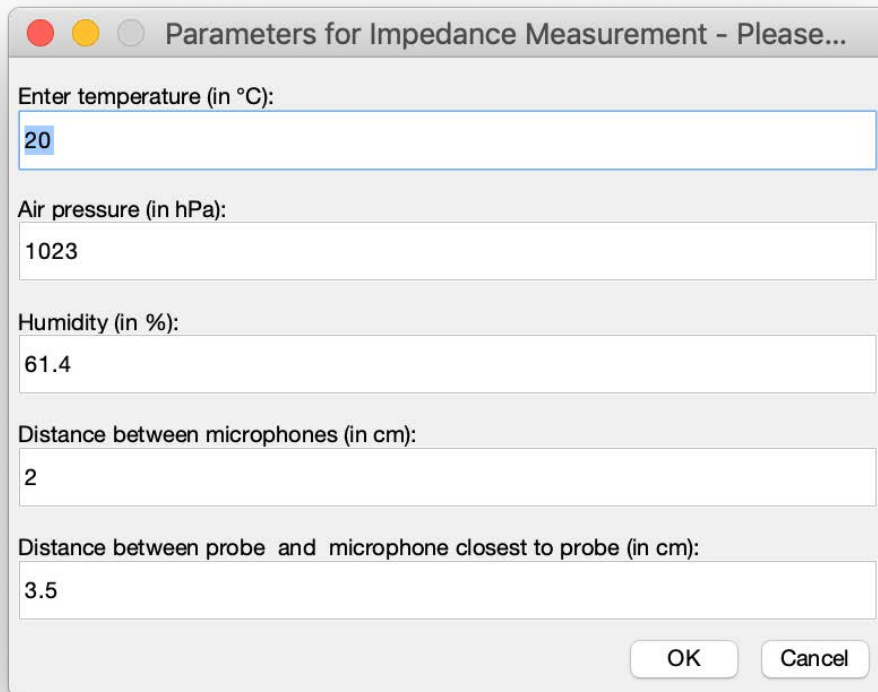


Fig. B.6: Level calibration module UI of 'ImpedanceMeasurement' program

functionImpedanceMeasurement_UIParametersBeforeMeasurement

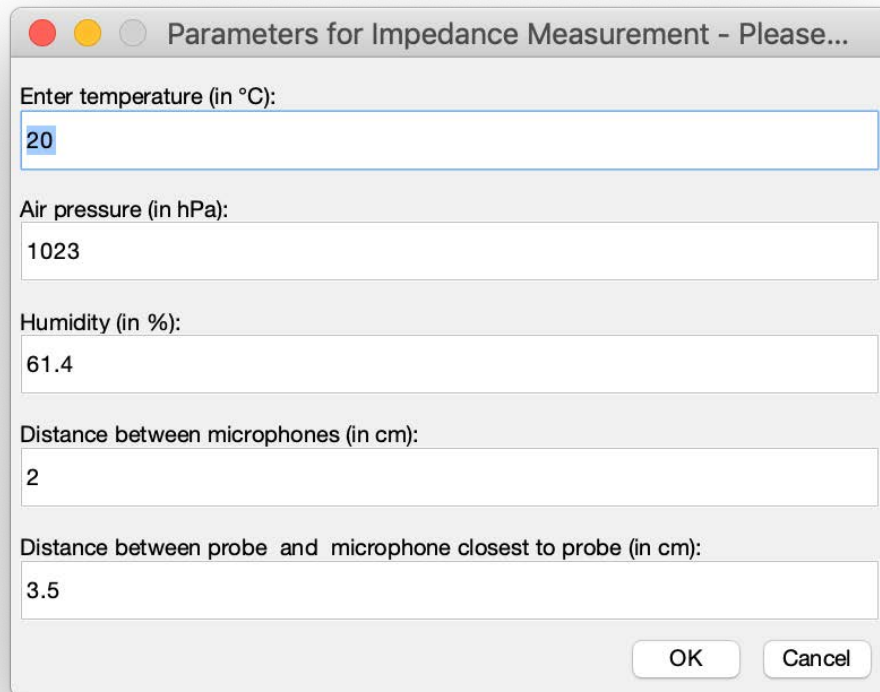


The image shows a dialog box titled "Parameters for Impedance Measurement - Please...". It contains five input fields for environmental and setup parameters, each with a label above it. The values entered in the fields are: 20 for temperature, 1023 for air pressure, 61.4 for humidity, 2 for microphone distance, and 3.5 for probe distance. At the bottom right, there are "OK" and "Cancel" buttons.

Parameter	Value
Enter temperature (in °C):	20
Air pressure (in hPa):	1023
Humidity (in %):	61.4
Distance between microphones (in cm):	2
Distance between probe and microphone closest to probe (in cm):	3.5

Fig. B.8: UI of 'ImpedanceMeasurement' program to set important environmental and setup parameters before the measurement


```
function ImpedanceMeasurement_UIParametersAfterMeasurement
```



Parameters for Impedance Measurement - Please...

Enter temperature (in °C):
20

Air pressure (in hPa):
1023

Humidity (in %):
61.4

Distance between microphones (in cm):
2

Distance between probe and microphone closest to probe (in cm):
3.5

OK Cancel

Fig. B.9: UI of 'ImpedanceMeasurement' program to set important environmental and setup parameters after the measurement

ImpedanceMeasurement_Check4ITA_Figure

App Designer - Object

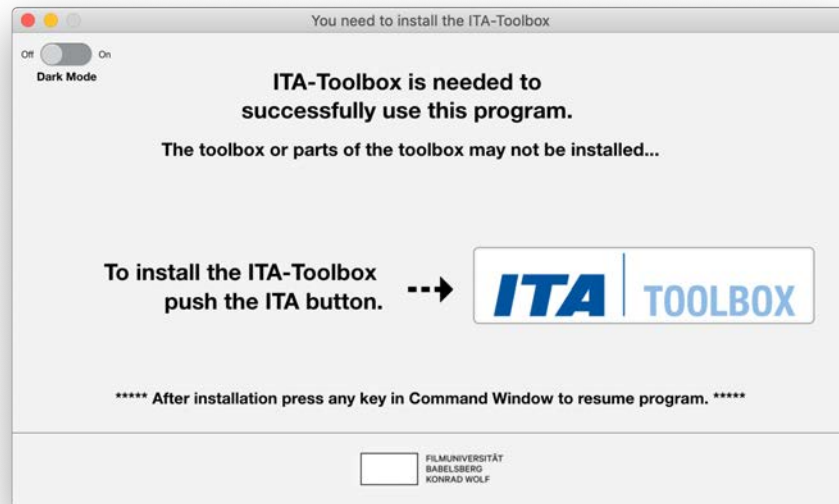


Fig. B.10: UI module of 'ImpedanceMeasurement' program that is called should the ITA-Toolbox not be installed

B.5 Visualization modules

function ImpedanceMeasurement_ParameterVisualization

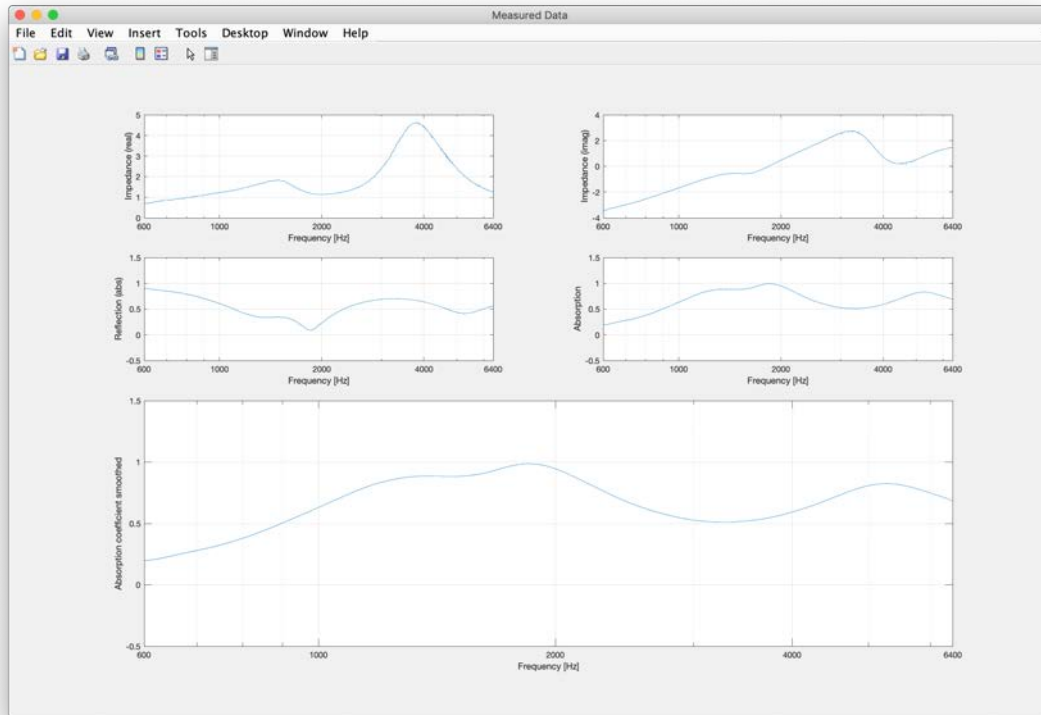


Fig. B.11: Example of figure module used to visually represent measurement results

B.7 Protocol module

function

ImpedanceMeasurement_Measurement_Protocol_ita_fillInTemplate

```

function ImpedanceMeasurement_Measurement_Protocol_ita_fillInTemplate(varargin)
%%%%%%%%%%%%%%%%%%%%%%%%%%%%%%%%%%%%%%%%%%%%%%%%%%%%%%%%%%%%%%%%%%%%%%%%
% Impedance Measurement using the 2-microphone wave separation method
%%%%%%%%%%%%%%%%%%%%%%%%%%%%%%%%%%%%%%%%%%%%%%%%%%%%%%%%%%%%%%%%%%%%%%%%
% Script functionality: script using ita_fillInTemplate functionalities
%                       + adds more tex sign translations
%                       + find ita_fillInTemplate Header attached to this
%                       header
%
% editor:   Ingolf-Christopher Facius
%           (ingolf-christopher.facius@filmuniversitaet.de)
%
% Date: August 08, 2020
%
% Version: 0.1
%
% Syntax:   ImpedanceMeasurement_Measurement_Protocol_ita_fillInTemplate(varargin)
%
% input parameters:   varargin
% output parameters:  none
%
% toolboxes:   Audio Toolbox
%              Communications Toolbox
%              Data Acquisition Toolbox
%              Simulink Control Design
%              Wavelet Toolbox
%
%              -----
%              ITA-Toolbox - get @ http://www.ita-toolbox.org
%
% Notes:
% ---
%
% Bug Info:
% no known bugs
%%%%%%%%%%%%%%%%%%%%%%%%%%%%%%%%%%%%%%%%%%%%%%%%%%%%%%%%%%%%%%%%%%%%%%%%
% ITA_FILLINTEMPLATE - replaces keyword in *.tex file by given strings
% This function ++++ FILL IN INFO HERE +++
%
% Syntax:
% audioObjOut = ita_fillInTemplate(audioObjIn, options)
%
% Options (default):
% 'opt1' (defaultopt1) : description
% 'opt2' (defaultopt1) : description
%
%
% 'opt3' (defaultopt1) : description
%
% Example:
% audioObjOut = ita_fillInTemplate(audioObjIn)
%
% See also:
% ita_toolbox_gui, ita_read, ita_write, ita_generate
%
% Reference page in Help browser
% <a href="matlab:doc ita_fillInTemplate">doc ita_fillInTemplate</a>
%
% <ITA-Toolbox>
% This file is part of the application Kundt for the ITA-Toolbox. All rights reserved.
% You can find the license for this m-file in the application folder.
% </ITA-Toolbox>
%
% Author: Martin Guski -- Email: martin.guski@akustik.rwth-aachen.de
% Created: 13-Oct-2010
%
% TODO:
% - sonderzeichen ersetzen: &AaUuOo\

```

function ImpedanceMeasurement_Measurement_Protocol

Function to generate Measurement protocol by using a LaTeX-template, filling in all the information and exporting to PDF. This function is language dependent, therefore creating either an English or a German measurement protocol.

```
function [] = ImpedanceMeasurement_Measurement_Protocol(audioSetup, probeInfo, completeUserParameters, measurement, TF, xs, \
absorptionSmooth, figureFileName, tubeTypeStr, airPressureDif)
%%%%%%%%%%%%%%%%%%%%%%%%%%%%%%%%%%%%%%%%%%%%%%%%%%%%%%%%%%%%%%%%%%%%%%%%
% Impedance Measurement using the 2-microphone wave separation method
%%%%%%%%%%%%%%%%%%%%%%%%%%%%%%%%%%%%%%%%%%%%%%%%%%%%%%%%%%%%%%%%%%%%%%%%
% Script functionality: script to generate test protocol
% based on and using functionalities from
% ita_kundt_protocol
%
% editor:   Ingolf-Christopher Facius
%           (ingolf-christopher.facias@filmuniversitaet.de)
%
% Date: August 08, 2020
%
% Version: 0.1
%
% Syntax:   [] = ImpedanceMeasurement_Measurement_Protocol(audioSetup, probeInfo, ...
%               completeUserParameters, measurement, TF, xs, ...
%               absorptionSmooth, figureFileName)
%
% input parameters:
%   audioSetup
%   probeInfo
%   completeUserParameters
%   measurement
%   TF
%   xs
%   absorptionSmooth
%   figureFileName
%   tubeTypeStr
%   airPressureDif
%
% output parameters:   none
%
% toolboxes:   Audio Toolbox
%               Communications Toolbox
%               Data Acquisition Toolbox
%               Simulink Control Design
%               Wavelet Toolbox
%
%               -----
%               ITA-Toolbox - get @ http://www.ita-toolbox.org
%
% Notes:
% ---
%
% Bug Info:
% no known bugs
```


English protocol:

**MEASUREMENT PROTOCOL:
Determination of sound absorption coefficient in the impedance tube according to EN ISO 10534-2**

Description of the testing environment:

Impedance tube used: B&K 4206 impedance tube
 Impedance tube setup: Small Tube Setup
 Excitation: using random white noise
 Evaluation: in accordance to EN ISO 10534-2 using the transfer function method (two-microphone wave-separation method).

Test date: 2020/08/27
 Test Engineer: Ingolf-Christopher Fackius
 Location: Potsdam, Germany
 Testing station: Acoustics Lab A

Meteorological conditions: Temperature: 20 °C Humidity: 61,4 %
 Air pressure: 1023 hPa Air density: 1,1968 kg/m³

Description of the materials to be examined and the testing arrangement:

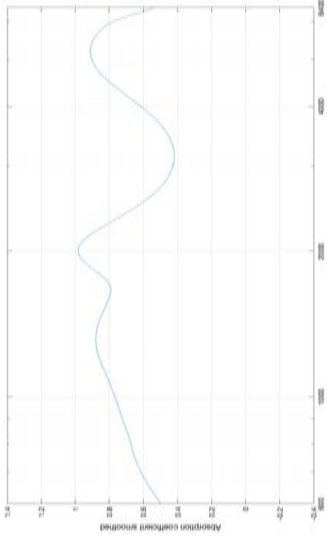
Anthracite-coloured, partly closed-pored cell foam. Thickness approx. 52 mm. Precise placement of the samples in the sample holder with tight closure to the wall. Installation of the samples without clearance in front of the soundproof tube end.

Designation of the sample: Probe A
 Thickness of probe: 2 cm
 Number of Repetitions: 3

Measurement System:

Sound source: B&K 4206 - built in driver + Waingine WPA-600PRO
 Sound Card: US-16x08
 Microphones: 2x Microtech Gefell measurement microphone capsule 1/4" MK301E (ser.no. 0556 + 0557) + measurement microphone preamp 1/2" P48 MV220 (ser.no. 1015 + 1033)

Pre-amps: between micro-phones: 2 cm
 Distance between microphones: 3,5 cm
 Signal to Noise Ratio: 60,487 dB
 Notes: no comments



Absorption coefficient α

f [Hz]

Figure 1: Frequency-dependent absorption coefficient. Calculation based on the measurements of 3 Repetitions. Curve smoothed by applying moving average: smoothing parameter: 1/12 octave, Gaussian window.

f [Hz]	630.00	800.00	1000.00	1250.00	1600.00	2000.00
α	0.54	0.67	0.77	0.86	0.82	0.93
f [Hz]	2500.00	3150.00	4000.00	6300.00	6300.00	
α	0.62	0.44	0.62	0.88	0.53	

German protocol:

Messprotokoll zur Messung des Absorptionsgrades im Impedanzmessrohr nach EN ISO 10534-2

Beschreibung der Prüfumgebung:

Verwendetes Impedanzrohr: B&K 4206 Impedanzrohr
 Aufbau des Impedanzrohrs: Kleines Rohr
 Anregung: mittels zufälligen weißem Rauschen
 Auswertung: nach EN ISO 10534-2 unter Anwendung des Übertragungsfunktionsverfahrens (Zwei-Mikrofonwellentrennungsverfahren).

Prüfdatum: 2020/08/27
 Prüfer: Ingolf-Christopher Factus
 Ort: Potsdam, Deutschland
 Prüfstelle: Akustiklabor

Meteorologische Bedingungen: Temperatur: 20 °C Luftfeuchtigkeit: 61,4 %
 Luftdruck: 1023 hPa Luftdichte: 1,1968 kg/m³

Beschreibung der zu untersuchenden Materialien und der Versuchsanordnung:

Auftragsfähigkeit: teils geschlossener-poriger Zellschaum. Dicke ca. 52 mm Passgenaue Platzierung der Samples im Probenhalter mit dichtem Abschluss zur Wandung. Einbau der Proben ohne Abstand vor dem schallharten Rohrabschluss.

Bezeichnung der Probe: Praeling A
 Dicke der Probe: 2 cm
 Anzahl der Wiederholungen: 3

Messsystem:

Schallquelle: B&K 4206 - eingebauter Treiber + Verstärker XY 50W @ 8 Ohm
 Soundkarte: US-16x08
 Mikrofone: 2x Microtech Gefell Messmikrofonkapsel 1/4" MK301E (Seriennummern 0556 + 0557) + Messmikrofonvorverstärker 1/2" P48 MV220 (Seriennummern 1015 + 1033)
 Vorverstärker: US-16x08 - eingebaute Vorverstärker
 Abstand zwischen den Mikrofonen: 2 cm
 Abstand zwischen Mikrofonen und Probe: 3,5 cm
 Signal-Rausch-Abstand: 60,2911 dB
 Notizen: keine Anmerkungen

Abbildung 1: Frequenzabhängiger Absorptionskoeffizient. Die Berechnung basiert auf den Messungen von 3 Wiederholungen. Kurve geglättet durch Anwendung des gleitenden Mittelwerts: Glättungsparameter 1/12 octave, Gaussfaster.

f/Hz	630,00	800,00	1000,00	1250,00	1600,00	2000,00
α	0,54	0,67	0,77	0,86	0,82	0,93
f/Hz	2500,00	3150,00	4000,00	6300,00	6300,00	
α	0,62	0,44	0,62	0,88	0,53	

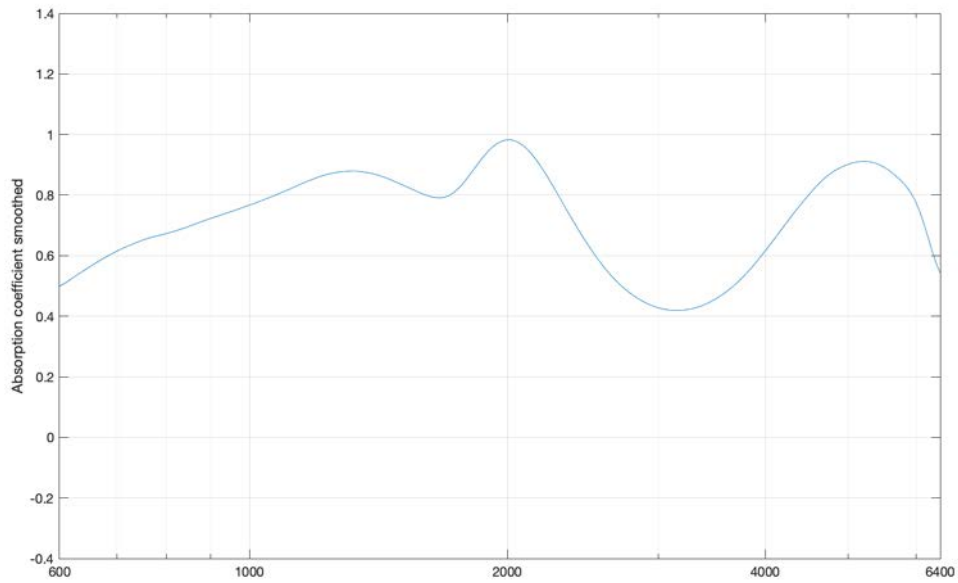
`function ImpedanceMeasurement_ProtocolFigure`

Fig. B.12: Example of figure module used to visually represent smoothed absorption data for measurement protocol

C Measurement data for phase comparison of different microphone pairs

C.1 Product and measurement data of Microtech Gefell MK301E

C.1.1 Product Data (Microtech Gefell n.d.)



MICROTECH GEFELL 
microphones & acoustic systems - founded 1928 by Georg Neumann

Kondensator-Messmikrofonkapsel MK 301 E

Die 1/4" Messmikrofonkapsel MK 301 E ist für akustische Messungen in Forschung, Entwicklung und Industrie konzipiert und wird unter anderem auch in der Bauakustik und der Audiometrie eingesetzt.

■ Frequenzbereich 5 Hz bis 100 kHz, Freifeld ■ Schalldruckpegel bis 158 dB



Die Messmikrofonkapsel verfügt über eine fixierte Ladungsträgerschicht (Backelektret) zur Bereitstellung der Polarisationsspannung. Der sorgfältige Aufbau und das konstruktive Konzept der Mikrofonkapsel garantieren eine hohe zeitliche Konstanz der elektroakustischen Parameter. Alle wichtigen Teile, einschließlich der in einem speziellen galvanischen Verfahren hergestellten und befestigten Membran, bestehen aus Nickel. Die Membran ist durch eine Schutzkappe vor mechanischen Beschädigungen geschützt.

Der statische Druckausgleich zwischen dem inneren Hohlraum und der Atmosphäre wird über eine seitliche Kapillare gewährleistet. Zur einfachen Kontrolle des Druckfrequenzganges kann ein separates Eichgitter verwendet werden, z.B. UA 0033 mit DB 0264. Der international übliche Gewindetyp (60 UNS) für den Anschluss der Mikrofonkapsel gestattet die Austauschbarkeit mit anderen 1/4" Mikrofonkapseln und ermöglicht den Anschluss an alle geeigneten 1/4" bzw. 1/2" Kalibrier- und Messgeräte.

Condenser Measuring Microphone Cartridge Type MK 301 E

The 1/4" measuring microphone cartridge MK 301 E is designed for acoustical measurements in research and development and also for industrial use. Some applications include audiology, the measurement of building acoustics and noise levels.

■ Frequency range 5 Hz to 100 kHz, free-field ■ Sound pressure levels up to 158 dB

The microphone cartridge has a fixed layer of backelectret to supply the polarization voltage. It is designed and very carefully constructed to ensure excellent long-time stability of the electroacoustical parameters. All essential components including the diaphragm are made of nickel and the diaphragm is bonded by a special galvanic process. The rear electrode is insulated from the cartridge housing by a quartz glass plate. The diaphragm is protected against mechanical damage by a protection grid in which an insulated calibration grid is integrated.

The equalization of the static air pressure between the inside and outside of the MK 301 E cartridge is by means of a capillary tube side-vented. The individual pressure frequency response curves can be conveniently measured by using a calibration grid, e.g. UA 0033 by means of the adaptor DB 0264. The cartridge uses the international standard thread 60 UNS which ensures compatibility with a wide range of calibration equipment and measurement devices available from many manufactures.

Lieferumfang/ Delivery

Messmikrofonkapsel	MK 301 E im Holzetui	Best.-Nr./ Order-No. Best.Nr. 311111
Measuring Microphone Cartridge	MK 301 E in wooden case	

Technische Daten/ Specifications MK 301 E

Wandlertyp Transducer type	Kapazitiver Druckempfänger Capacitive pressure transducer
■Frequenzbereich des Freifeldübertragungsmaßes ■Frequency range free-field response	5 Hz ... 100 kHz (± 2 dB)
■Feld-Leerlauf-Übertragungsfaktor/ Sensitivity	4 mV/ Pa
Grenzschalldruckpegel für 3 % Klirrfaktor bei 1 kHz Max. SPL for THD ≤ 3 % at 1 kHz	158 dB
Eigenrauschen mit Vorverstärker MV 310 Inherent noise with preamplifier MV 310	36 dBA
Polarisationsspannung/ Polarization	backelectret
■Kapazität mit Polarisationsspannung bei 1 kHz ■Polarized cartridge capacitance at 1 kHz	4,5 pF
Arbeitstemperaturbereich Operating temperature range	-20 ... +100 °C
Feuchtigkeit/ Humidity	bis/ to 70 °C, 90 %
Temperaturkoeffizient Main ambient temperature coefficient	≤ 0,01 dB/K
Statischer Druckkoeffizient Main ambient pressure coefficient	-5 -1x10 ⁻⁵ dB/Pa
Durchmesser/ Diameter	
mit Schutzkappe/ with protection grid	7,0 ± 0,02 mm
ohne Schutzkappe/ without protection grid	6,35 ± 0,02 mm
Höhe/ Height	9,7 mm
Gewicht/ Weight Gewinde für Gewinde für Vorverstärker/ Preamplifier thread	2 g
Gewinde für Schutzkappe/ Protection grid thread	5,7 mm 60 UNS 6,35 mm 60 UNS

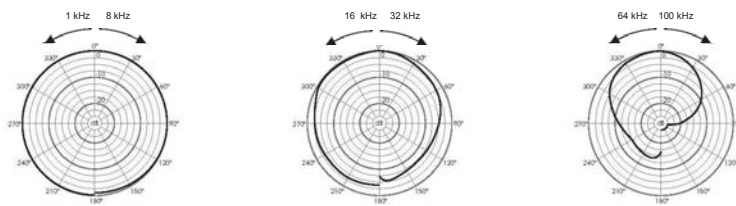
Wartung und Instandhaltung

Zur Gewährleistung der Funktionstüchtigkeit ist die Messmikrofonkapsel vor mechanischen Beschädigungen zu schützen und in Abhängigkeit von den Einsatzbedingungen in festzulegenden Intervallen im betriebsspannungsfreien Zustand allseitig auf Verschmutzung zu überprüfen. Nach Entfernen der Schutzkappe sind die Verunreinigungen in deren Innenraum sowie auf der Membran äußerlich vorsichtig mit einem weichen Pinsel oder Tuch zu entfernen. Die Messmikrofonkapsel ist nicht für den Einsatz in chemisch aggressiven Medien und leitendem Staub geeignet. Kondensatbildung ist auszuschließen.

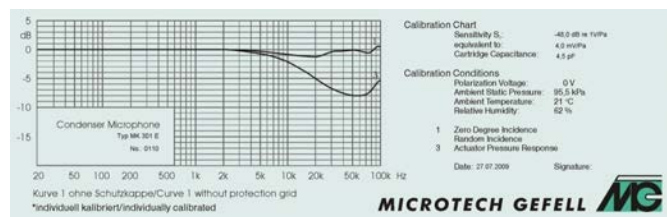
Maintenance and upkeep

In order to maintain its functioning the measurement microphone cartridge should be protected against mechanical damage. It should be disconnected from its power source and completely checked for any pollution in regular intervals that have to be defined depending on the operating conditions. After removal of the protection grid the pollution within the grid and on the diaphragm should be cleaned very carefully with a soft clean cloth or brush. The measurement microphone cartridge is not suitable for use in chemical aggressive conditions and in conductible dust. Condensation must be avoided.

Polardiagramme/ Polar patterns



Frequenzgänge/ Frequency responses



Microtech Gefell GmbH • Georg-Neumann-Platz • 07926 Gefell • Germany
Phone +49 (0)36649 882-0 • Fax +49 (0)36649 882-11 • www.microtechgefell.de • info@microtechgefell.de

C.1.2 Measurement Data

Calibration data of MK301E with serial number 0556

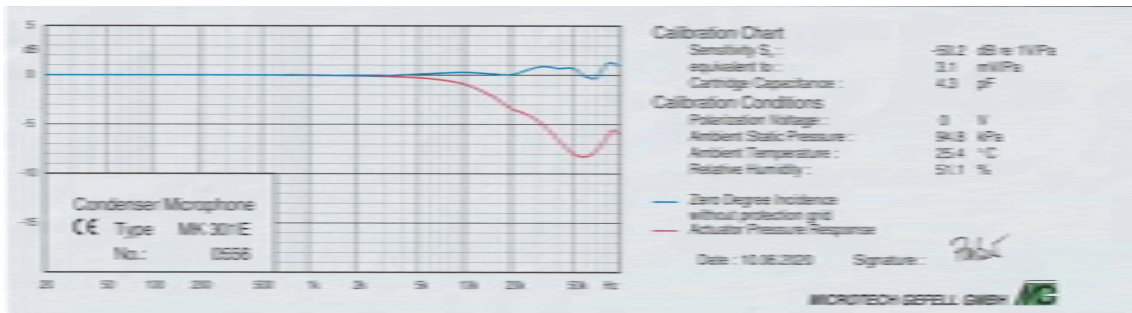


Fig. C.1: Original calibration data of MK301E (ser. 0556)

Calibration data of MK301E with serial number 0557

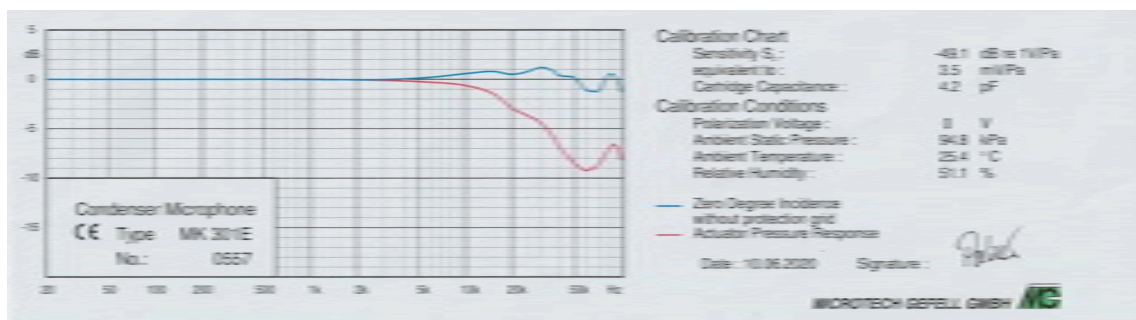


Fig. C.2: Original calibration data of MK301E (ser. 0557)

Calibration data of difference in phase response of MK301E with serial numbers 0556 and 0557

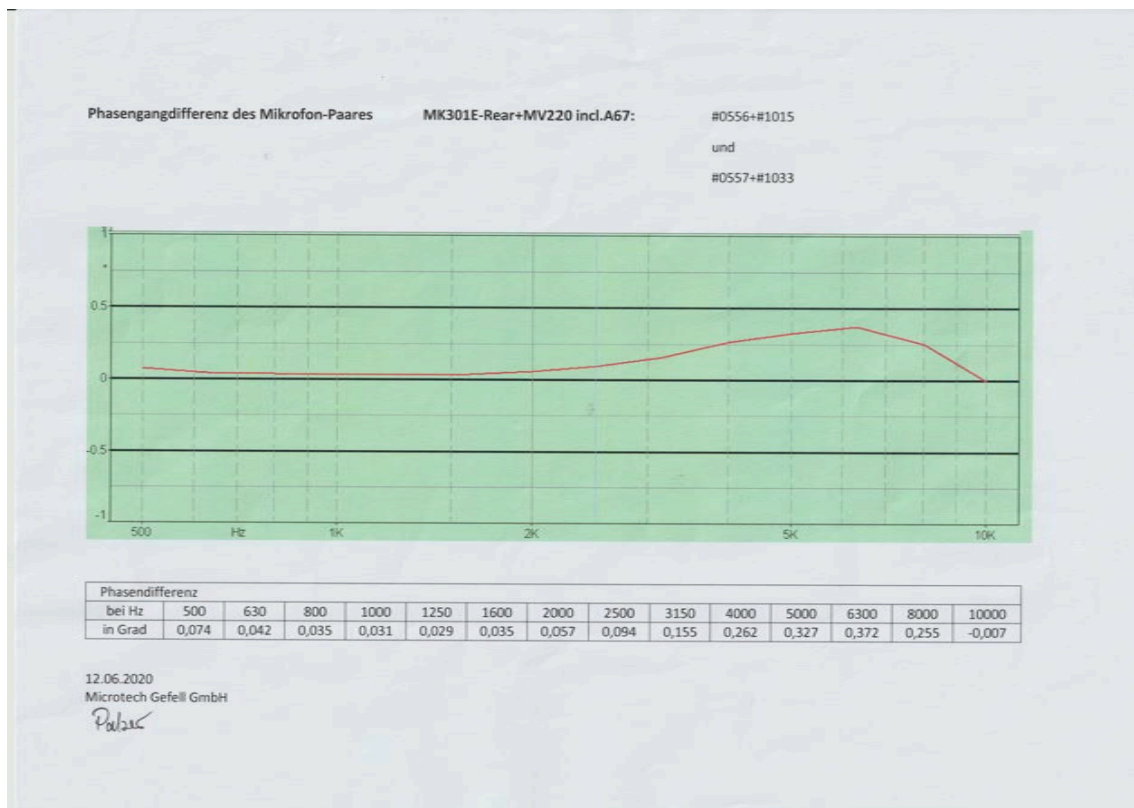
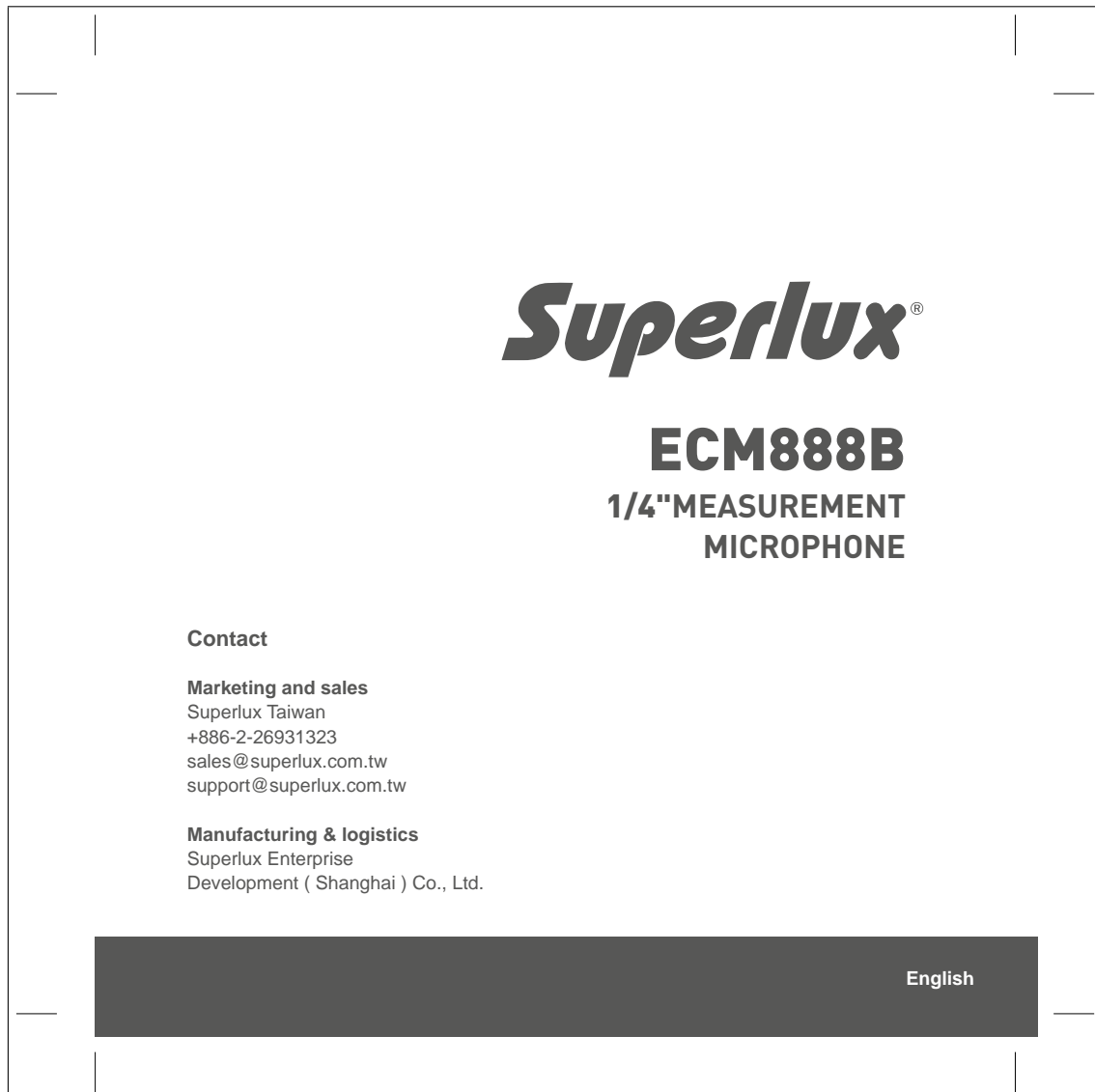


Fig. C.3: Original measurement of differences in phase frequency response of both MK301E

C.2 Product data of Superlux ECM888B (Superlux 2018: 1-5)



ECM888B

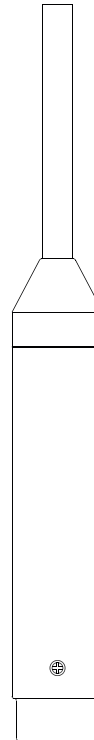
1/4" MEASUREMENT MICROPHONE

GENERAL DESCRIPTION

The ECM888B is a 1/4" standard measurement microphone powered by an internal battery. There is no external power needed for easier connection to various devices such as a real time analyzer, PC, or palm-size devices. Its wide and flat frequency response makes the ECM888B an ideal measurement and recording microphone.

FEATURES

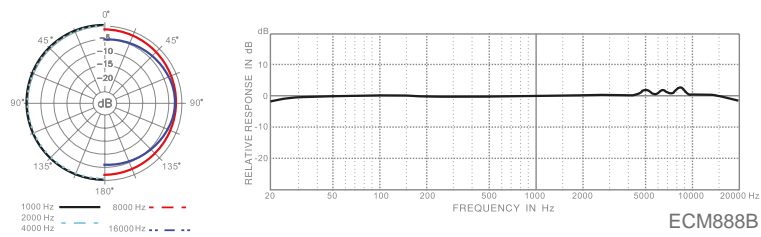
- Metal structure with champagne silver finish
- Wide frequency response from 20 Hz to 20 kHz
- Suitable for spectrum analyzer, audio testing and measurement applications
- Internal battery, 6V 4LR44 battery
- 1/4" industrial standard diameter



APPLICATIONS

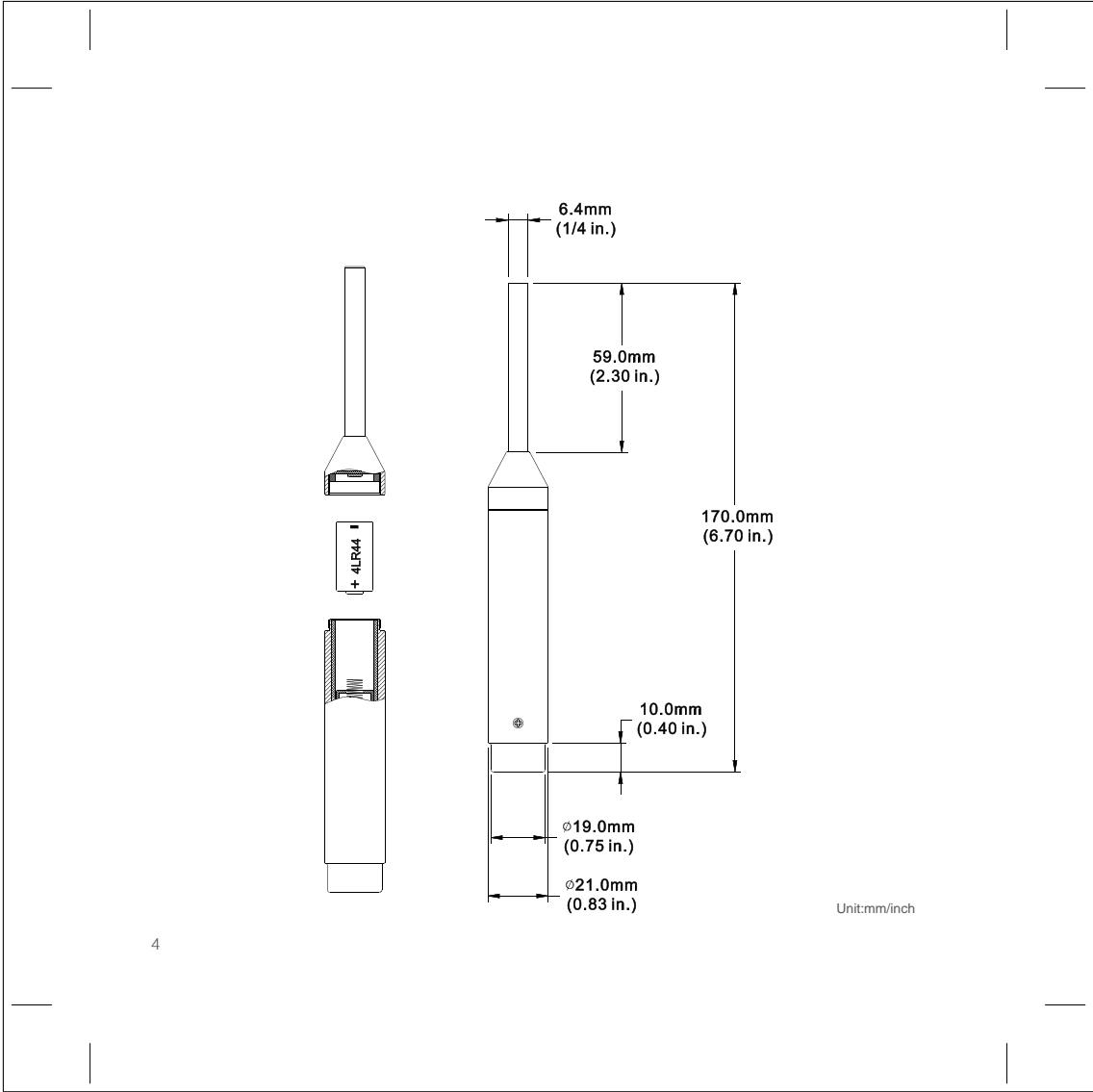
Measurement / Recording

ECM888B FREQUENCY RESPONSE (Omni)



Omni

With equal sensitivity in all directions, an omni microphone doesn't need to point toward the sound source. It features low handling and wind noise. It is welcomed for news gathering and music recording applications.



*Note: Specifications are subject to change.

SPECIFICATIONS

Type	Back electret, Ø6 mm (Ø0.24")
Polar Pattern	Omni
Frequency Response	20-20,000 Hz
Sensitivity	-43 dBV/Pa (4 mV)
Output Impedance	800 Ω
Min. Load Impedance	3 kΩ
S/N Ratio	72 dB
Equivalent Output Noise	22 dB
Max. SPL	132 dB SPL
Dynamic Range	110 dB
Power Requirements	6V 4LR44, 0.5 mA, >200 hours
Finish	Champagne silver
Connector	XLR3M
Dimensions	Ø21 × 170 mm Ø0.83" × 6.7"
Net Weight	150 g (5.3 oz), without battery

CAUTIONS

- When the microphone is connected, do not un-screw the microphone that may cause impact signal to the connected system.
- Turn off the level on the audio system before disconnecting the microphone.
- Battery life time is 300 hours. If the signal is low or no signal, replace the battery.
- Before replace the battery, disconnect the microphone from the system.
- Insert the battery according to the illustrated polarity on the body. Anode shall point toward the XLR3M plug. Cathode shall point to the capsule tip. If the battery is not properly inserted, the microphone will not be damaged, but will not work either.
- To save the battery power, remove the battery when the microphone will not be used for a long period.
- Place foam wind screen when in outdoor to reduce wind noise.

C.3 Measuring the microphones' phase frequency responses

C.3.1 Microtech Gefell MK301 with serial number 0556

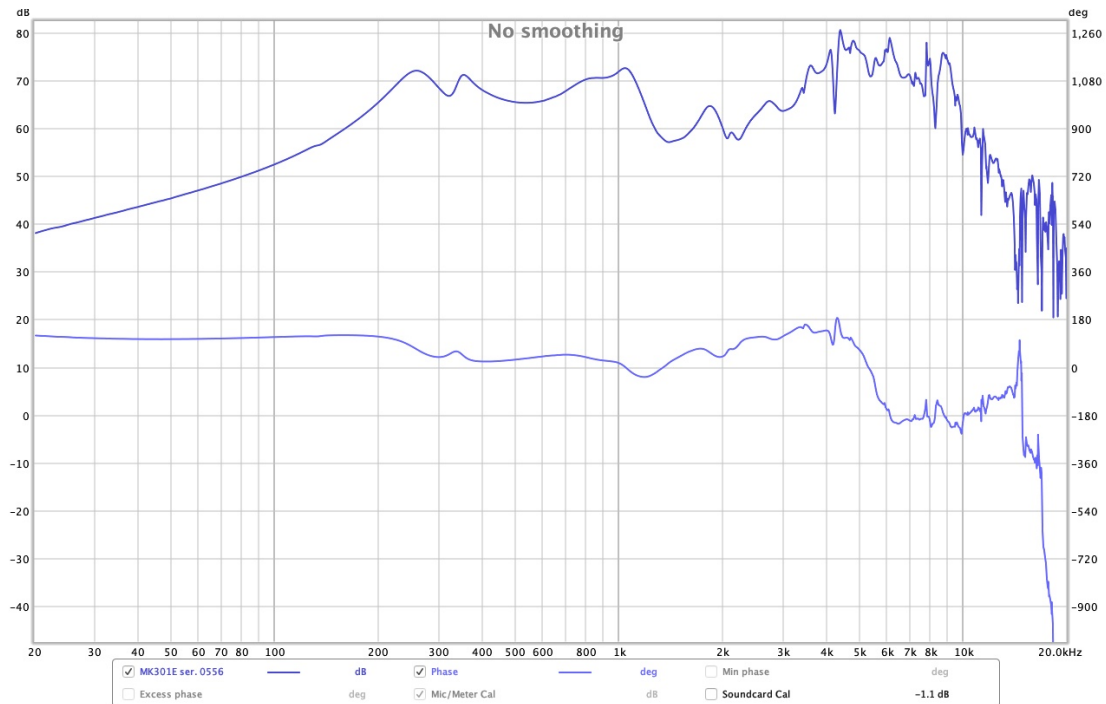


Fig. C.4: Amplitude and phase frequency response of MK301E (ser. 0556)

C.3.2 Microtech Gefell MK301 with serial number 0557

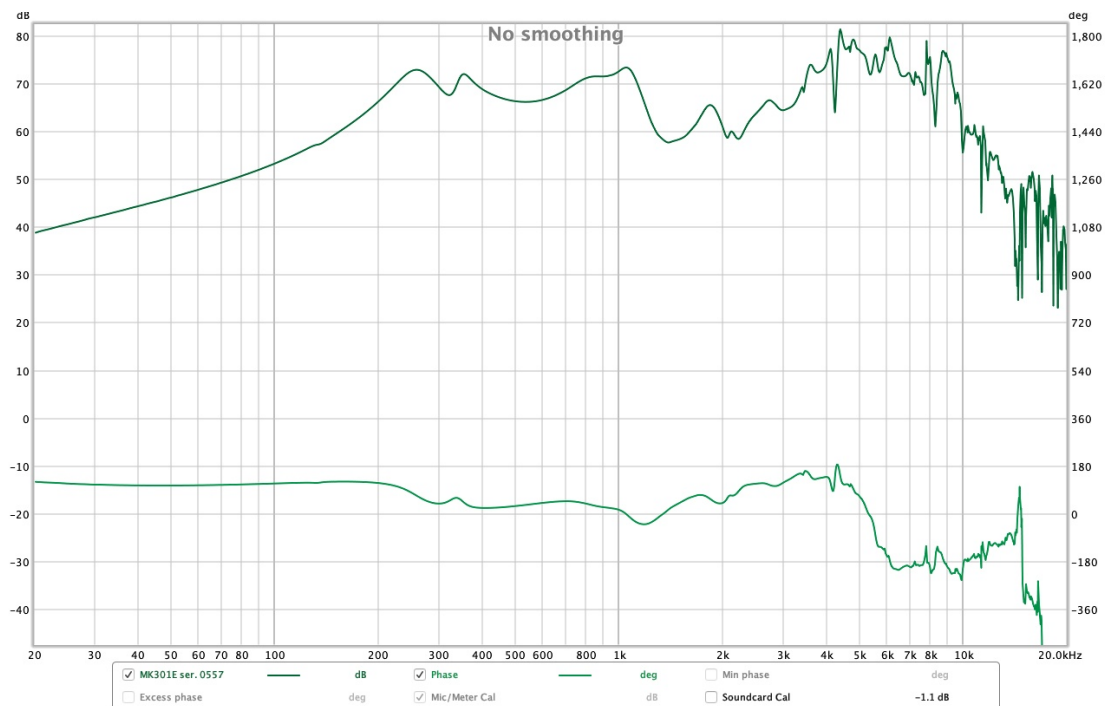


Fig. C.5: Amplitude and phase frequency response of MK301E (ser. 0557)

C.3.3 Superlux ECM888B with serial number E888B5A0528

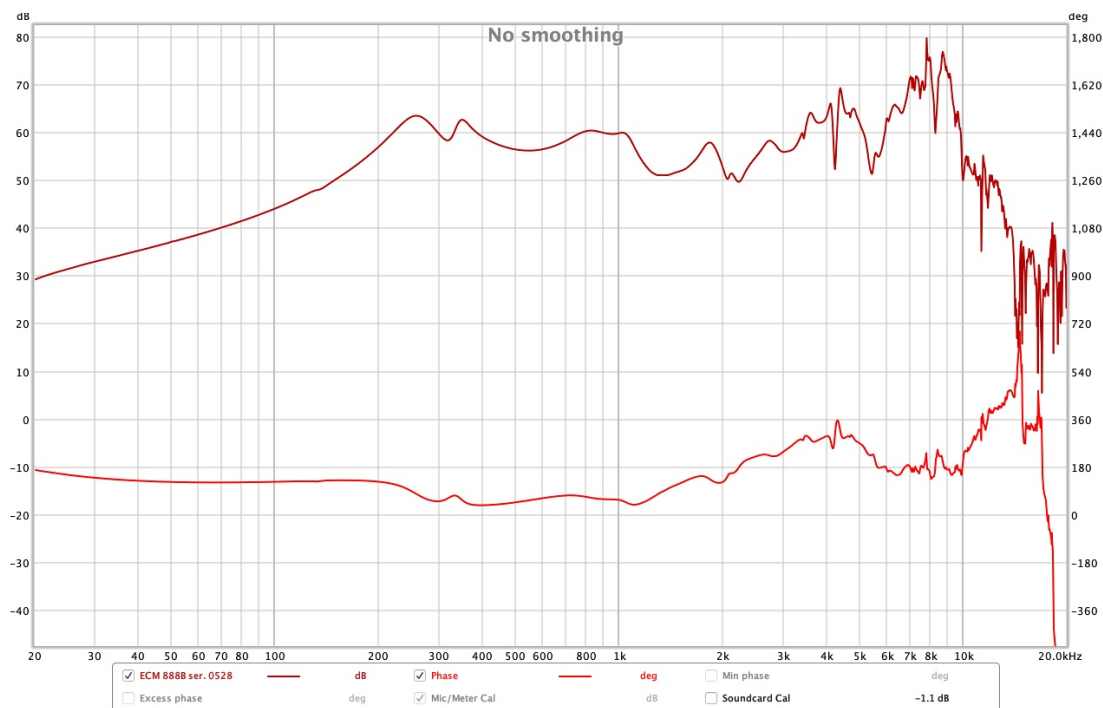


Fig. C.6: Amplitude and phase frequency response of ECM888B (ser. E888B5A0528)

C.3.4 Superlux ECM888B with serial number E888B5A0530

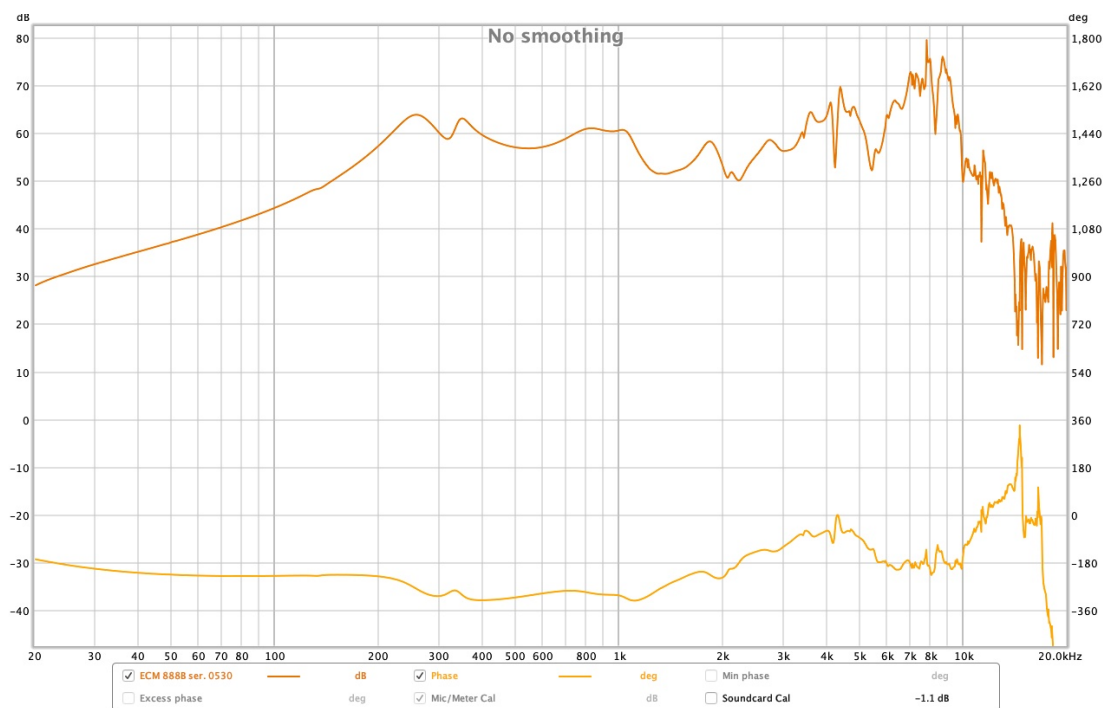


Fig. C.7: Amplitude and phase frequency response of ECM888B (ser. E888B5A0530)

C.4 Comparing the microphones' phase frequency responses

C.4.1 Complete comparison of all four microphones

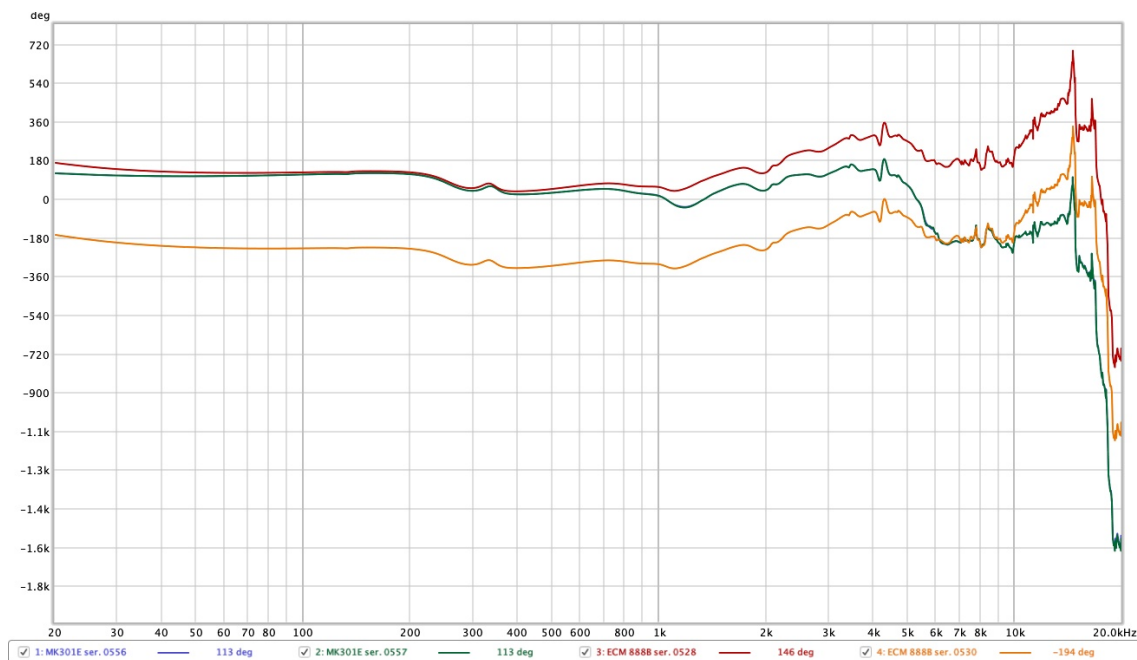


Fig. C.8: Phase frequency responses of all four microphones

C.4.2 Comparison of both Microtech Gefell MK301E

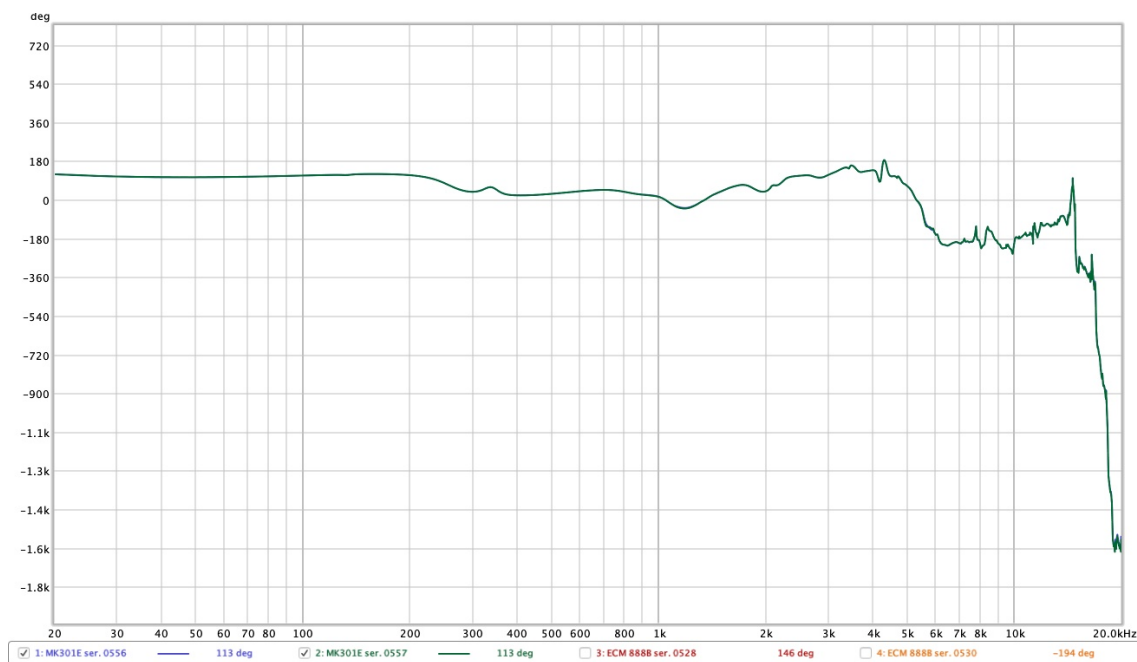


Fig. C.9: Phase frequency responses of both Microtech Gefell MK301E

C.4.3 Comparison of both Superlux ECM888B

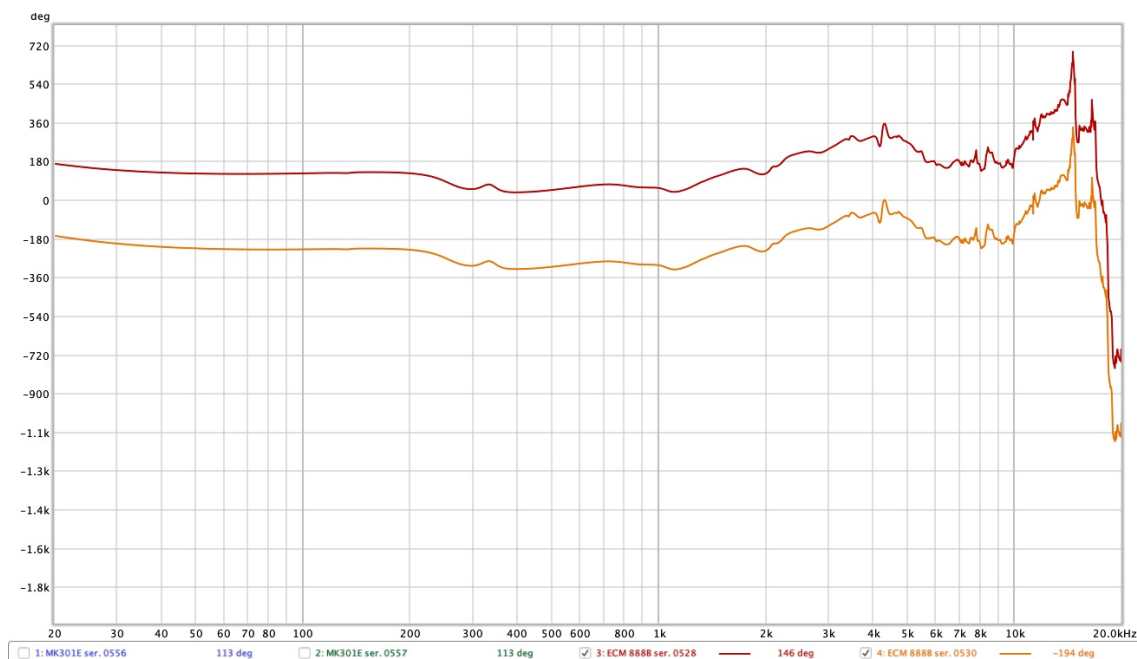


Fig. C.10: Phase frequency responses of both Superlux ECM888B

C.4.4 Comparison of Microtech Gefell MK301E with serial number 0556 and Superlux ECM888B with serial number E888B5A0528



Fig. C.11: Phase frequency responses of both MKE301E (ser. 0556) and ECM888B (ser. E888B5A0528)

C.4.5 Comparison of Microtech Gefell MK301E with serial number 0556 and Superlux ECM888B with serial number E888B5A0530

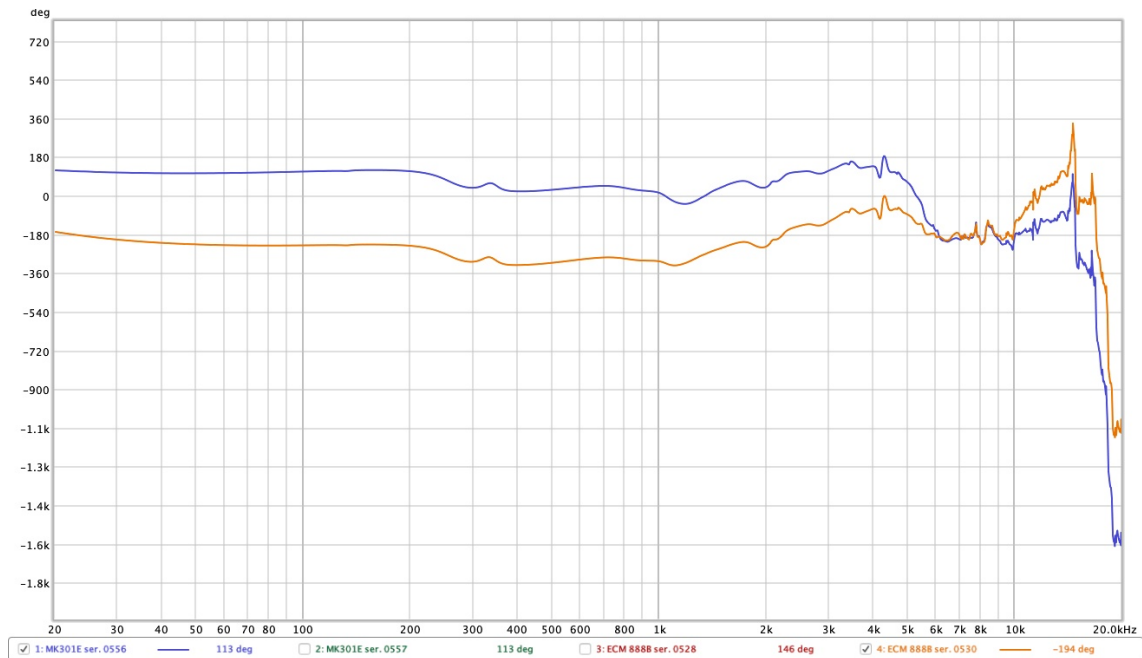


Fig. C.12: Phase frequency responses of both MKE301E (ser. 0556) and ECM888B (ser. E888B5A0530)

C.4.6 Comparison of Microtech Gefell MK301E with serial number 0557 and Superlux ECM888B with serial number E888B5A0528

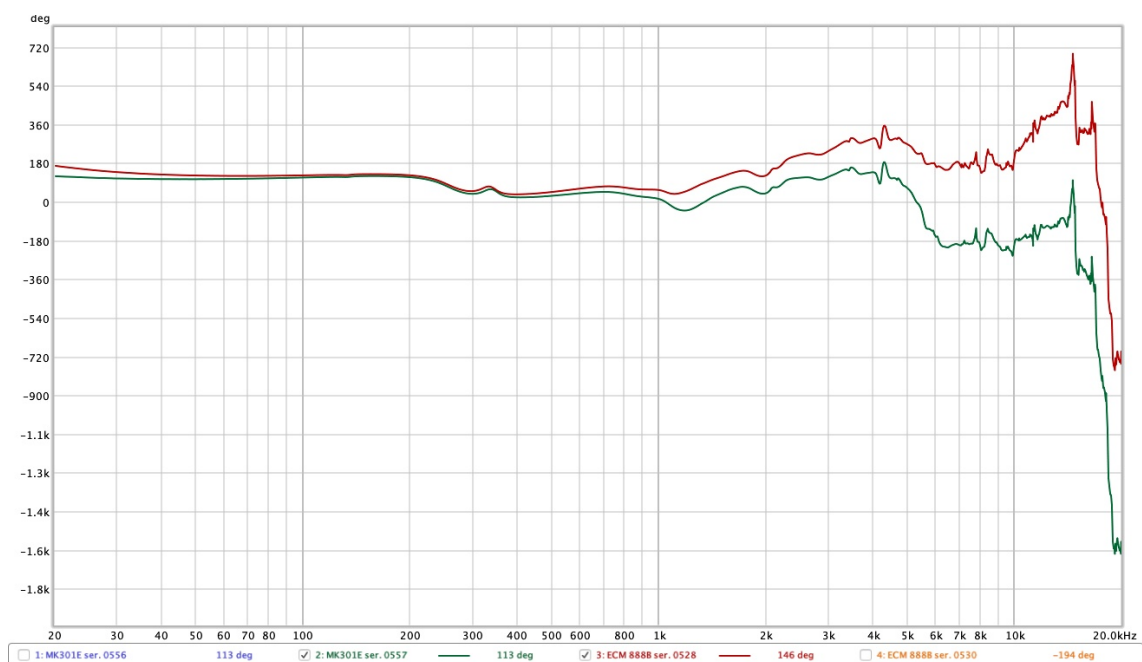


Fig. C.13: Phase frequency responses of both MKE301E (ser. 0557) and ECM888B (ser. E888B5A0528)

C.4.7 Comparison of Microtech Gefell MK301E with serial number 0557 and Superlux ECM888B with serial number E888B5A0530

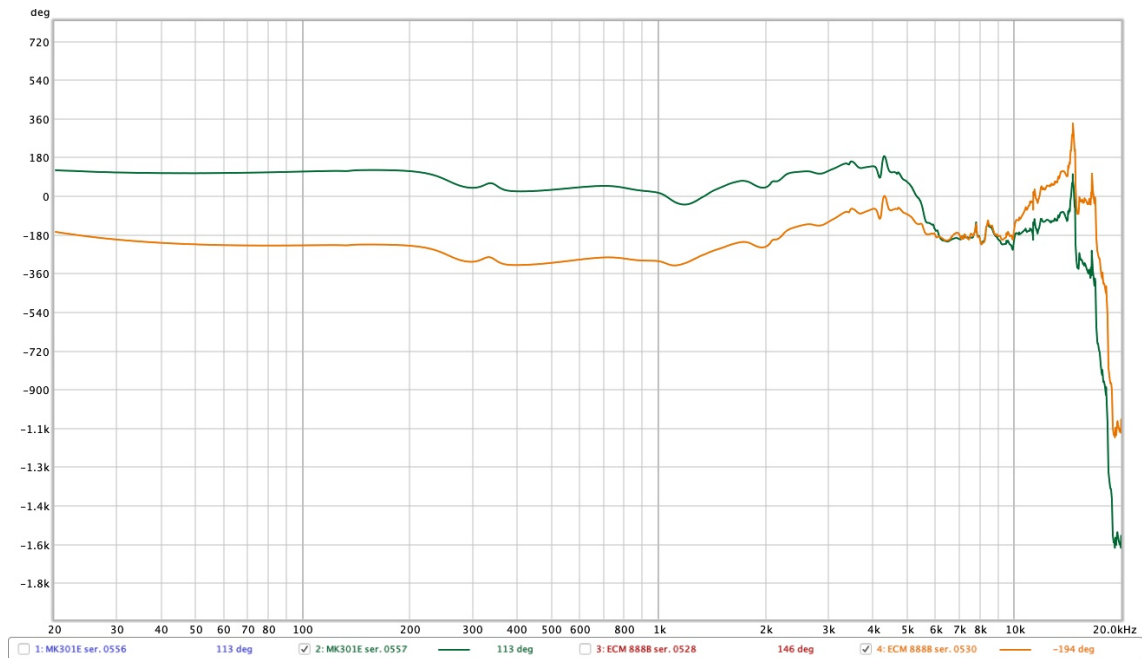


Fig. C.14: Phase frequency responses of both MKE301E (ser. 0557) and ECM888B (ser. E888B5A0530)

D Measurement data for the observation of the influences of different phase responses

To evaluate the influences of different measurement microphone's phase frequency responses in chapter 4, six different measurements were performed, as introduced in 4.3.1.

Subsequently, the characteristics of the sample used for the calibration process, as well as the measurement specimen will be introduced. Thereafter, the measurement results of the relevant individual measurements are presented.

D.1 Specimen

Hereafter, the relevant information on the utilized specimens is presented.

D.1.1 Calibration specimen

The following specimen was used to perform all calibration processes for the individual microphone combinations.

MEASUREMENT PROTOCOL:
Determination of sound absorption coefficient in the impedance tube according to EN ISO 10534-2

Description of the testing environment:

Impedance tube used: B&K 4206 impedance tube
 Impedance tube setup: Small Tube Setup
 Excitation: using random white noise in accordance to EN ISO 10534-2 using the transfer function method (two-microphone wave-separation method).
 Evaluation: method (two-microphone wave-separation method).

Test date: 2020/08/27
 Test Engineer: Inggolf-Christopher Facius
 Location: Potsdam, Germany
 Testing station: Acoustics Lab

Metereological conditions: Temperature: 23,6 °C Humidity: 38 %
 Air pressure: 1016,1 hPa Air density: 1,1743 kg/m³

Description of the materials to be examined and the testing arrangement:

Anthracite-coloured, partly closed-pored cell foam. Thickness approx. 50 mm Precise placement of the samples in the sample holder with tight closure to the wall. Installation of the samples without clearance in front of the soundproof tube end.

Designation of the sample: Own Calibration Probe
 Thickness of probe: 5 cm
 Number of Repeats: 6

Measurement System:

Sound source: B&K 4206 - built in driver + Wainghe WPA-600PRO
 Sound Card: US-16x08
 Microphones: 2x Microtech Gefell measurement microphone capsule 1/4" MK301E (ser.no. 0556 + 0557) + measurement microphone preamp 1/2" P48 MV220 (ser.no. 1015 + 1033)
 US-16x08 - built in pre-amps

Pre-amps: between micro-
 Distance: 2 cm
 Distance between microphones: 3,5 cm
 and probe:
 Signal to Noise Ratio: 62,2747 dB
 Notes: no comments

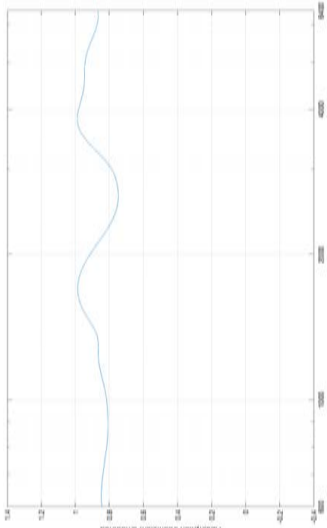



Figure 1: Frequency-dependent absorption coefficient. Calculation based on the measurements of 6 Repeats. Curve smoothed by applying moving average: smoothing parameter 1/12 octave, Gaussian window.

f/Hz	630.00	800.00	1000.00	1250.00	1600.00	2000.00
α	0.84	0.82	0.82	0.87	0.96	0.90
f/Hz	2500.00	3150.00	4000.00	6300.00	6300.00	
α	0.76	0.85	0.97	0.93	0.88	


D.1.2 Specimen under investigation (measurement specimen)

A sample of Cellofoam CELLO® 521 was used for all measurement processes:

PUR FOAM



DATA SHEET




CELLO® 521

Noise-absorbing, three-dimensionally structured PUR-ester foam, with an air-permeable sealed surface (special Cello® process).

Thanks to the rippled surface embossing, the material achieves excellent sound attenuation effectivity across all frequency bands.

Applications: Construction and farm machinery, cabins/ casings/hoods, machine construction



TECHNICAL DATA

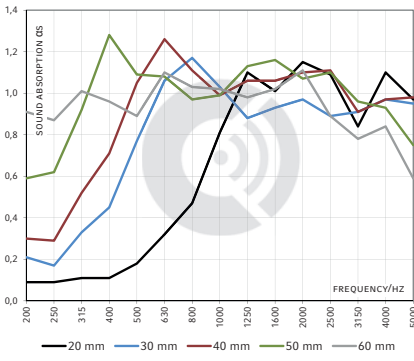
FLAMMABILITY	▶ FMVSS 302, DIN 75 200, fulfilled ▶ ISO 3795, burning rate < 100 mm/min
TEMPERATURE RESISTANCE	-40°C to +100°C
THERMAL CONDUCTIVITY / EN 12667	≤ 0.040 W/(m·K) at 10°C
DENSITY PUR-FOAM / DIN EN ISO 845	25 kg/m ³

DIMENSIONS

PRODUCT	THICKNESS [mm]	THICKNESS TOLERANCE [mm]	SHEETS* [mm]
521	20, 30, 40, 50, 60	≤ 30 mm ± 10% > 30 mm ± 3 mm	1000 x 1500 or 2000 x 1500

Other thicknesses / dimensions on request. Ready-to-use parts according to your specifications or drawing.
*Untrimmed: Effective dimensions guaranteed as ordered, may be exceeded by some layers (foam, film, non-woven etc.).

REVERBERATION ROOM / DIN EN ISO 354



BENEFITS

- ▶ Attractive and distinctive design
- ▶ Dirt-resistant and oil-, water- and fuel-repellent surface
- ▶ Excellent absorption values across all frequency ranges
- ▶ Effortless to cut with a cardboard cutter

OPTIONS

521 NK: no self-adhesive equipment
521 SK: with self-adhesive finish

PLEASE SEE OUR PROCESSING AND STORAGE INSTRUCTIONS

ISO 9001 CERTIFIED

CELLOFOAM GMBH & CO. KG

Details and values given in this leaflet are average values and have been compiled with care. They are not binding, however, and Cellofoam GmbH & Co. KG disclaims any liability for any damages and detriments, also in connection with to any third party's rights. The information given does not release the buyers from making the necessary experiments and tests themselves. Subject to technical changes. For updates of this data sheet, please go to our website.

sales@cellofoam.de
www.cellofoam.de

08/19

01

D.2 Individual measurements

D.2.1 Impedance measurement using 2 Microtech Gefell MK301E with Calibration

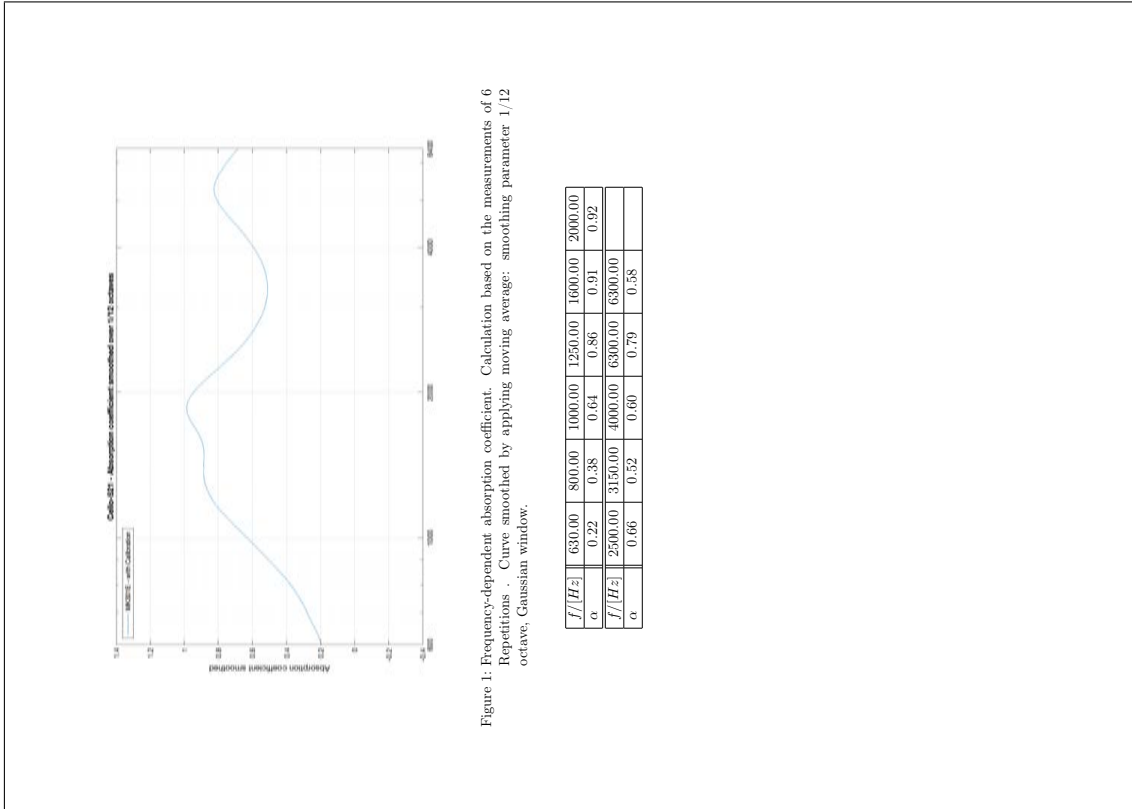
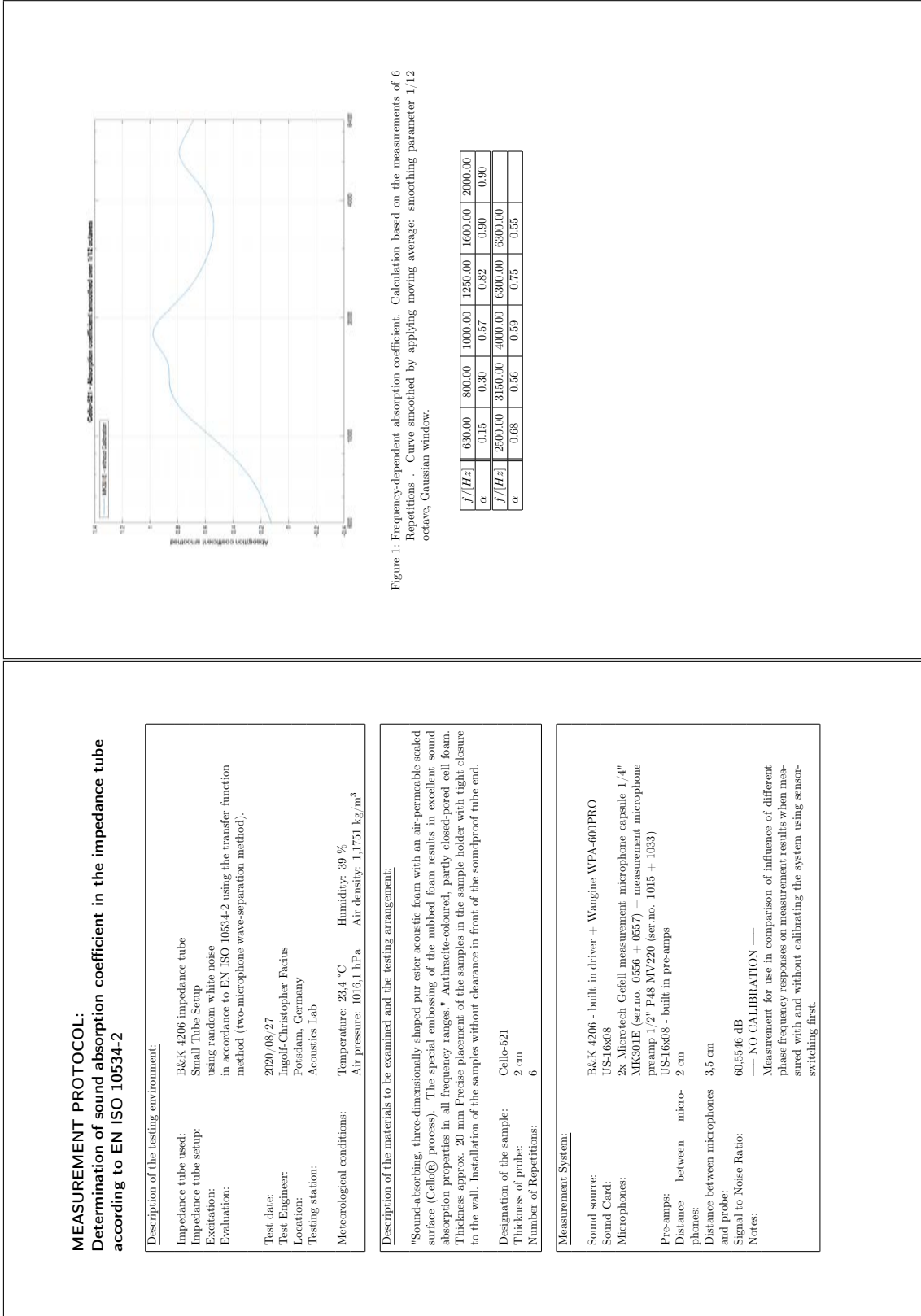


Figure 1: Frequency-dependent absorption coefficient. Calculation based on the measurements of 6 Repetitions. Curve smoothed by applying moving average: smoothing parameter 1/12 octave, Gaussian window.

MEASUREMENT PROTOCOL: Determination of sound absorption coefficient in the impedance tube according to EN ISO 10534-2	
<u>Description of the testing environment:</u>	<p>Impedance tube used: B&K 4206 impedance tube</p> <p>Impedance tube setup: Small Tube Setup</p> <p>Excitation: using random white noise in accordance to EN ISO 10534-2 using the transfer function method (two-microphone wave-separation method).</p> <p>Test date: 2020/08/27</p> <p>Test Engineer: Ingo-Christoph Focius</p> <p>Location: Potsdam, Germany</p> <p>Testing station: Acoustics Lab</p> <p>Meteorological conditions: Temperature: 23,4 °C Humidity: 39 % Air pressure: 1016,1 hPa Air density: 1,1751 kg/m³</p>
<u>Description of the materials to be examined and the testing arrangement:</u>	<p>"Sound-absorbing, three-dimensionally shaped par ester acoustic foam with an air-permeable sealed surface (Cello process). The special embossing of the nubbled foam results in excellent sound absorption properties in all frequency ranges." Anthracite-coloured, partly closed-pored cell foam. Thickness approx. 20 mm. Precise placement of the samples in the sample holder with tight closure to the wall. Installation of the samples without clearance in front of the soundproof tube end.</p> <p>Designation of the sample: Calib-521</p> <p>Thickness of probe: 2 cm</p> <p>Number of Repetitions: 6</p>
<u>Measurement System:</u>	<p>Sound source: B&K 4206 - built in driver + Wangine WPA-600PRO</p> <p>Sound Card: US-16x08</p> <p>Microphones: 2x Microtech Gefell measurement microphone capsule 1/4" MK301E (ser.no. 0556 + 0557) + measurement microphone preamp 1/2" P48 MV220 (ser.no. 1015 + 1033)</p> <p>Pre-amps: US-16x08 - built in pre-amps</p> <p>Distance between micro-phones: 2 cm</p> <p>Distance between microphones and probe: 3,5 cm</p> <p>Signal to Noise Ratio: 60,5546 dB</p> <p>Notes: Measurement for use in comparison of influence of different phase frequency responses on measurement results when measured with and without calibrating the system using sensor-switching first. Calibration probe: 50mm anthracite colored open pore foam</p>

D.2.2 Impedance measurement using 2 Microtech Gefell MK301E without Calibration



D.2.3 Impedance measurement using 2 Superlux ECM 888B with Calibration

**MEASUREMENT PROTOCOL:
Determination of sound absorption coefficient in the impedance tube according to EN ISO 10534-2**

Description of the testing environment:

Impedance tube used: B&K 4206 impedance tube
 Impedance tube setup: Small Tube Setup
 Excitation: using random white noise in accordance to EN ISO 10534-2 using the transfer function method (two-microphone wave-separation method).
 Test date: 2020/08/27
 Test Engineer: Ingolf-Christopher Fuchs
 Location: Potsdam, Germany
 Testing station: Acoustics Lab

Meteorological conditions: Temperature: 23,4 °C Humidity: 39 %
 Air pressure: 1016,1 hPa Air density: 1,1751 kg/m³

Description of the materials to be examined and the testing arrangement:

"Sound-absorbing, three-dimensionally shaped poly ester acoustic foam with an air-permeable sealed surface (Cello process). The special embossing of the nubbled foam results in excellent sound absorption properties in all frequency ranges." Anthracite-coloured, partly closed-pored cell foam. Thickness approx. 20 mm. Precise placement of the samples in the sample holder with tight closure to the wall. Installation of the samples without clearance in front of the soundproof tube end.

Designation of the sample: Cello-521
 Thickness of probe: 2 cm
 Number of Repetitions: 6

Measurement System:

Sound source: B&K 4206 - built in driver + Wangine WPA-600PRO
 Sound Card: US-16808
 Microphones: E8885A0528 + E8885A0530
 Pre-amps: US-16808 - built in pre-amps
 Distance between microphones: 2 cm
 Distance between microphones and probe: 3,5 cm
 Signal to Noise Ratio: 65,4566 dB
 Notes: Measurement for use in comparison of influence of different phase frequency responses on measurement results when measured with and without calibrating the system using sensor-switching first. Calibration probe: 50mm anthracite colored open pore foam

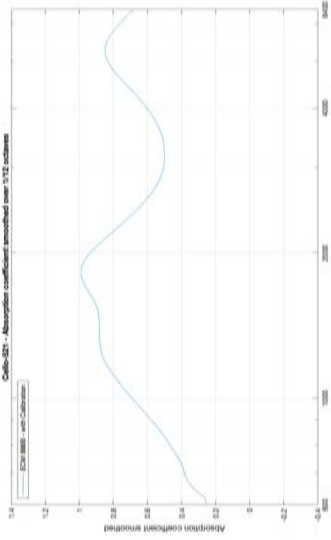


Figure 1: Frequency-dependent absorption coefficient. Calculation based on the measurements of 6 Repetitions. Curve smoothed by applying moving average; smoothing parameter 1/12 octave, Gaussian window.

f / [Hz]	630.00	800.00	1000.00	1250.00	1600.00	2000.00
α	0.31	0.47	0.69	0.86	0.92	0.92
f / [Hz]	2500.00	3150.00	4000.00	6300.00	6300.00	
α	0.64	0.51	0.61	0.81	0.45	

D.2.4 Impedance measurement using 2 Superlux ECM 888B without Calibration

MEASUREMENT PROTOCOL:
Determination of sound absorption coefficient in the impedance tube according to EN ISO 10534-2

Description of the testing environment:

Impedance tube used: B&K 4206 impedance tube
 Impedance tube setup: Small Tube Setup
 Excitation: using random white noise in accordance to EN ISO 10534-2 using the transfer function method (two-microphone wave-separation method).
 Test date: 2020/08/27
 Test Engineer: Ingolf-Christopher Fuchs
 Location: Potsdam, Germany
 Testing station: Acoustics Lab

Meteorological conditions: Temperature: 23.4 °C Humidity: 39 %
 Air pressure: 1016.1 hPa Air density: 1.1751 kg/m³

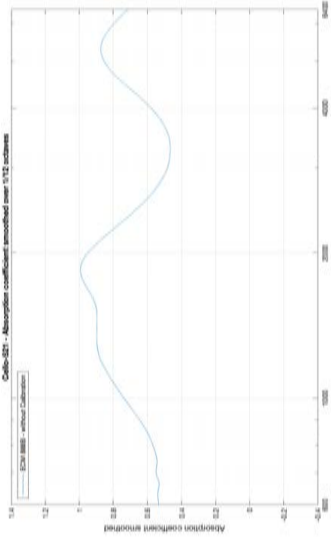
Description of the materials to be examined and the testing arrangement:

"Sound-absorbing, three-dimensionally shaped poly ester acoustic foam with an air-permeable sealed surface (Cello process). The special embossing of the nubbed foam results in excellent sound absorption properties in all frequency ranges." Anthracite-coloured, partly closed-pored cell foam. Thickness approx. 20 mm. Precise placement of the samples in the sample holder with tight closure to the wall. Installation of the samples without clearance in front of the soundproof tube end.

Designation of the sample: Cello-521
 Thickness of probe: 2 cm
 Number of Repetitions: 6

Measurement System:

Sound source: B&K 4206 - built in driver + Wangine WPA-600PRO
 Sound Card: US-16808
 Microphones: 2x Superlux measurement microphone ECM 888B (ser.no. E888B5A0528 + E888B5A0530)
 Pre-amps: US-16808 - built in pre-amps
 Distance between microphones: 2 cm
 and probe: 3.5 cm
 Signal to Noise Ratio: 65.4566 dB
 Notes: — NO CALIBRATION —
 Measurement for use in comparison of influence of different phase frequency responses on measurement results when measured with and without calibrating the system using sensor-switching first.



f/[Hz]	630.00	800.00	1000.00	1250.00	1600.00	2000.00
α	0.54	0.57	0.74	0.88	0.93	0.93

f/[Hz]	2500.00	4000.00	6300.00	6300.00
α	0.64	0.48	0.59	0.83

Figure 1: Frequency-dependent absorption coefficient. Calculation based on the measurements of 6 Repetitions. Curve smoothed by applying moving average; smoothing parameter 1/12 octave, Gaussian window.

D.2.5 Impedance measurement using Microtech Gefell MK301E (ser. 0557) and Superlux ECM 888B (ser. E888B5A0530) with Calibration

MEASUREMENT PROTOCOL: Determination of sound absorption coefficient in the impedance tube according to EN ISO 10534-2

Description of the testing environment:
 Impedance tube used: B&K 4206 impedance tube
 Impedance tube setup: Small Tube Setup
 Excitation: using random white noise in accordance to EN ISO 10534-2 using the transfer function method (two-microphone wave-separation method).
 Test date: 2020/08/27
 Test Engineer: Ingolf-Christopher Fuchs
 Location: Potsdam, Germany
 Testing station: Acoustics Lab
 Meteorological conditions: Temperature: 23.4 °C Humidity: 39 %
 Air pressure: 1016.1 hPa Air density: 1.1751 kg/m³

Description of the materials to be examined and the testing arrangement:
 "Sound-absorbing, three-dimensionally shaped pur ester acoustic foam with an air-permeable sealed surface (Cello process). The special embossing of the nubbled foam results in excellent sound absorption properties in all frequency ranges." Anthracite-coloured, partly closed-pored cell foam. Thickness approx. 20 mm. Precise placement of the samples in the sample holder with tight closure to the wall. Installation of the samples without clearance in front of the soundproof tube end.
 Designation of the sample: Cello-521
 Thickness of probe: 2 cm
 Number of Repetitions: 6

Measurement System:
 Sound source: B&K 4206 - built in driver + Waugine WPA-600PRO
 Sound Card: US-16x08
 Microphones: Microtech Gefell measurement microphone capsule 1/4" MK301E (ser.no. 0557) + measurement microphone preamp 1/2" P48 MV220 (ser.no. 1033) + Superlux measurement microphone ECM 888B (ser.no. E888B5A0530)
 Pre-amps: US-16x08 - built in pre-amps
 Distance between microphones: 2 cm
 Distance between microphones and probe: 3.5 cm
 Signal to Noise Ratio: 62.9577 dB
 Notes: Measurement for use in comparison of influence of different phase frequency responses on measurement results when measured with and without calibrating the system using sensor-switching first. Calibration probe: 50mm anthracite colored open pore foam

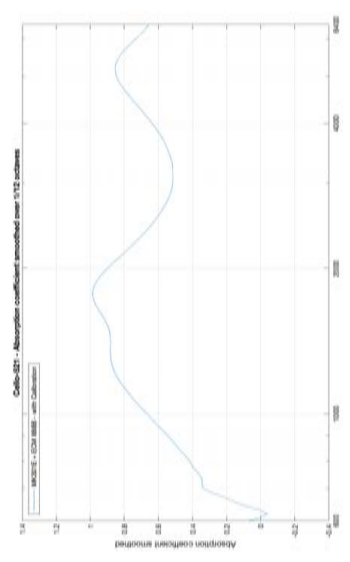


Figure 1: Frequency-dependent absorption coefficient. Calculation based on the measurements of 6 Repetitions. Curve smoothed by applying moving average: smoothing parameter 1/12 octave, Gaussian window.

$f/[Hz]$	630.00	800.00	1000.00	1250.00	1600.00	2000.00
α	0.16	0.42	0.67	0.86	0.93	0.89
$f/[Hz]$	2500.00	3150.00	4000.00	6300.00	6300.00	
α	0.63	0.52	0.64	0.82	0.71	

D.2.6 Impedance measurement using Microtech Gefell MK301E (ser. 0557) and Superlux ECM 888B (ser. E888B5A0530) without Calibration

MEASUREMENT PROTOCOL: Determination of sound absorption coefficient in the impedance tube according to EN ISO 10534-2

Description of the testing environment:

Impedance tube used: B&K 4206 impedance tube
 Impedance tube setup: Small Tube Setup using random white noise in accordance to EN ISO 10534-2 using the transfer function method (two-microphone wave-separation method).
 Test date: 2020/08/27
 Test Engineer: Ingolf-Christopher Fuchs
 Location: Potsdam, Germany
 Testing station: Acoustics Lab
 Meteorological conditions: Temperature: 23.4 °C Humidity: 39 %
 Air pressure: 1016.1 hPa Air density: 1.1751 kg/m³

Description of the materials to be examined and the testing arrangement:

"Sound-absorbing, three-dimensionally shaped par ester acoustic foam with an air-permeable sealed surface (Cello process). The special embossing of the nubbled foam results in excellent sound absorption properties in all frequency ranges." Anthracite-coloured, partly closed-pored cell foam. Thickness approx. 20 mm. Precise placement of the samples in the sample holder with tight closure to the wall. Installation of the samples without clearance in front of the soundproof tube end.

Designation of the sample: Cello-521
 Thickness of probe: 2 cm
 Number of Repetitions: 6

Measurement System:

Sound source: B&K 4206 - built in driver + Wangine WPA-600PRO
 Sound Card: US-16x08
 Microphones: Microtech Gefell measurement microphone capsule 1/4" MK301E (ser.no. 0557) + measurement microphone preamp 1/2" P48 MV220 (ser.no. 1033) + Superlux measurement microphone ECM 888B (ser.no. E888B5A0530)
 Pre-amps: US-16x08 - built in pre-amps
 Distance between microphones: 2 cm
 Distance between microphones and probe: 3.5 cm
 Signal to Noise Ratio: 62.9377 dB
 Notes: — NO CALIBRATION —
 Measurement for use in comparison of influence of different phase frequency responses on measurement results when measured with and without calibrating the system using sensor-switching first.

f/[Hz]	630.00	800.00	1000.00	1250.00	1600.00	2000.00
α	0.36	0.50	0.67	0.83	0.91	0.87

f/[Hz]	2500.00	3150.00	4000.00	6300.00	8300.00
α	0.58	0.58	0.75	0.75	0.34

Figure 1: Frequency-dependent absorption coefficient. Calculation based on the measurements of 6 Repetitions. Curve smoothed by applying moving average; smoothing parameter 1/12 octave, Gaussian window.

D.3 Comparison of measurements

D.3.1 Impedance measurements using 2 Microtech Gefell MK301E

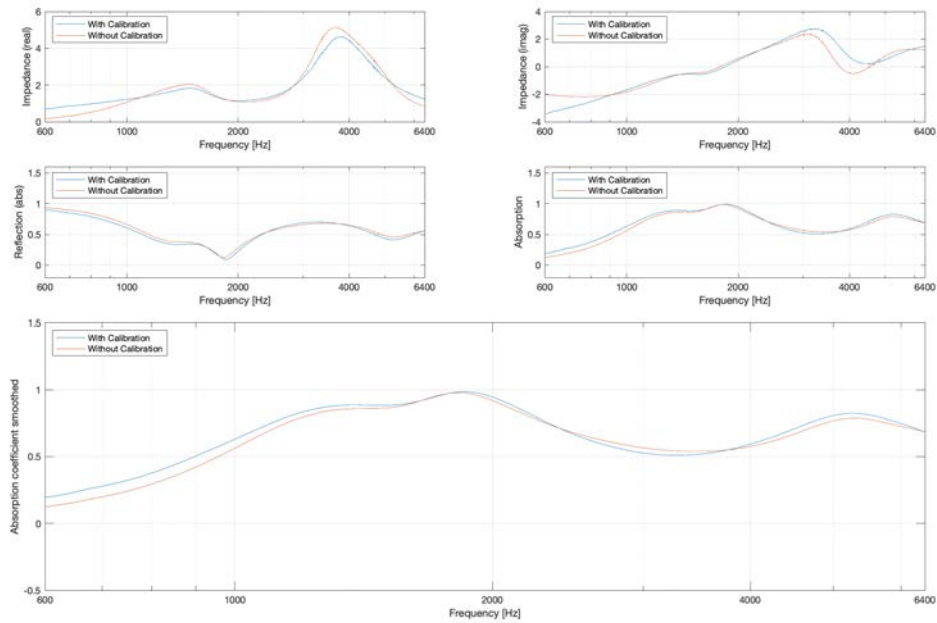


Fig. D.1: Measured data of impedance measurements using two MK301E

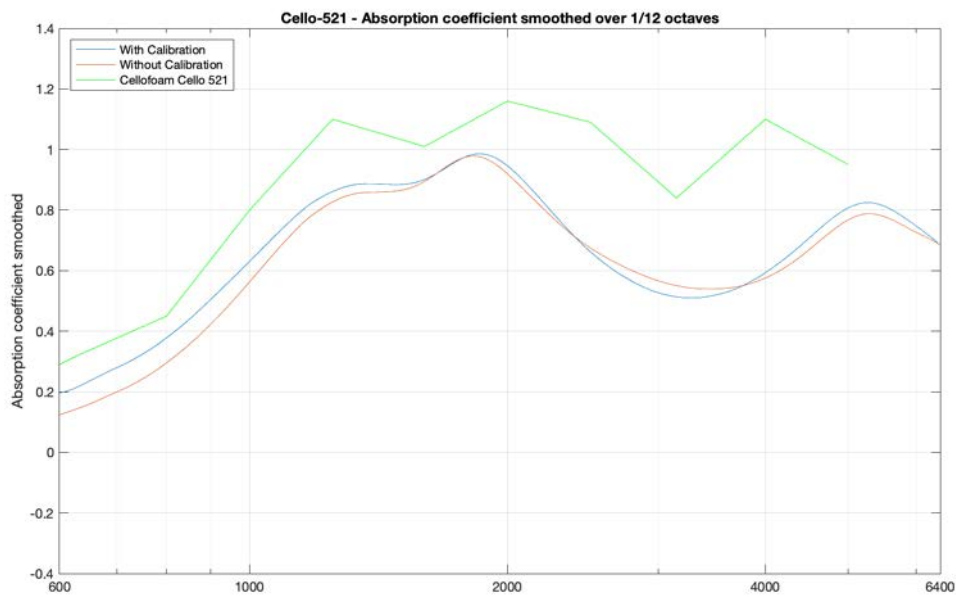


Fig. D.2: Smoothed absorption data of impedance measurements using two MK301E

D.3.2 Impedance measurements using 2 Superlux ECM 888B

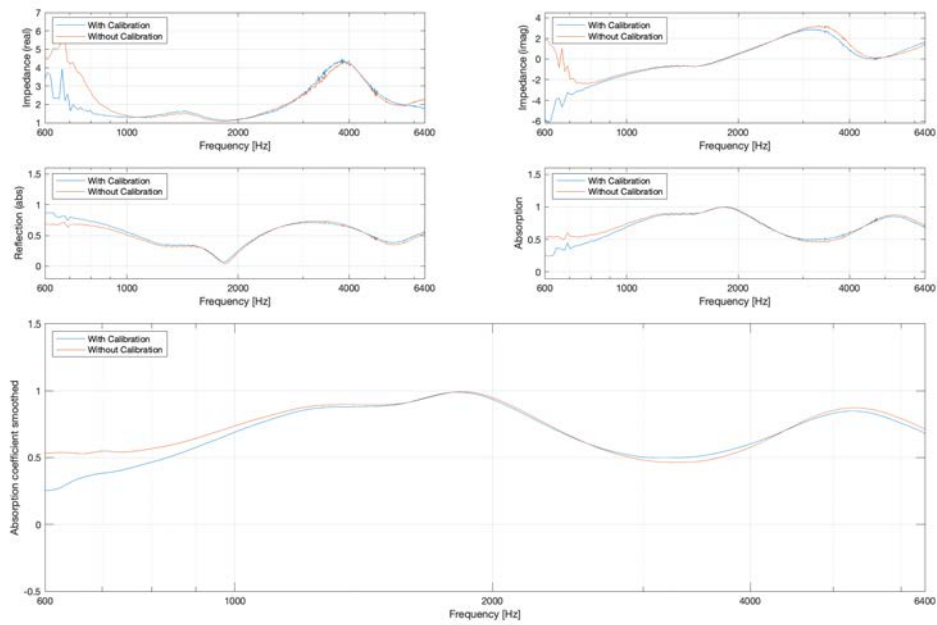


Fig. D.3: Measured data of impedance measurements using two ECM888B

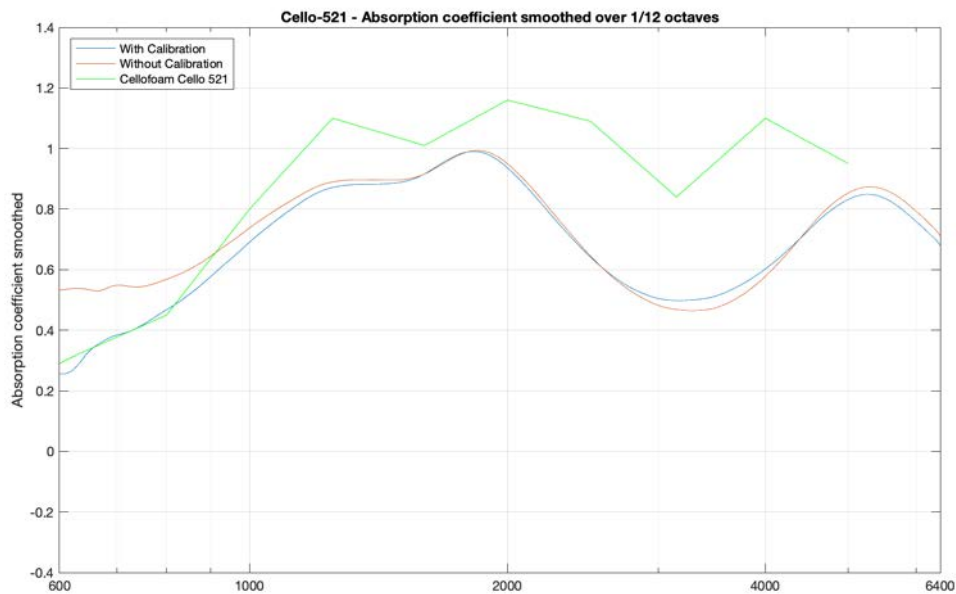


Fig. D.4: Smoothed absorption data of impedance measurements using two ECM888B

D.3.3 Impedance measurements using Microtech Gefell MK301E (ser. 0557) and Superlux ECM 888B (ser. E888B5A0530)

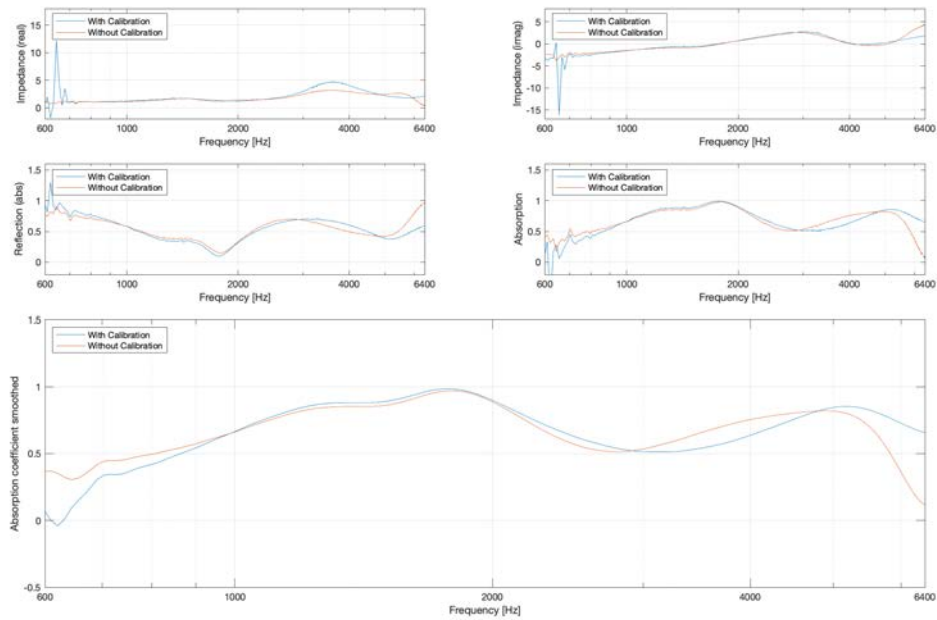


Fig. D.5: Measured data of impedance measurements using MK301E (ser. 0557) & ECM888B (ser. E888B5A0530)

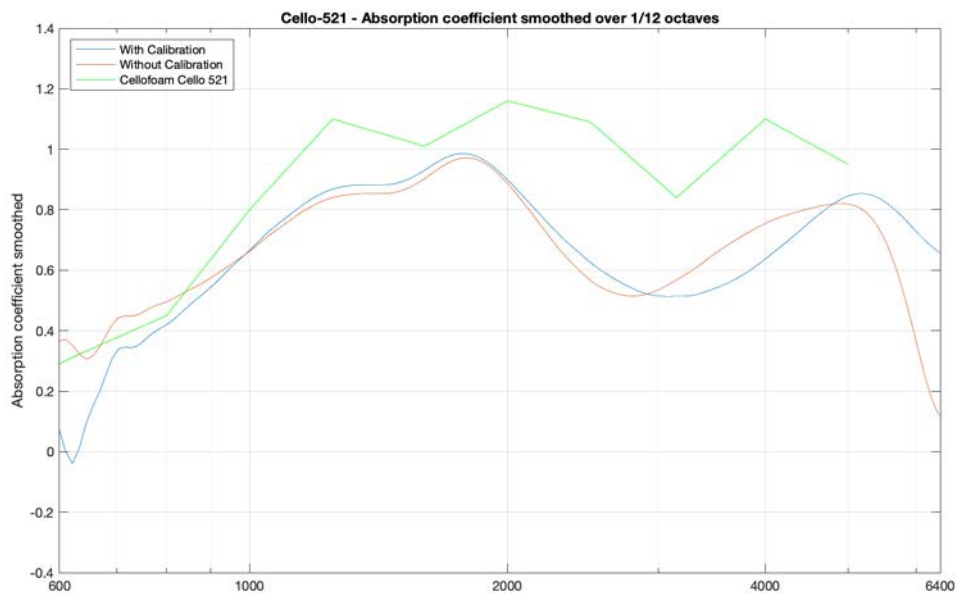


Fig. D.6: Smoothed absorption data of impedance measurements using MK301E (ser. 0557) & ECM888B (ser. E888B5A0530)

D.3.4 All impedance measurements with Calibration

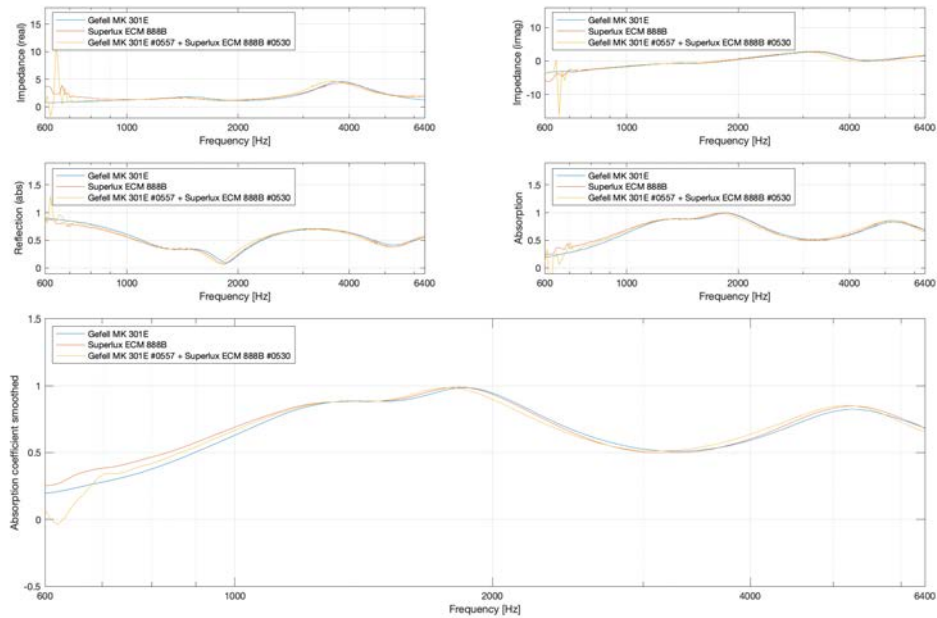


Fig. D.7: Measured data of impedance measurements of all microphone combinations using Calibration

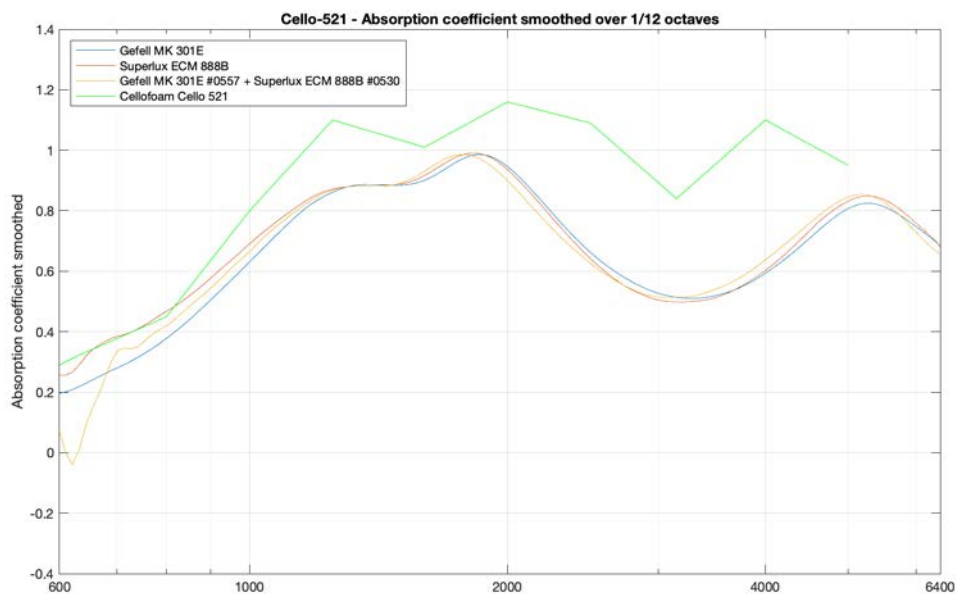


Fig. D.8: Smoothed absorption data of impedance measurements of all microphone combinations using Calibration

D.3.5 All impedance measurements without Calibration

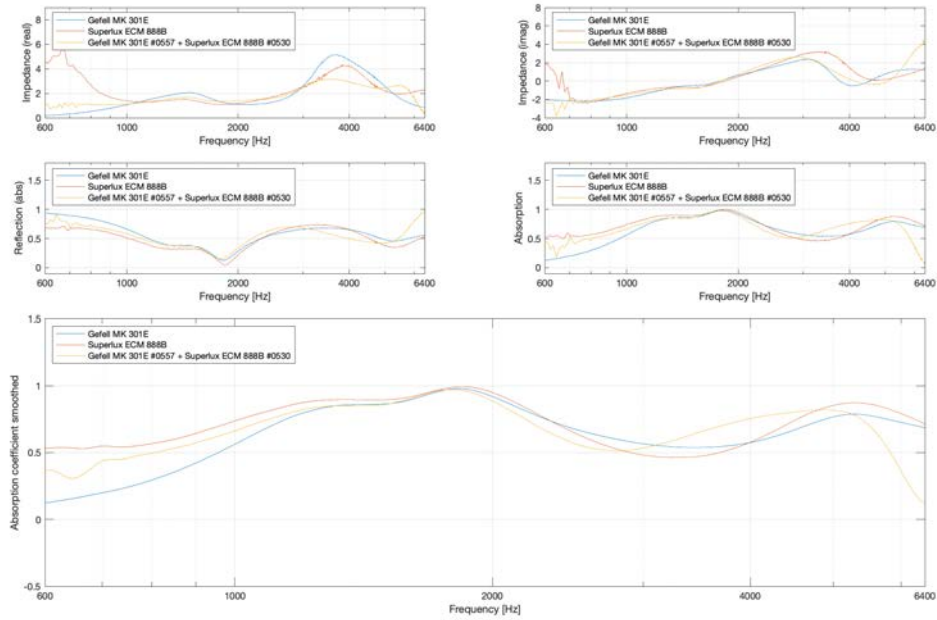


Fig. D.9: Measured data of impedance measurements of all microphone combinations not using Calibration

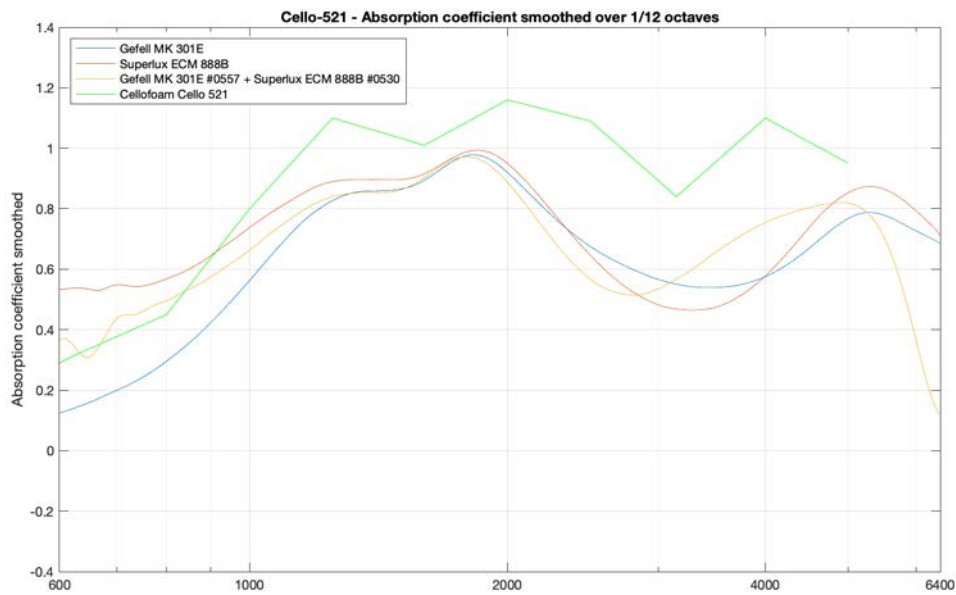


Fig. D.10: Smoothed absorption data of impedance measurements of all microphone combinations not using Calibration

D.4 Comparison of calibration data

D.4.1 Calibration data of measurement using 2 Microtech Gefell MK301E

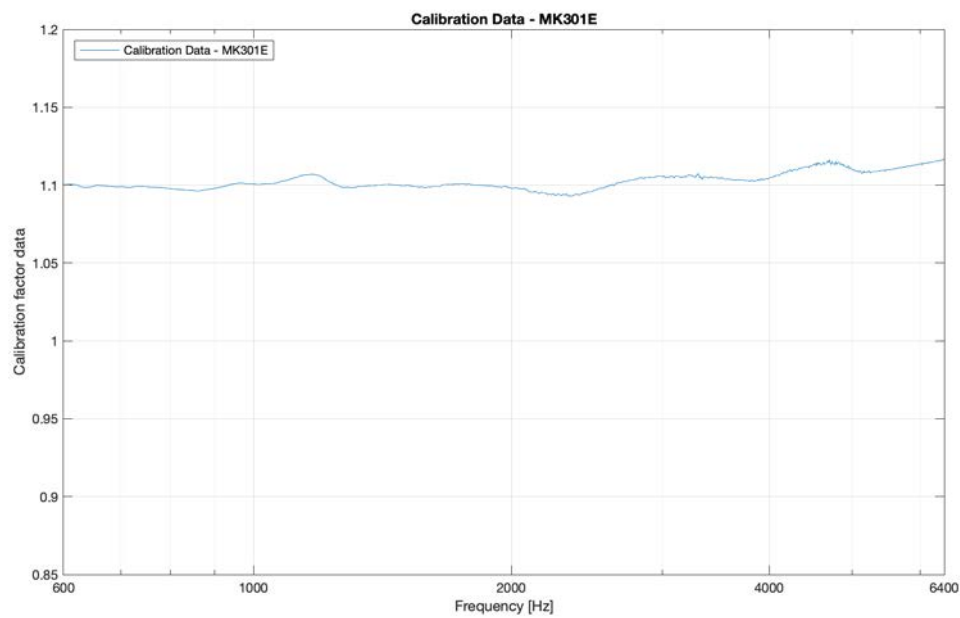
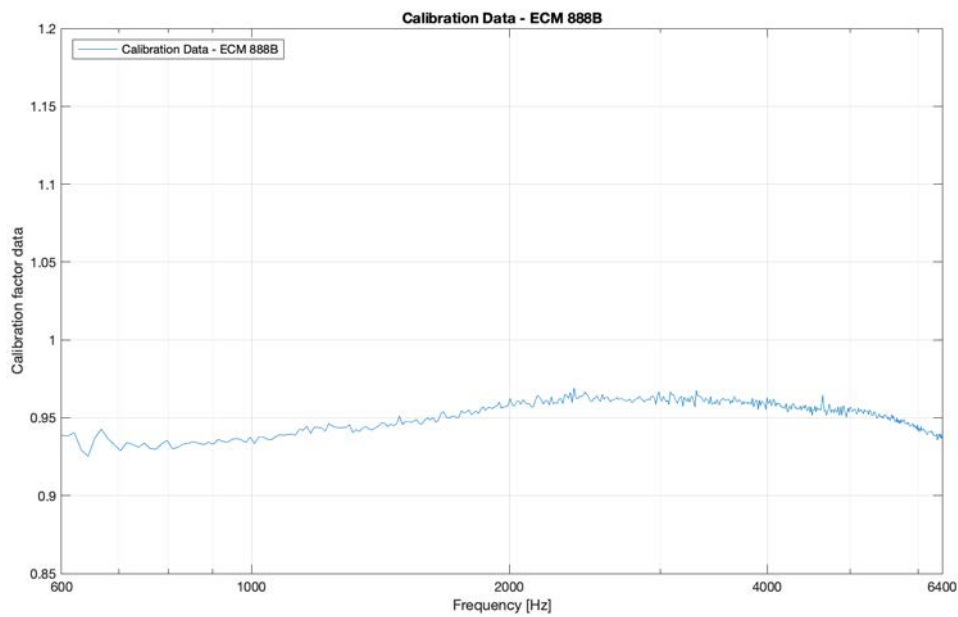


Fig. D.11: Calibration data H_c of measurement using two MK301E

D.4.2 Calibration data of measurement using 2 Superlux ECM 888B

Fig. D.12: Calibration data H_c of measurement using two ECM888B

D.4.3 Calibration data of measurement using Microtech Gefell MK301E (ser. 0557) and Superlux ECM 888B (ser. E888B5A0530)

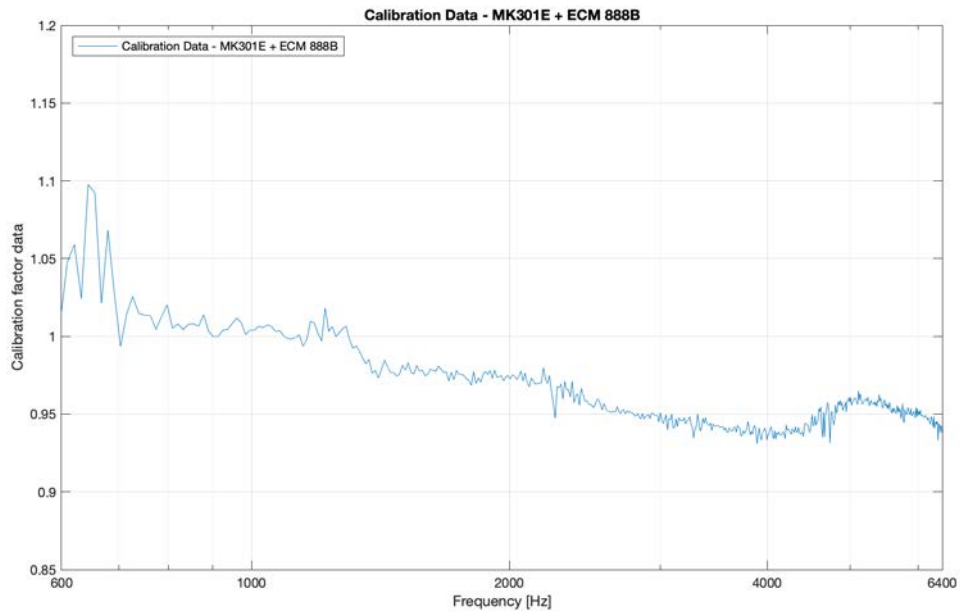
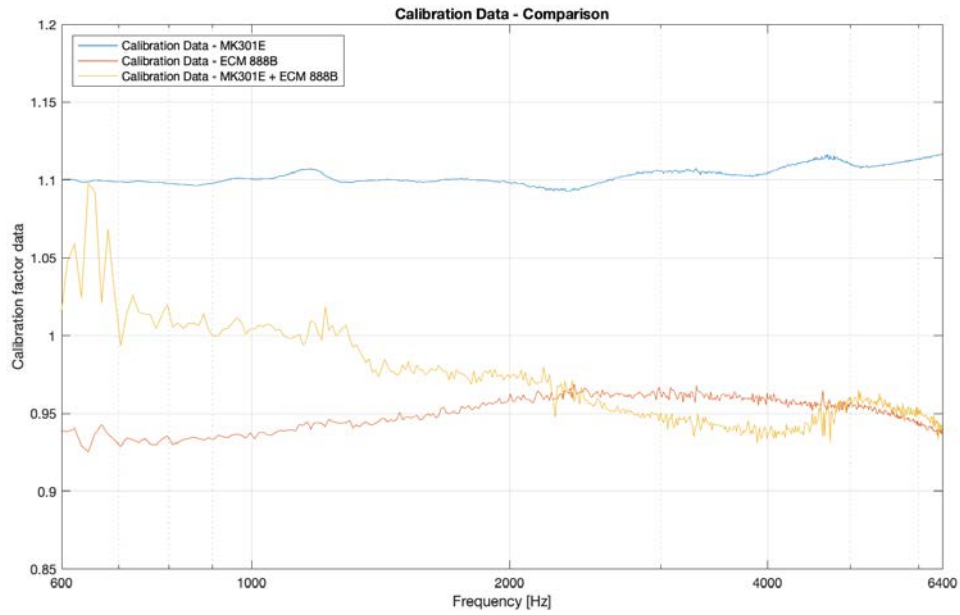


Fig. D.13: Calibration data H_c of measurement using MK301E (ser. 0557) & ECM888B (ser. E888B5A0530)

D.4.4 Calibration data of all microphone combinations

Fig. D.14: Comparison of calibration data H_c of all microphone combinations

Declaration/Selbstständigkeitserklärung

I hereby declare that I have written this bachelor's thesis independently and only using the sources and aids indicated. I have marked the passages extracted from the sources used, either literally or in terms of content, as such.

Ich versichere, dass ich diese Bachelorarbeit selbständig und nur unter Verwendung der angegebenen Quellen und Hilfsmittel angefertigt und die den benutzten Quellen wörtlich oder inhaltlich entnommenen Stellen als solche kenntlich gemacht habe.

Potsdam, September 15, 2020

.....

Signature